GEOLOGICA ULTRAIECTINA

Mededelingen van de
Faculteit Aardwetenschappen der
Rijksuniversiteit te Utrecht

No. 78

Single-channel Marine Seismic Profiling and The Analysis of Reverberatory Sequences

Eén-kanaals Marien Seismisch Onderzoek en De Analyse van Resonantie in Tijdreeksen

THOMAS MARTIN McGEE

GEOLOGICA ULTRAIECTINA

Mededelingen van de
Faculteit Aardwetenschappen der
Rijksuniversiteit te Utrecht

No. 78

Single-channel Marine Seismic Profiling and The Analysis of Reverberatory Sequences

Eén-kanaals Marien Seismisch Onderzoek en De Analyse van Resonantie in Tijdreeksen

Single-channel Marine Seismic Profiling and The Analysis of Reverberatory Sequences

Eén-kanaals Marien Seismisch Onderzoek en De Analyse van Resonantie in Tijdreeksen

(met een samenvatting in het Nederlands)

PROEFSCHRIFT

TER VERKRIJGING VAN DE GRAAD VAN DOCTOR AAN DE RIJKSUNIVERSITEIT TE UTRECHT, OP GEZAG VAN DE RECTOR MAGNIFICUS PROF. DR. J.A. VAN GINKEL VOLGENS BESLUIT VAN HET COLLEGE VAN DEKANEN IN HET OPENBAAR TE VERDEDIGEN OP DONDERDAG 11 APRIL 1991 DES NAMIDDAGS TE 12.45 UUR

DOOR

THOMAS MARTIN McGEE

GEBOREN OP 3 NOVEMBER 1939 TE MISSOURI

PROMOTOR: PROF. DR. K. HELBIG

CIP-GEGEVENS KONINKKLIJKE BIBLIOTHEEK, DEN HAAG

McGee, Thomas Martin

Single-channel marine seismic profiling, and the analysis of reverberatory sequences/ Thomas Martin McGee. - [Utrecht: Instituut voor Aardwetenschappen der Rijksuniversiteit Utrecht]. - (Geologica Ultraiectina, ISSN 0072-1026 ; no. 78)
Proefschrift Utrecht. - Met lit. opg. - Met samenvetting in het Nederlands.
ISBN 90-71577-28-7
Trefw.: seismologie / tunnelbouw.

for my family

Contents

Samenvatting

Eén-kanaals metingen worden reeds jaren gebruikt voor marien seismische profielen om de dikte en samenstelling van ongeconsolideerde en semi-geconsolideerde sedimenten in met water bedekte gebieden te bestuderen. Als de reflekties digitaal worden opgenomen is het theoretisch ook mogelijk enkele van hun fysische eigenschappen te schatten. De mogelijkheid om dergelijke schattingen te kunnen vaststellen zou een middel vormen om mariene bodemsoorten te bepalen en een waardevolle bijdrage in een samenhang, variërend van geotechnische en technische studies tot het in de gaten houden van bezinking van afvalwater-stoffen. Met dit doel worden in dit proefschrift de digitale opname en verwerking besproken van bijna zero-offset mariene reflectie gegevens.

Onder geschikte condities kunnen één-kanaals mariene profielen een beeld geven van de zeebodem tot honderden meters dik, terwijl een resolutie in de orde van een meter of minder behouden blijft. Een dergelijke afbeelding bevat niet alleen de primaire reflecties maar ook de multipels. Deze multipels verschijnen in de tijdserie als een golfpatroon dat zich herhaalt, en dikwijls interfereren met, of ten onrechte worden beschouwd als primaire reflekties. Om die reden worden multipels gewoonlijk beschouwd als ruis en wordt met veel moeite gepoogd ze te onderdrukken, vaak met weinig succes. De stelling die hier geponeerd wordt is, dat zelfs als het niet praktisch haalbaar is om de multipels uit een data-set te verwijderen, het toch nog mogelijk is om multipels te gebruiken als bron van informatie.

Voorbeelden van multipels die zijn waargenomen in industriële waterwegen worden gepresenteerd. Een theorie wordt ontwikkeld die laat zien hoe de verkregen informatie betreffende akoestische impedantie-overgangen en absorptie-coëfficienten besloten ligt in de mate van demping en de verandering van golfvorm tussen opeenvolgende golfreeksen in de tijdserie. Het is bekend dat het gebruik van bepaalde veld-technieken tot doel heeft de de identificatie van primaire reflekties en multipels te vereenvoudigen. Er van uitgaande dat deze technieken worden toegepast, wordt een wiskundig model ontwikkeld dat als kader dient voor de analyse. Een deterministisch 'dereverberatie'-filter wordt vastgesteld, dat gebruikt kan worden om multipels te onderdrukken zodra schattingen van fysische eigenschappen verkregen zijn. Het effekt van dit filter wordt toegelicht aan de hand van synthetische voorbeelden en het resultaat van zo'n 'dereverberatie'-filter wordt in detail beschouwd. Knelpunten worden besproken en er worden conclusies getrokken.

Summary

Analogue recordings of single-channel marine seismic profiles have been used for years to study the thickness and configuration of unconsolidated and semiconsolidated sediments in water-covered areas. If the signals are recorded digitally, it is theoretically possible to estimate some of their physical properties as well. The ability to make such estimates would constitute a means of remotely classifying marine soils and would be a valuable asset in contexts ranging from geotechnical and engineering studies to the monitoring of effluent accumulation. Toward such an end, this dissertation considers the digital recording and analysis of near-to-zero-offset marine reflection data.

Under proper conditions, single-channel marine profiles can image sea-floor soil hundreds of metres thick while retaining resolution on the order of a metre or less. Such an image contains not only primary reflections but also multiple reflections. These multiples occur in reverberatory sequences of wavelets that often interfere with, or are mistakenly identified as, primary reflections. For this reason multiple sequences are usually classified as noise and much effort is spent trying to suppress them, often with little success. The thesis propounded here is that, even should it not be practical to "remove" multiple reflections from a data set, it is still possible to use sequences of multiples as a source of information.

Examples of multiple sequences observed in industrial waterways are presented. Theory is developed showing how information concerning acoustic impedance contrasts and absorption coefficients is encoded in the rate of sequence decay and the change in shape between successive wavelets. It is recognized that the use of certain field techniques serves to simplify the decoding procedure. Under the assumption that these techniques are followed, a mathematical model is developed to act as a framework for the analysis. A deterministic "dereverberation filter" is identified which would be useful for supressing multiples once estimates of physical properties have been obtained. Its effect is demonstrated on the synthetic examples and the result of such "dereverberation" is considered in detail. Points of difficulty are discussed and conclusions are drawn.

Chapter 1

Introduction

Single-channel marine seismic profiling has been successfully used for more than a quarter of a century to study unconsolidated and semiconsolidated sediments in water-covered areas. It utilizes a seismic source that is triggered periodically and a single receiver, usually a linear array of hydrophones, that produces a time trace of variable voltage referenced to the instant that the source is triggered. Its simplest application involves recording the hydrophone output on paper in a grey scale format. One trace is recorded for each triggering of the source, or shot, and traces from successive shots are recorded in adjacent positions on the paper. The result is a profile whose vertical dimension is "time-after-the-shot-instant", herein called record time, and whose horizontal dimension is measured in distance between shots. The grey scale format accurately displays the record times of the onset of seismic wavelets but gives only a rough indication of their amplitudes. Thus it is not uncommon to be able to observe the configuration of geologic features in great detail but not to be able to determine the relative amplitude, or even the polarity, of individual wavelets. The result is that the amplitude and phase information present in the data is usually disregarded. Since such profiles often represent a principal source of data for purposes such as engineering design and environmental assessment, there is some impetus to make better use of the information in them. This thesis is concerned with using seismic amplitude and phase to obtain estimates of the reflection coefficients at submarine soil interfaces and, in favorable situations, of the effect of seismic absorption within soil units. Toward that end, the digital recording and analysis of single-channel marine seismic data are considered in detail.

Digital technology has been widely applied to seismic reflection profiling for hydrocarbon exploration since 1961. Many techniques of data processing have been developed which are highly successful in that context. Often, however, the same techniques are found to be not very useful when applied to single-channel marine data. The extension from exploration data with dominant frequencies in the range of tens of hertz to high-resolution data with frequencies on the order of kilohertz seems to be nontrivial. A major difficulty is associated with the fact that high-resolution data do not always satisfy certain assumptions that are basic to the methods devised for the exploration data, the most prominent examples being the assumptions of *statistical stationarity* and *minimum phase*. This means that processing techniques for engineering or environmental use often must be developed without the benefit of the large body of experience associated with hydrocarbon exploration. For that reason the following discussion is pursued on a rather basic level and digresses at times to consider details that would be taken for granted in a hydrocarbon exploration context. In an effort to avoid obscuring

the mainstream of discussion, many such details are presented in separate chapters and appendices. The intention is that the result be complete in regard to all salient aspects and that no assumptions be made without justification.

Under proper conditions, single-channel marine profiles can image sea-floor soil hundreds of metres thick while retaining resolution on the order of a metre or less. Such an image contains not only primary reflections but also multiple reflections. These multiples occur in reverberatory sequences that often interfere with, or are mistakenly identified as, primary reflections. For this reason multiple sequences are usually classified as noise and much effort is spent trying to suppress them, often with little success. However, even when it is not practical to "remove" multiple reflections from a data set, it is still possible to use sequences of multiples as a source of information. In the case of some submarine soils that are so sensitive to mechanical disturbance that they cannot be sampled without altering their *in–situ* properties, these sequences may represent the only source from which information concerning those properties is available.

The information in a multiple sequence is contained in the changes between successive seismic wavelets. Information concerning the magnitudes of reflection coefficients is encoded as the rate at which wavelet amplitude decays. Whether the coefficients are positive or negative is indicated by the relative polarity of successive wavelets. Progressive changes in wavelet shape are the result of frequency-dependent absorption in the materials through which the wavelet propagates. Since the information is associated with relative changes within a sequence, its extraction is not strictly dependent on knowledge of the source wavelet. Rather, it depends on an ability to identify wavelets associated with particular sequences of multiples and to compare their amplitudes and phases. This requires a thorough understanding of the temporal structure of the data. The choice of field technique is very important in this regard because the structure of the data can be greatly simplified by following certain procedures when the data are recorded. The identification and comparison of wavelets can then be done by modelling the data in a way that exploits those simplifications. Stochastic modelling methods that rely on data being statistically stationary often are not effective when used with high-resolution data. For that reason, the development here favors a more deterministic approach to the modelling and chooses to accomplish it in the time domain.

In the simplest reverberatory situation, that of plane-wave propagation and no absorption, a one-dimensional model is sufficient if the seismic reflectors exhibit little dip, if they are smooth enough that the wavelengths comprising the signal are reflected specularly and if recording is done using approximately zero-offset field geometry so that the direction of propagation is nearly perpendicular to the reflectors. Sequences of multiple wavelets then exhibit a temporal regularity that is useful for identifying wavelets within them. The amplitudes of wavelets thus identified can be compared to obtain estimates of the reflection coefficients between layers. Since the incidence is nearly normal, the estimated reflection coefficients can be assumed to be Rayleigh coefficients from which acoustic impedance contrasts are easily determined. The impedance contrasts principally indicate density contrasts because the speed of compressional propagation usually does not vary much from one sea-floor soil to another. The density of the sediments can be determined from the contrasts because the density of the top layer (water) is known.

Estimates of the density of sea-floor soils can be applied to environmental assessment. Since much single-channel profiling has been done as part of industrial development, sometimes for the express purpose of monitoring effluent accumulation, engineering geophysicists have become familiar with the appearance of high-resolution reflection data in areas where the natural sea floor has been modified by human activity. In particular, it has become known that anomalously reflective sediments are a rather common occurrence in harbours and industrial rivers. Such sediments are clearly indicated by the presence of strong sequences of multiple reflections in the data. Since the density of effluent often differs greatly from that of naturally occurring materials, an accumulation of effluent in a sediment can alter the strength of seismic reflections between it and the water or between it and adjacent sediments. Such a change of reflection coefficient affects the decay rate of multiple sequences and so it can be an indicator of effluent accumulation.

The principal difficulties encountered in the modelling of multiple sequences are associated with the effects of two processes; geometric attenuation and absorption. Both render the data nonstationary in that they cause the amplitude and phase of seismic wavelets to be dependent on distance from the source. This results in a model of more than one dimension being required. Geometric attenuation includes the effects of wave-front divergence, receiver directivity and the curvature of reflectors. Wave-front divergence is always present because the seismic source is necessarily of limited physical size and therefore produces a curved wave front which diverges as it propagates. Divergence results in nonstationarity because the power density of the wave front, and hence the amplitude of the seismic pulse, decreases as a function of distance from the source. For seismic wavelengths that are very large compared to the dimensions of the source, such as those produced by an airgun, the curvature of the wave front is approximately spherical and the rate of amplitude loss can be considered to be independent of frequency. For shorter wavelengths, comparable to or less than source dimensions, the curvature is less and the rate of amplitude decrease is less but can be dependent on frequency. The frequency-dependent directivity of a "boomer" source is an example of this. Thus, when modelling broad-band data, the geometrical spreading of the wave front may have to be considered to be a function of frequency with low frequencies being subject to more attenuation per unit distance than are high frequencies. A similar geometric effect is associated with the size and shape of the receiver. In practical situations, the overall effect of geometric attenuation can be so complicated that it is more accurately measured than calculated.

Absorption is related to inelastic behavior of the medium through which the seismic wave propagates. It is quantified in terms of power lost during each cycle of the seismic signal. The total loss experienced during propagation over a certain distance depends on the number of seismic wavelengths that the distance represents. In this way absorption also establishes a relationship between seismic amplitude and distance from the source and thereby results in nonstationarity. It is known that absorption depends on the type of material through which propagation occurs, but opinions vary concerning the mechanism by which it occurs, and whether or not the loss per cycle is a function of frequency. If it is, there seems to be less loss per cycle at lower frequencies than at higher. Futterman (1962) argues that this must be the case for arbitrarily low frequencies if the theory of wave propagation is to be linear. At more moderate frequencies, however, the loss per cycle seems to be constant. In either case, high

frequencies experience more absorption per unit distance than do low frequencies. This effect is opposite to the effect of frequency-dependent geometric attenuation and gives rise to the possibility of the two effects masking each other. Also, it is theoretically possible that the effect of absorption is strongest near some particular frequency or set of frequencies. Meissner and Theilen (1986) discuss this and present evidence for such behavior in water-saturated soils, suggesting that the effect might be exploited for the acoustic determination of marine soil types.

This thesis is founded on the fact that reverberatory sequences of multiple events have been observed on paper recordings of single-channel marine seismic profiles. The observations include sequences which are not confined to the water layer and therefore may be expected to contain information concerning the sediments within which they reverberate. The possibility of recovering this information is considered to justify the development of a theory for analyzing such sequences. It is apparent from the outset that digital recording is required and that it entails considerations that go beyond what is common practice in hydrocarbon exploration. Also, it is recognized that the use of certain field procedures serves to simplify subsequent analysis. Under the assumption that these procedures are followed, a mathematical model is developed to act as a framework for the analysis. A point of difficulty is the accounting for geometric attenuation. This is discussed thoroughly and a scheme devised for empirically measuring the effect of geometric attenuation from a data set recorded for the purpose. An example is then given of estimating reflection coefficients from real data, taking the geometric effect into account. The measurement of absorption is also discussed, and nominally realistic examples of modelling absorption are presented. Synthetic reflectivity sequences corresponding to these models are shown. A deterministic "dereverberation filter" is identified which may be convolved with a reflectivity sequence to suppress multiples. Its effect on the synthetic examples is demonstrated and the result of such "dereverberation" is considered in detail. Conclusions are drawn.

Chapter 2

Observations of Reverberatory Sequences on Single-channel Profiles

Single-channel marine seismic profiles have traditionally been black-and-white recordings of the polarity of the hydrophone output voltage on paper. Although little quantitative information can be extracted from such records, the presence of reverberations is obvious on them, and they are useful for becoming acquainted with the phenomenon. Toward that end, several profiles on which reverberatory sequences can be observed are presented below.

The profile shown in fig.1a crosses the Saint Clair River from Sarnia, Ontario, to Port Huron, Michigan. It is interesting as an example of reverberations confined to the water layer, the so-called water-layer multiples. The most salient features are depicted in the line drawing of fig.1b. The event near 5 ms record time is the direct arrival from the source to the hydrophone array. The time of its onset varies by about ±0.4 ms because the distance from source to the nearest hydrophone in the array is not constant. This is due to the current in the river. Since the speed of compressional propagation in water is about 1500 metres per second, the source/receiver offset distance is indicated to be 7.5±0.6 m. The concave downward event near the center is the reflection from the top of a railway tunnel that passes beneath the river. The shape of the event is somewhat distorted because the profile crosses the tunnel obliquely. The first water-layer multiple reflection from the tunnel is visible below its primary reflection. (The presence of this multiple implies that the primary event is, indeed, a reflection and not a diffraction.) After construction was completed, a detailed description of the sediment through which the tunnel passed was published in the Port Huron Daily Times (1890). That description and information from nearby bore holes make it possible to interpret fig.1a rather extensively. The dredged area on the extreme left is associated with a commercial wharf on the Canadian side of the river. The soil there is soft clay over firm clay. On the extreme right the soil is sand over firm clay. Except for those localities, the tunnel was dug entirely in firm clay containing large boulders and lenses of sand and gravel. Diffraction patterns visible on the profile are apparently caused by the boulders. The lower part of the tunnel rests in a sand layer, which explains the weak reflection located in the center of the profile immediately above the first water-layer multiple . The strong reflector beneath it is bedrock; the Detroit Sandstone. Water-layer multiple reflections from both the water bottom and the bedrock are strong enough to be visible to the fifth order or more. Water-layer multiples in the vicinity of the dredged shipping berth clearly illustrate the effect of reflector curvature on the strength of reverberations. The water bottom is convex upward in the center of the berth and concave upward on

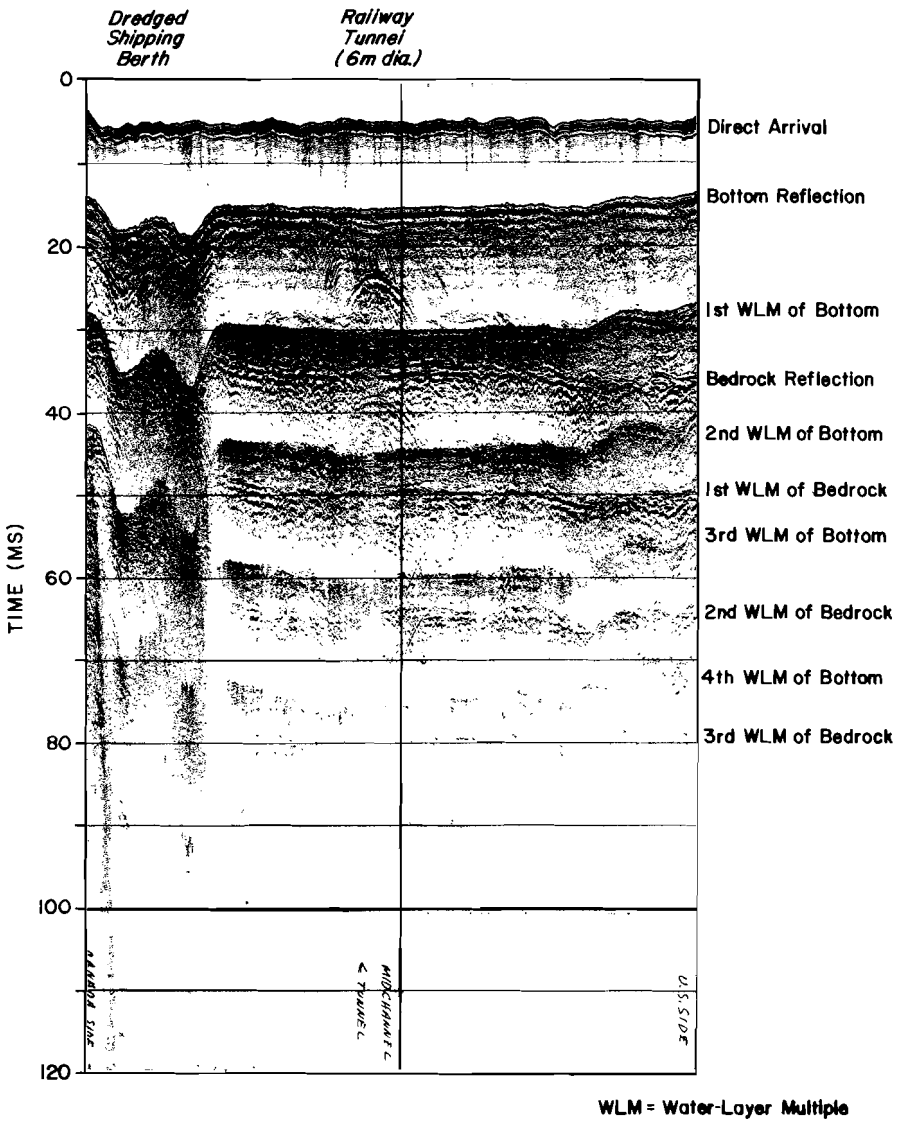

Fig.1a: Seismic profile across the Saint Clair River in the vicinity of the railway tunnel showing water-layer multiples and the effect of reflector geometry.

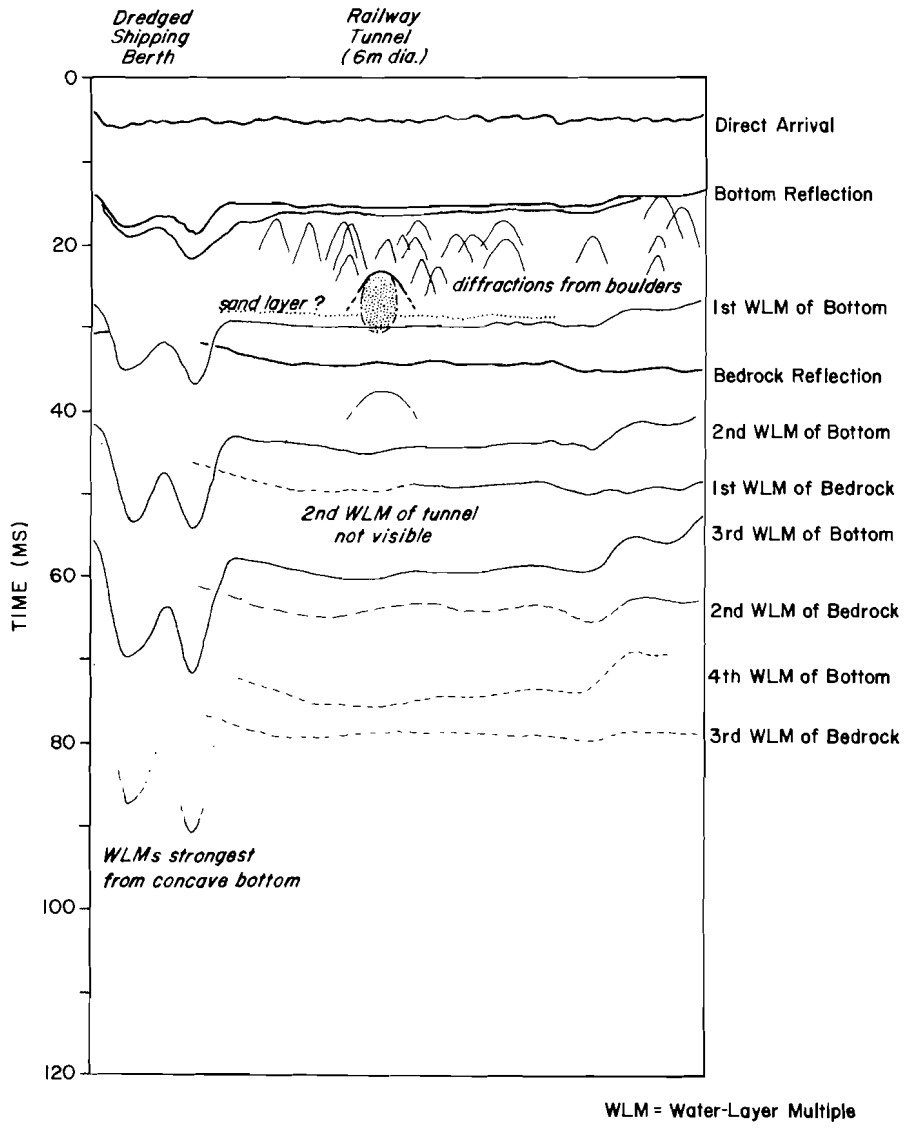

Fig.1b: Line drawing of the salient features in fig.1a.

either side of center. Reverberations are visible to higher order on the sides than in the center because the concave curvature focuses the reflected wave fronts while the convex curvature causes them to diverge. The energy density of the wave front decays more rapidly in the divergent portion than in the focused portion. A similar observation can be made concerning the reflection from the tunnel. Even though the tunnel is a strong reflector, the strength of its water-layer multiples decreases rapidly due to its curvature.

It is often possible to observe multiple sequences other than those confined to the water layer. The profile shown in fig.2 was recorded some distance downstream from the tunnel, near the river's entrance into Lake Saint Clair. No direct groundtruth is available there, but the interpretation appears to be similar to that of fig.1a, i.e. water and two layers of soil over bedrock. Again, water-layer multiples are visible to about the fifth order. In addition, two other types of multiple are faintly discernable near the bottom of the record. They can be identified on the basis of arrival time. The one with longer arrival time is a reverberation between the bedrock interface and the water surface. It is said to be a *surface-related multiple*. The one with shorter arrival time is a reverberation between the bedrock interface and the water bottom. It is said to be an *internal multiple* and is sometimes called a *pegleg multiple* because its "leg" within the soil layer is shorter than it would be if it were surface related. Both are generated by a strong acoustic impedance contrast between the lower soil and the bedrock. The impedance contrast between the two soil layers, on the other hand, is strong enough to produce a primary reflection but not to generate discernable multiples.

A profile recorded nearby is shown in fig.3. The interpretation is water and two layers of soil over bedrock, again without the benefit of groundtruth, but an important difference can be seen. Near the left-hand side of the figure there is a locality where a pegleg multiple is generated by the acoustic impedance contrast between the two soil layers. The reflectivity of the interface between the two soil layers is anomalously large there. The anomaly cannot be a geometric effect because the multiple events have no curvature. Thus it is surmised that the impedance contrast between the soils is much greater at that locality than elsewhere in the vicinity.

Similar observations can be made on profiles from other portions of the river. The profile in fig.4, for example, shows several localities of strong reflectivity between the sediment layers. The portion of fig.4 immediately to the right of the vertical line is enlarged in fig.5 to show more detail. Several orders and combinations of water-layer and pegleg multiples can be identified on the basis of arrival time. (Slight differences in dip between the water-bottom reflection and the anomalous reflection have an exaggerated appearance on the higher-order events because the travel-time differences are added with each successive reverberation.) A hole drilled nearby found a soft grey clay over a firm blue clay. The interface between them was encountered within 30 cm of the depth calculated from the reflection time by assuming the speed of seismic propagation be 1500 metres per second in both the water and the upper soil. It is not apparent from the bore hole information why the multiples should decay so slowly in some places. If the anomalous reflector were concave upward, it could perhaps be due to geometric focusing. It can be seen clearly in fig.5, however, that the reflector is convex upward which would result in a faster rate of amplitude decay. The conclusion is that the impedance contrast between the two clays is anomalously large in certain localities. Since the river is heavily industrialized, there is the possibility that accumulations of

dense effluent are responsible.

Not all pegleg multiples are caused by anomalous conditions. They sometimes can be observed where the sea-floor sediments consist of a soft soil overlying a more competent material. Such a situation is illustrated in fig.6, which is a portion of an air-gun profile recorded in the Mediterranean Sea near the island of Crete. The water is more than a thousand metres deep and therefore the reverberation time in the water layer is too long for water-layer multiples to be visible in the portion of the record shown. Pegleg multiples are clearly seen, however, and can be identified on the basis of their reverberatory period. There appear to be two orders of them; one with a period equal to the travel time in the uppermost soil layer and one with a period equal to the travel time in the two uppermost soil layers.

The foregoing figures illustrate reverberatory sequences associated with various layered systems. Different sequences are seen to be dominant in different situations because the magnitudes of the reflection coefficients are distributed differently. It would be possible to estimate the magnitudes and signs of the reflection coefficients if the data were in digital form. The following development considers what that entails.

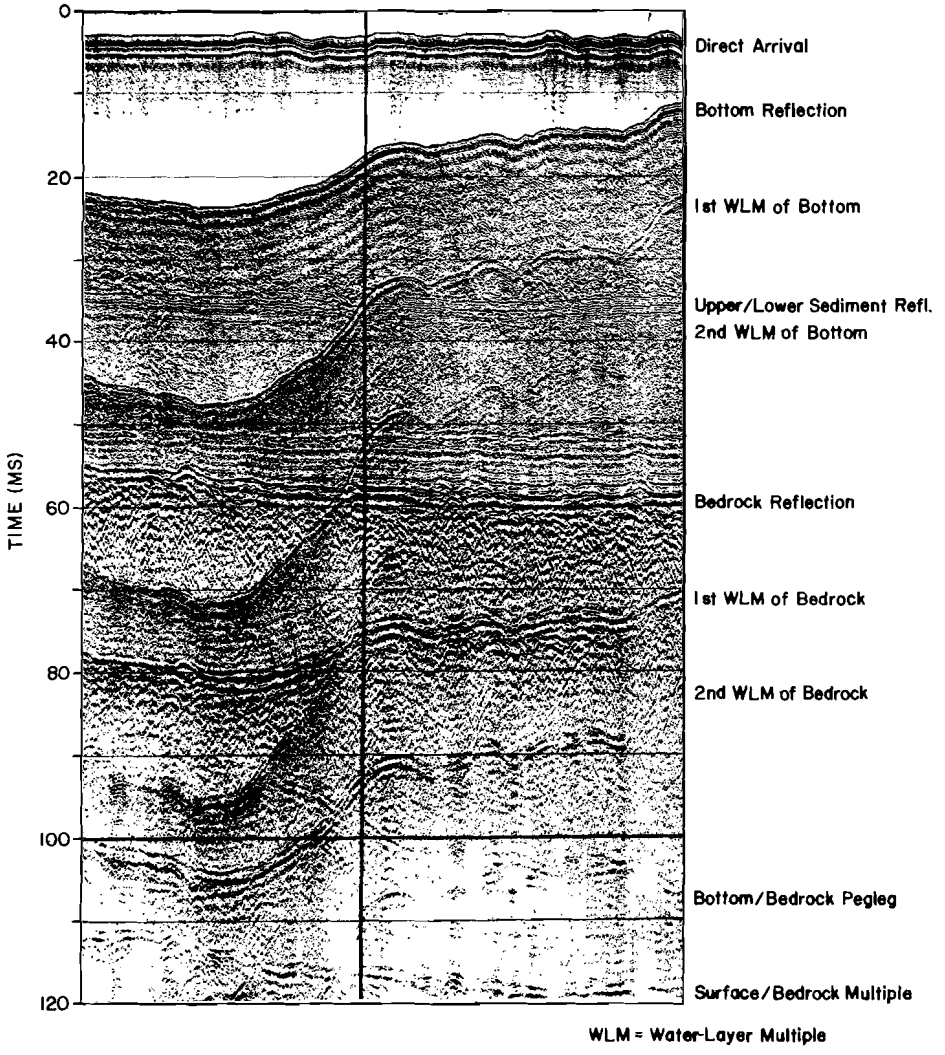

Fig.2: Seismic profile across the Saint Clair River on which it is possible to identify all types of multiples for a two-layer situation

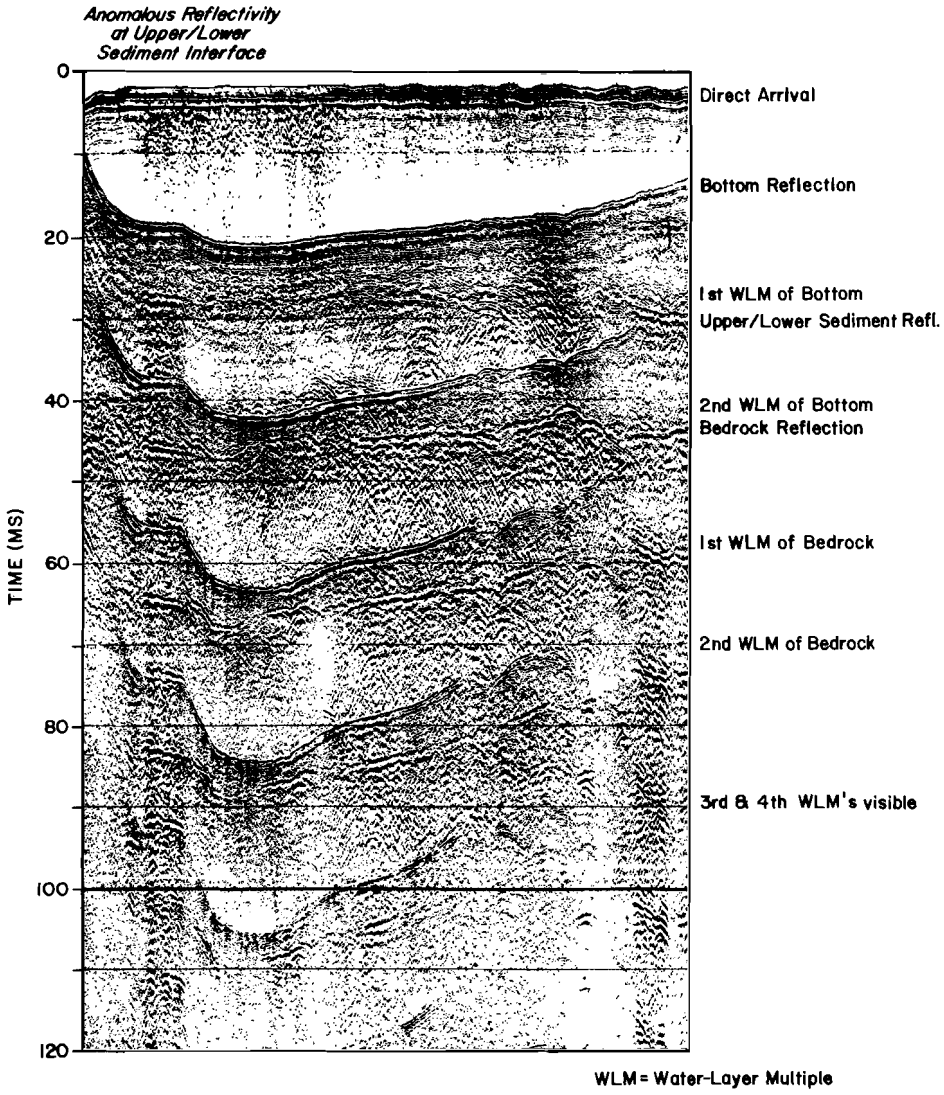

Fig.3: Seismic profile across the Saint Clair River showing anomalous reflectivity indicated by pegleg multiples.

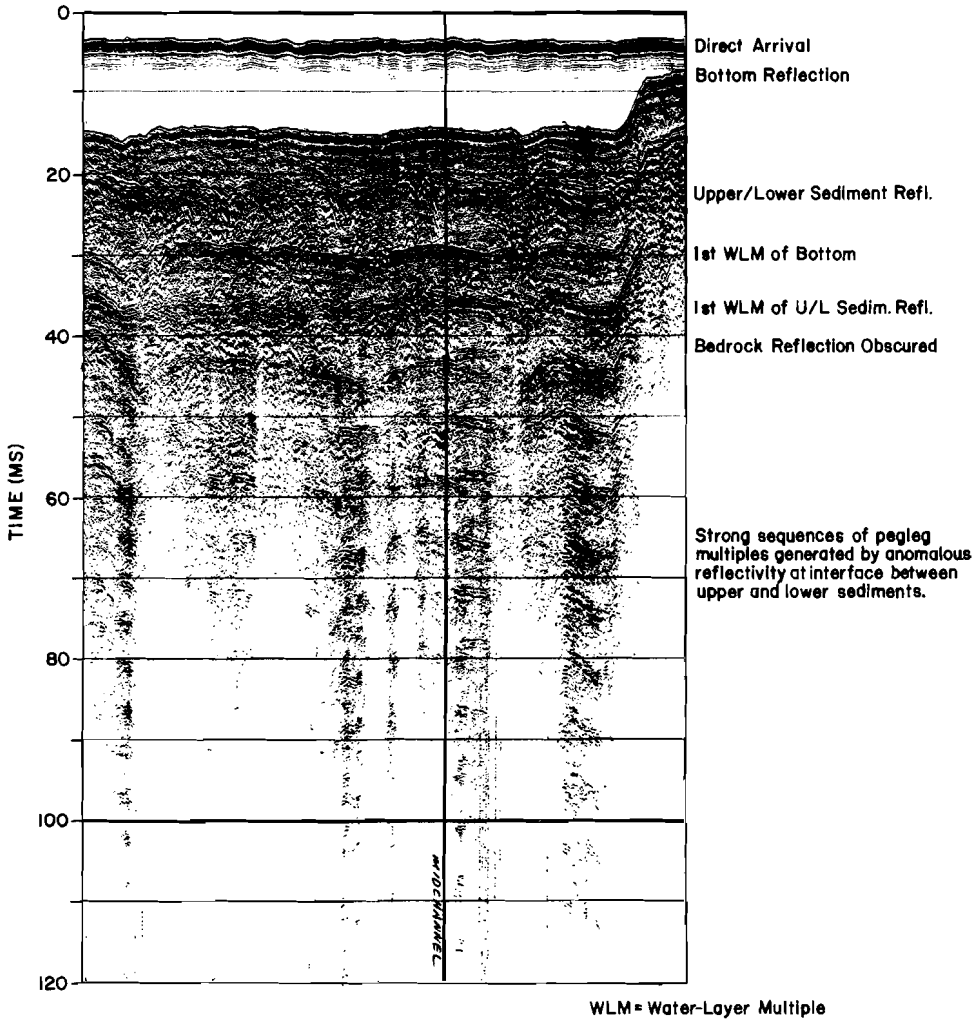

Fig.4: Seismic profile across the Saint Clair River showing numerous patches of anomalous reflectivity indicated by pegleg multiples.

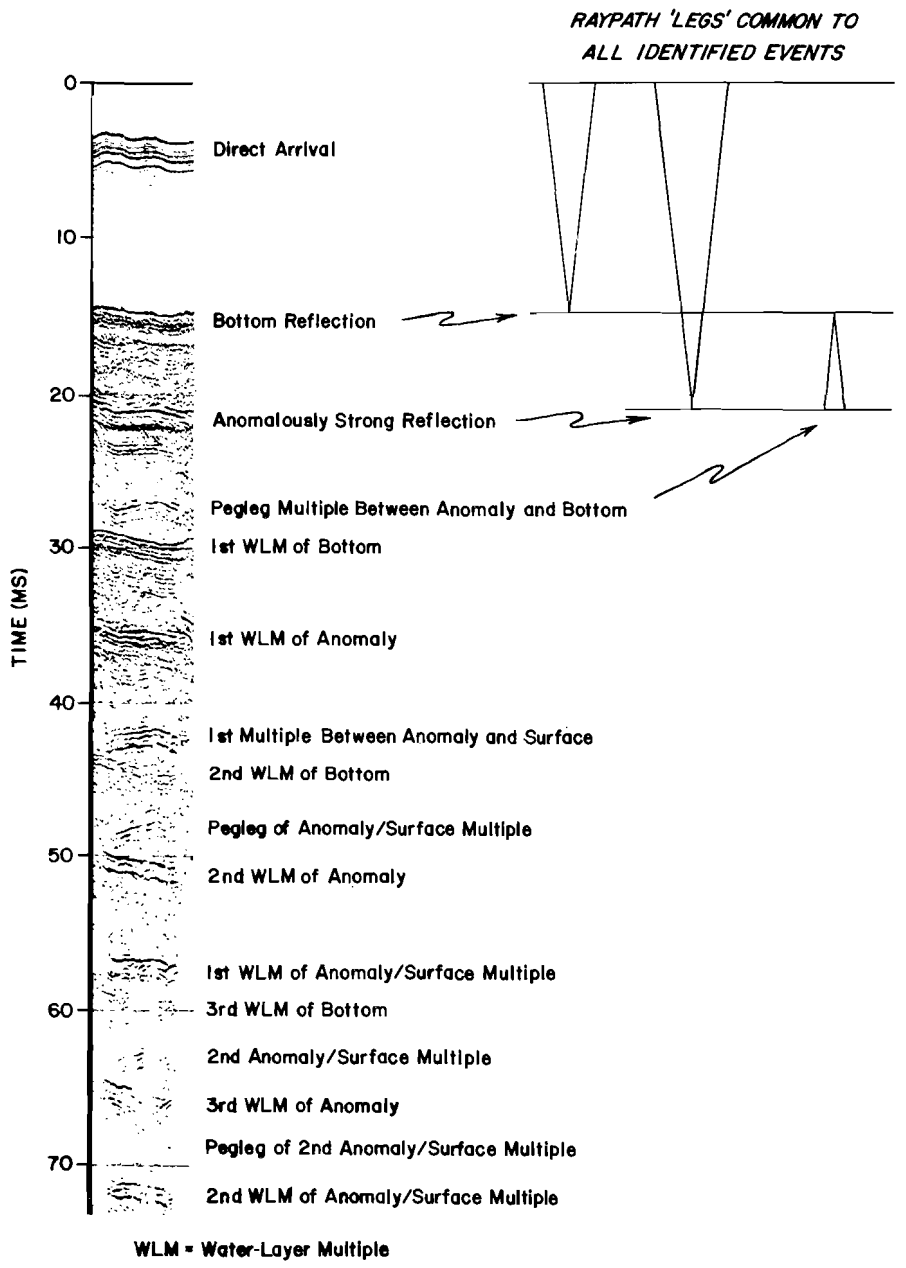

Fig.5: Enlargement of the portion of fig.4 immediately to the right of the vertical line showing the multiple sequences in detail.

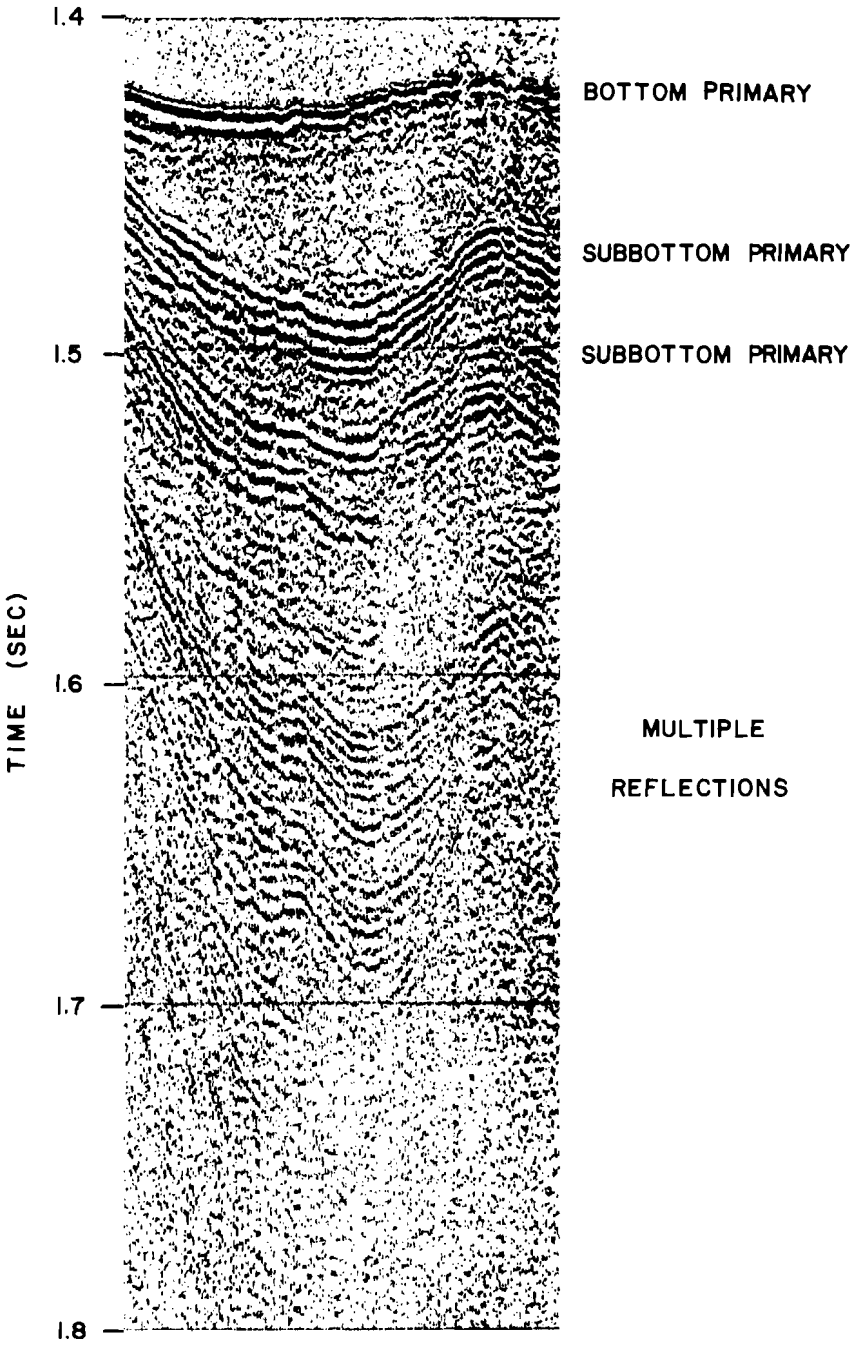

Fig.6: Seismic profile near Crete showing pegleg multiples.

Chapter 3

Acquiring Digital Data for Reverberatory Sequence Analysis

The ability to observe and analyze reverberatory sequences largely depends on the way that the data are acquired. Since the amplitudes of wavelets in a sequence can decay rapidly, the dynamic range (the ratio between maximum and minimum measurable wavelet magnitudes) of the data should be as large as possible. Assuming the quality of the recording equipment to be adequate, the dominant factor in this regard is signal-to-noise ratio. For a given signal strength, the dynamic range of the data increases as the level of noise decreases. Frequency filtering, often relied upon to discriminate between signal and noise, is usually ineffective because the two occur in similar frequency bands. In general, the most reliable way to improve signal-to-noise ratio is to decrease noise at its source. Many sources of noise contribute to the total noise level. Most may be catagorized as electrical, operational or geometrical. Several that are commonly encountered are discussed in Appendix A together with procedures for reducing their effects on data quality. In addition, there are some further considerations that serve to facilitate the analysis of reverberatory sequences. These are discussed below.

First, the water surface should be as calm as possible while recording is being done. This not only results in an improved signal-to-noise ratio but also enhances multiple sequences by minimizing the scatter of energy at the air/water interface. That interface is an almost perfect reflector for acoustic wavelengths that are large compared to the scale of disturbance it exhibits. A smooth surface coherently reflects shorter wavelengths than does a rough surface so that the high frequency cutoff of a reflected signal increases with surface smoothness. Thus it is possible for the coherent frequency band width of a multiple sequence to be significantly greater if the surface is calm than if it is choppy or stormy. The width of the coherent frequency band is especially important for observing effects of absorption.

Next, the acoustic wavelet travelling directly from source to receiver should be clearly separable from reflected wavelets. If so, the source pulse does not interfere with the sea-floor reflection and thereby contaminate the reflection sequence. This is facilitated if the seismic source is located close to the hydrophone array and if it produces a wavelet of short duration.

A small source/receiver distance is desirable for other reasons as well. It ensures that the direction of wave propagation is nearly perpendicular to reflecting interfaces so

that it is not necessary to consider the conversion of energy between compressional and shear modes of propagation. Also, in the case of parallel interfaces, it produces a nearly constant time interval between successive wavelets in a multiple sequence. Both these conditions serve to greatly simplify the mathematical form of the theoretical model. They are fulfilled exactly when there is no distance between source and receiver. That arrangement is called zero-offset recording geometry. In practice, of course, there is always some distance between source and receiver. It is sufficient if the offset distance is small enough that the angle of incidence is less than ten degrees. If the speed of propagation in the water is constant, such is the case whenever the offset distance is less than one-fifth of the water depth. In practice, it is easy to check whether or not a particular recording geometry is approximately zero offset because, when the condition is fulfilled, the record time of the direct arrival is less than one-tenth of the record time of the reflection from the water bottom.

It is very important, particularly in regard to measuring the effects of absorption, that the data be digitized at a rate that is high enough to adequately describe the shapes of individual wavelets. To a large extent, the choice of sampling rate depends on the information that the data are expected to provide. It is customarily made by appealing to the theorem stated in the following quote (Shannon, 1949):

"Let us suppose that the channel has a certain band width W in cps starting at zero frequency, and that we are allowed to use this channel for a certain period of time T. Without any further restrictions this would mean that we can use as signal functions any functions of time whose spectra lie entirely within the band W, and whose time functions lie within the interval T. Although it is not possible to fulfill both of these conditions exactly, it is possible to keep the spectrum within the band W, and to have the time function very small outside the interval T. Can we describe in a more useful way the functions which satisfy these conditions? One answer is the following:

> *THEOREM 1: If a function f(t) contains no frequencies higher than W cps, it is completely determined by giving its ordinates at a series of points spaced 1/2W seconds apart.*

This is a fact which is common knowledge in the communications art. The intuitive justification is that, if $f(t)$ contains no frequencies higher than W, it cannot change to a substantially new value in a time less than one-half cycle of the highest frequency, that is, $1/2W$."

Shannon then shows that, if $f(t)$ is a sequence of discrete samples separated by an interval of $1/2W$ time units, it can be written

$$f(t) = \sum_{n=-\infty}^{\infty} x_n \frac{\sin \pi(2Wt - n)}{\pi(2Wt - n)} \tag{3-1}$$

where x_n is the amplitude of the nth sample. He also shows that if, in addition to being band limited, $f(t)$ is exactly zero outside a time interval T, it is completely specified by its value at $2TW$ sample points. Referring to Nyquist (1928), he calls the time interval $1/2W$ "the Nyquist interval corresponding to the band W."

It is important to realize that Shannon did not prove his sampling theorem for functions that are limited in both time and frequency. He could not have done so because, as mentioned early in the quote, it is not possible for a function to be exactly zero outside both an interval of time and a band of frequency. A function limited in time is transient and a function limited in frequency is periodic. A periodic transient does not exist except as the mathematical concept of a set of isolated values that span zero area (the Paley-Wiener criterion, Appendix B). In particular, since seismic wavelets are causal (identically zero prior to their onset), they cannot be band limited. This is substantiated by Eisner (1984) who shows that a causal function represented by eq.(3-1) must be identically zero. Shannon's theorem is useful when applied to long time functions that oscillate many times within their time interval (he gives an example of a television signal lasting for an hour) but,strictly speaking, it cannot be applied to individual seismic wavelets that describe a few oscillations in a short time. Justification for doing so relies on the fact that the power spectra of seismic wavelets approach zero in the high frequency limit, as is true of any finite energy wave form (Robinson, 1967a). This allows a frequency band to be chosen outside of which spectral power is as small as desired. The justifying assumption is that, if sufficiently small, the power outside the band can be considered to be zero. Since the power spectrum is a density function, it is the integral of the portion of the spectrum outside the band that should be "sufficiently small" compared to the integral of the portion of the spectrum inside the band. Criteria for choosing the band remain rather ambiguous, however, because it is difficult to describe how small "sufficiently small" actually is.

It is much more straightforward to simply make the choice of digitization rate in the time domain. This may be done by appealing to the intuitive justification described in the quote. Thus, paraphrasing Shannon, digitization should be done at a rate high enough that the seismic signal "cannot change to a substantially new value in a time less than" the digitizing interval. The choice of rate then relies on the meaning of the term "substantial" in the particular situation being considered. This can be illustrated as follows. Wavelets produced by a plasma gun and a boomer source are shown in fig.7. The rise time of the plasma gun pulse is about 0.1 ms and that of the boomer pulse somewhat less. If it is supposed that one-fifth of the onset magnitude is a "substantial" change, a digitization rate of 50 kHz is indicated. A suite of boomer pulses fired randomly and digitized at a 50 kHz rate is shown in fig.8. The onset times are random so that the location of sample points relative to pulse onset is different for each. It can be seen that the shape of the principal excursion changes from pulse to pulse; some being "squared off" and others "pointed". The variation in shape is a form of noise that has an increasing effect toward the higher-frequency portions of the pulse spectra. If the accuracy of high-frequency information is significant, as it would be for observing effects of absorption, it would be better to consider one-tenth of the onset magnitude to be a "substantial" change and to digitize at a rate of 100 kHz. On the other hand, if accuracy at high frequencies is less important, such as when simply estimating reflection coefficients, one-half or more of the onset magnitude might be considered "substantial" and a rate of 20 kHz or less be adequate. Of course, after a digitizing rate has been selected, the analog signal should be passed through an appropriate antialias filter before being digitized.

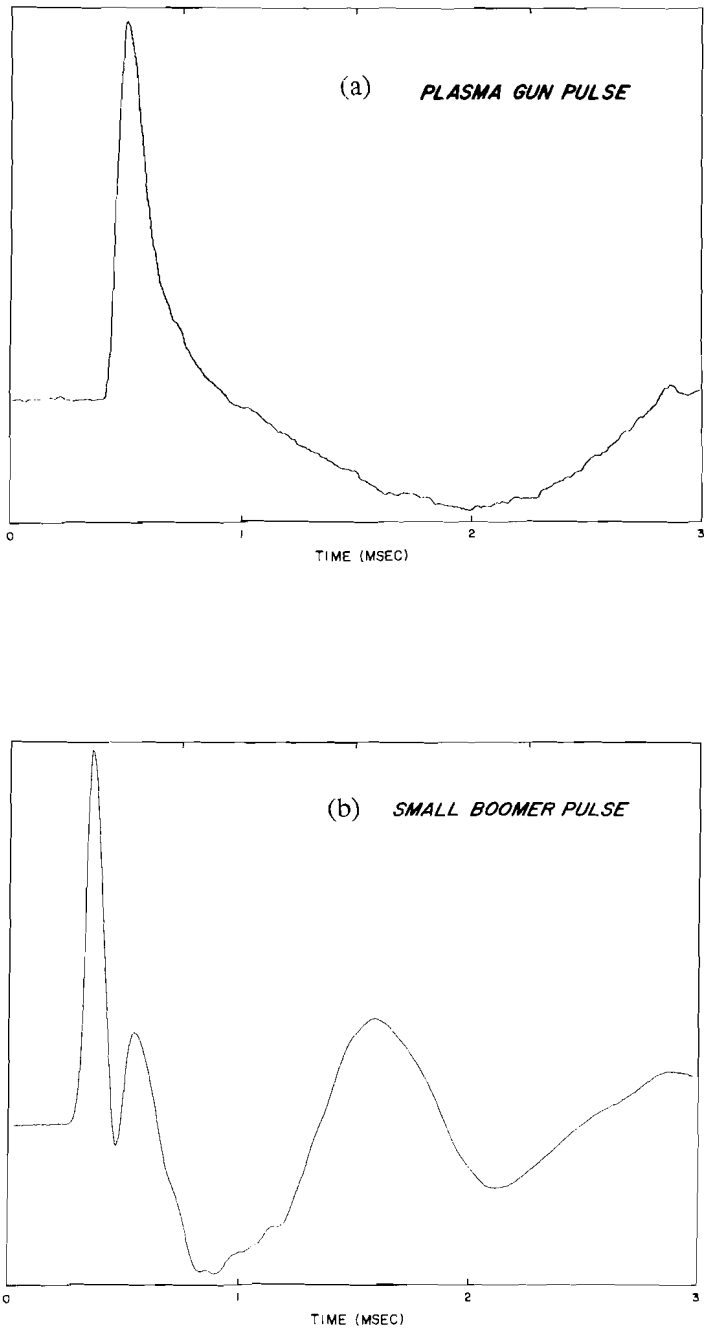

Fig.7: Typical high-resolution marine seismic pulses; (a) plasma gun pulse and (b) small boomer pulse.

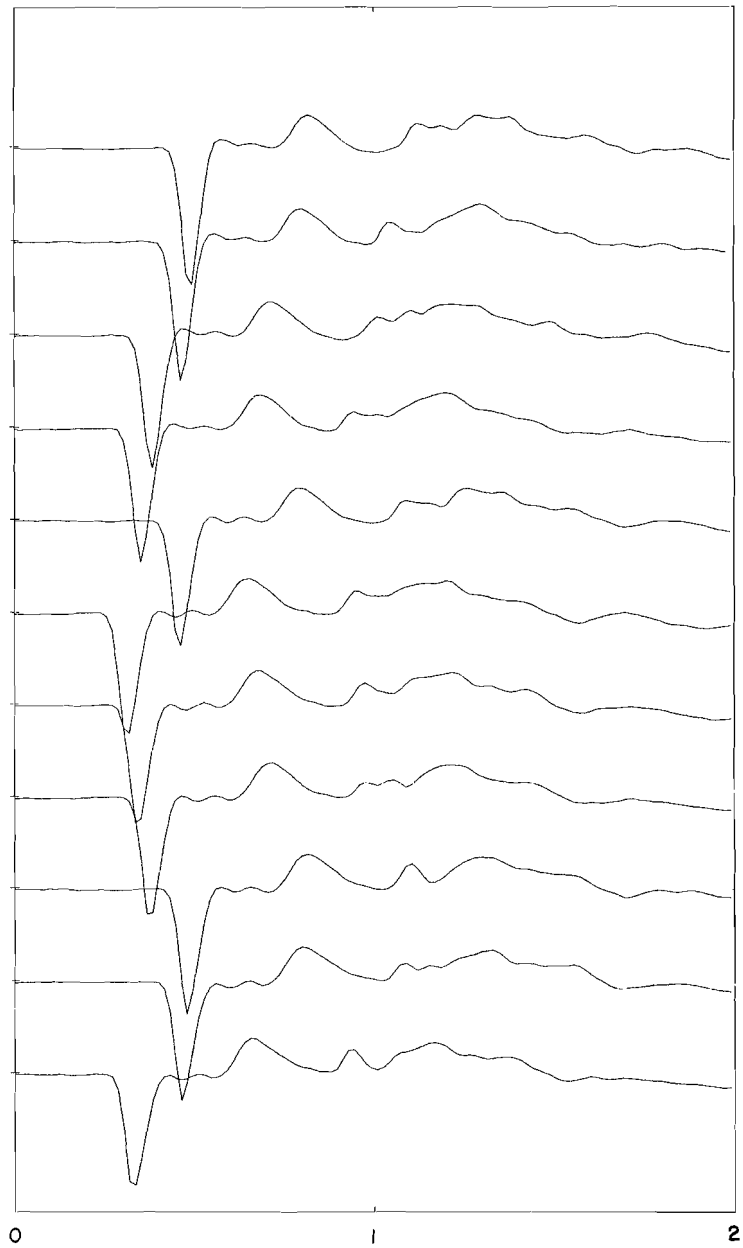

Fig.8: Suite of randomly triggered boomer pulses digitized at a 50 kHz. rate. Note that the representation of the principal excursion varies considerably.

Finally, the length of data digitized must be adequate for the needs of reverberation analysis. Since seismic signals decay in time, an effective limit to their length is always imposed by the digital dynamic range (the number of bits available for recording). In the absence of noise, this limit is reached when the magnitude of the signal decreases below the level of the least significant bit and further digitization is vacuous. Otherwise, it is best if digitization continues until the signal is lost in the noise. However, practical considerations (such as available storage space or repetition rate) often require that digitization stop after a fixed amount of time regardless of signal magnitude. In the context of harmonic analysis of brain waves, Wiener (1958) suggests that the length of data be 100 times the longest period of interest. Others would consider that more than sufficient; a rule-of-thumb common in oil exploration requiring only a factor of ten. Even this may be unrealistically large because it is not common to observe as many as ten wavelets in a reverberatory sequence. Generally speaking, it is desirable to digitize as many reverberatory wavelets as possible. Thus, if other considerations allow, digitization should continue as long as multiple reflections are observable.

Chapter 4

Modelling Zero-offset Reflections from Sea-floor Soils

A way of analyzing multiple sequences is to model the seismograms in which they occur and determine the values of model parameters that best duplicate the observed sequences. Insofar as sea-floor soils exhibit little dip, they may be considered to be horizontal layers separated by reflecting interfaces. If all interfaces are located in the Fraunhofer far field of the seismic receiver (as discussed in Appendix A) and if the recording geometry is approximately zero offset, the propagation of recorded waves is nearly vertical. It can then be assumed that the reflection seismogram represents only two directions of propagation; up and down. Such a seismogram is said to be bidirectional and, if the waves are plane waves, can be modelled in a single dimension. A plane-wave model is not very realistic, however, because real seismic sources produce curved wave fronts that diverge as a function of range (distance along the ray path). The effect of wave-front divergence is to change the amplitude, and possibly the shape, of seismic wavelets. For a bidirectional seismogram representing propagation along the axis of source symmetry, the effect can be expressed as a function of speed of propagation and record time with, possibly, some frequency dependence to account for changes in wavelet shape. The function is not necessarily single valued because the speed of propagation may vary with distance from the source and cause wavelets at more than one range to be recorded at the same time.

It is a common procedure to first "correct" a seismogram for wave-front divergence and then model it with a plane-wave model. The results are not always satisfactory, however, because the correction tends to distort individual wavelets (Ziolkowski, 1984) and can thereby have an adverse effect on parameter estimates. The cause of the distortion can be explained by considering the seismogram to be associated with more than one temporal dimension. In the simplest (bidirectional) case, two "kinds" of time are involved; record time which measures the occurence of wavelets relative to the origin of the seismogram and "interwavelet time" which measures the duration of a wavelet relative to its onset. Range is a function of record time for given speeds of propagation and wavelet shape is a function of "interwavelet time" for a given frequency dependence. The two "kinds" of time are independent if wavelet shape does not depend on range, i.e. if there is no absorption and the speed of propagation does not depend on frequency. It is difficult to distinguish between the two on a seismic record, however, especially when wavelets overlap. If data are "corrected" for divergence effects on the basis of record time alone, without considering wavelet duration, different "corrections" are applied at different "interwavelet" times within the same wavelet and thus distort its shape. The difficulty can be made explicit, at least formally, by expressing the model in both temporal dimensions.

It is customary to describe digital reflection seismograms in terms of three types of sequences; a "wavelet" sequence describing the generation and evolution of the seismic pulse, an "arrival" sequence describing the distribution of seismic pulses in space and time and a "noise" sequence describing all recorded amplitudes that are not described by the other two sequences. In order to distinguish between the two "kinds" of time, the "wavelet" sequence must be considered to be a "suite of sequences". If the time indices t and τ are sequential sets of nonnegative integers and the symbol * denotes convolution, a bidirectional seismogram with spreading wave front can be expressed as

$$s_{t,\tau} = x_{t,\tau} * y_t + n_t \tag{4-1}$$

where $x_{t,\tau}$ describes the suite of wavelets, y_t describes the distribution of wavelet arrivals, n_t describes the noise sequence, t indexes record time and τ indexes time after wavelet onset. The indices represent equivalent measures of time. Without loss of generality, the unit of time can be taken to be one index interval.

The shapes of wavelets present in a seismogram are broadly determined by the particular seismic source, but vary from near-field shapes in the immediate vicinity of the source to a far-field shape at infinite range from the source. The near field is defined to be that vicinity about the source within which wave-front divergence is characterized by frequency-dependent changes in wavelet shape. Outside the near field, seismic wavelets can be modelled as scaled versions of the far-field wavelet. Thus, if near-field ranges are associated with record times $t < t_{near\ field}$, the "suite of wavelet sequences" can be written

$$x_{t,\tau} = g_t\, w_\tau \qquad \text{for } t > t_{near\ field} \tag{4-2}$$

where the geometric attenuation factor g_t is independent of τ and the far-field wavelet w_τ is independent of t. The factor g_t is defined for ranges greater than or equal to a reference range outside the near field and is often expressed as the power law

$$g_t = \left[\frac{\text{reference range}}{\text{range at time } t}\right]^\gamma . \tag{4-3a}$$

The value of γ is nonnegative, $\gamma = 0$ being the plane-wave case, and therefore $0 < g_t \leq 1$ for ranges greater than the reference range. In the special case of a medium in which the speed of propagation is constant,

$$g_t = \left[\frac{(ct)_{reference}}{ct}\right]^\gamma = \left[\frac{t_{reference}}{t}\right]^\gamma \qquad \text{for } t \geq t_{reference} > t_{near\ field} . \tag{4-3b}$$

where c is the speed of propagation. In the very special case of a point source in a constant-speed-of-propagation medium, the geometry of the wave front is spherical,

$$\gamma = 1 \quad \text{and} \quad g_t = \frac{t_{reference}}{t} \qquad \text{for} \quad t \geq t_{reference} > t_{near\ field} \ . \tag{4-3c}$$

This is approximately valid in situations when signal wavelengths are long compared to source dimensions (so that there is effectively a point source) and the acoustic speed in sea-floor soils does not vary significantly from that in water. If signal wavelengths are comparable to source dimensions, the value of the exponent must be determined. In such cases it can be simpler to measure γ empirically than to deduce it from theoretical considerations. This is often done by "calibrating" the spacial characteristics of the field configuration being employed. As will be discussed later, for zero-offset marine seismograms it is possible to estimate γ directly from data recorded for the purpose.

The "arrival" sequence in eq.(4-1) describes the onset times of direct and reflected wavelets. It will be seen later that it also describes changes in wavelet shape due to absorption. Thus, if absorption is present, the arrival sequence is a function of both record time and "interwavelet time". For the present, however, it will be considered to be a function of record time only. If so, direct and reflected waves can be separated by writing

$$y_t = \delta_t + \xi_t \tag{4-4}$$

where $\delta_0 = 1$, $\delta_t = 0$ for $t \neq 0$ and ξ_t is the reflectivity of the medium. If the onset of reflected energy occurs at $t = t_r$ the reflectivity sequence is zero for $t < t_r$. Its first element vanishes in any case ($\xi_0 = 0$) because reflected waves cannot arrive before at least one unit of time has elapsed. Substituting eq.(4-4) into eq.(4-1),

$$s_{t,\tau} = x_{0,\tau} + x_{t,\tau} * \xi_t + n_t \tag{4-5}$$

where $x_{0,\tau}$ is the direct (near-field) wavelet. If the duration of the direct wavelet is short enough that it does not interfere with the onset of reflected waves, the direct wavelet vanishes for $\tau \geq t_r$ and eq.(4-5) can be partitioned into the pair of equations

$$s_{t,\tau} = x_{0,\tau} + n_t \qquad \text{for} \quad t < t_r \tag{4-6a}$$

and

$$s_{t,\tau} = x_{t,\tau} * \xi_t + n_t \qquad \text{for} \quad t \geq t_r \ . \tag{4-6b}$$

The first of the pair may be disregarded in the present context because reflected waves occur only in the second. If $t_r > t_{nf}$, eq.(4-2) is valid and can be substituted into eq.(4-6b) to give

$$s_{t,\tau} = g_t w_\tau * \xi_t + n_t \qquad \text{for} \quad t \geq t_r \ . \tag{4-7a}$$

or, since g_t is constant with respect to τ,

$$s_{t,\tau} = w_\tau * g_t \xi_t + n_t \qquad \text{for } t \geq t_r \ . \tag{4-7b}$$

In this form, the effect of geometric attenuation is a time-dependent scaling of the reflectivity sequence. Such a model would be used with uncorrected data.

The "noise" sequence is usually described statistically but can also have deterministic components. Rarely is it known well enough for accurate modelling. Thus it is usually accepted as the amplitude level below which results are expected to deteriorate. As discussed previously, it is best to reduce the level of noise at its source. The importance of this can be seen in following way. Since a seismic wavelet is causal its spectrum does not vanish over any range of frequencies and its inverse can, in principle, be determined. It can be done by a deterministic procedure if the far-field wavelet is known explicitly, or by a statistical procedure if the wavelet is minimum phase. In either case, the inverse wavelet w_τ^{-1} is a sequence that can be convolved with both sides of eq.(4-7b) to obtain

$$w_\tau^{-1} * s_{t,\tau} = \delta_\tau * g_t \xi_t + w_\tau^{-1} * n_t \qquad \text{for } t \geq t_r \ . \tag{4-8}$$

This is said to be the "spectrally whitened" seismogram. It is independent of τ in the absence of noise ($n_t \equiv 0$) because the wavelet "collapses" to a delta function of no duration and renders the concept of "interwavelet time" irrelevent. The "whitened" seismogram may then be "corrected" for divergence of the wave front and eq.(4-8) written

$$\frac{w_\tau^{-1} * s_{t,\tau}}{g_t} = \xi_t \qquad \text{for } t \geq t_r \ . \tag{4-9}$$

This result is strictly correct only in the absence of absorption. Theoretically, data should be distorted by the application of divergence "corrections" in the presence of absorption because, as seen later, absorption operators are described in terms of "interwavelet time". This distortion is not very great in the illustrative examples of Chapter 11.

Spectral "whitening" fails to be feasible if the noise level is not negligible, because the spectral magnitude of the inverse wavelet is large at frequencies in which the wavelet is deficient, and convolving it with the noise sequence causes noise to dominate those components of the "whitened" spectrum. Thus the modelling of geometric attenuation depends on noise level. If noise can be neglected, a seismogram may be spectrally "whitened" and then "corrected" for geometric attenuation as in eq.(4-9), the result being modelled as a reflectivity sequence. If the noise level is appreciably high, the effect of geometric attenuation must be accounted for by scaling the reflectivity sequence as done in eq.(4-7b). The result is then convolved with the far-field wavelet to obtain a model for the reflected portion of the seismogram. In either case, the reflectivity sequence is derived from theoretical considerations.

Chapter 5

One-dimensional Wave Propagation in a System of Absorbing Layers

The acoustic response of systems of parallel non-absorbing layers has been discussed in the literature many times. One of the classic approaches to the problem, but modified to include absorption, is presented here. The derivation is basically a modification of the traditional matrix formulation of Thompson (1950) and Haskell (1953). It employs the "unit-layer" indexing convention of Goupillaud (1961) and proceeds in the manner of Sherwood and Trorey (1965) to include effects of absorption in a rather general, but realistic, way. Since the phenomenon of absorption occurs in continuous time but the modelling is done in discrete time, this involves not only describing the effects of absorption but also considering the implications of representing them digitally. As Trorey (1962) has shown, computational efficiency is improved if unit layers are gathered into blocks within which the effects of absorption can be described on average. The transmissivity and reflectivity of systems composed of such blocks have succinct z-domain expressions in which reverberatory effects of the layered structure are easily identified. The reflectivity sequence corresponds to ξ_t in Chapter 4.

Consider a medium comprising N horizontal layers situated between two halfspaces, as illustrated in fig.9. Let a particular layer be designated by an integer k, $0 \le k \le N+1$, where $k=0$ corresponds to the upper halfspace and $k=N+1$ to the lower, and let the interfaces between layers be denoted by integers $0 \le i \le N$. Also, let the thickness of each layer be such that, for propagation normal to the interfaces, the time of propagation through the layer is one time unit. In this way, the time at which a normally propagating wave encounters each interface may be designated by an integer j. At each interface, the wave would be partially reflected and partially transmitted in such a way that the signal in any layer k at any time j could be considered to be a superposition of four possible types of waves. As illustrated in fig.10, these may be denoted

$d_{k,j}$ - a downward travelling wave immediately within the top of the layer,

$d'_{k,j}$ - a downward travelling wave immediately within the bottom of the layer,

$u_{k,j}$ - an upward travelling wave immediately within the top of the layer,

$u'_{k,j}$ - an upward travelling wave immediately within the bottom of the layer.

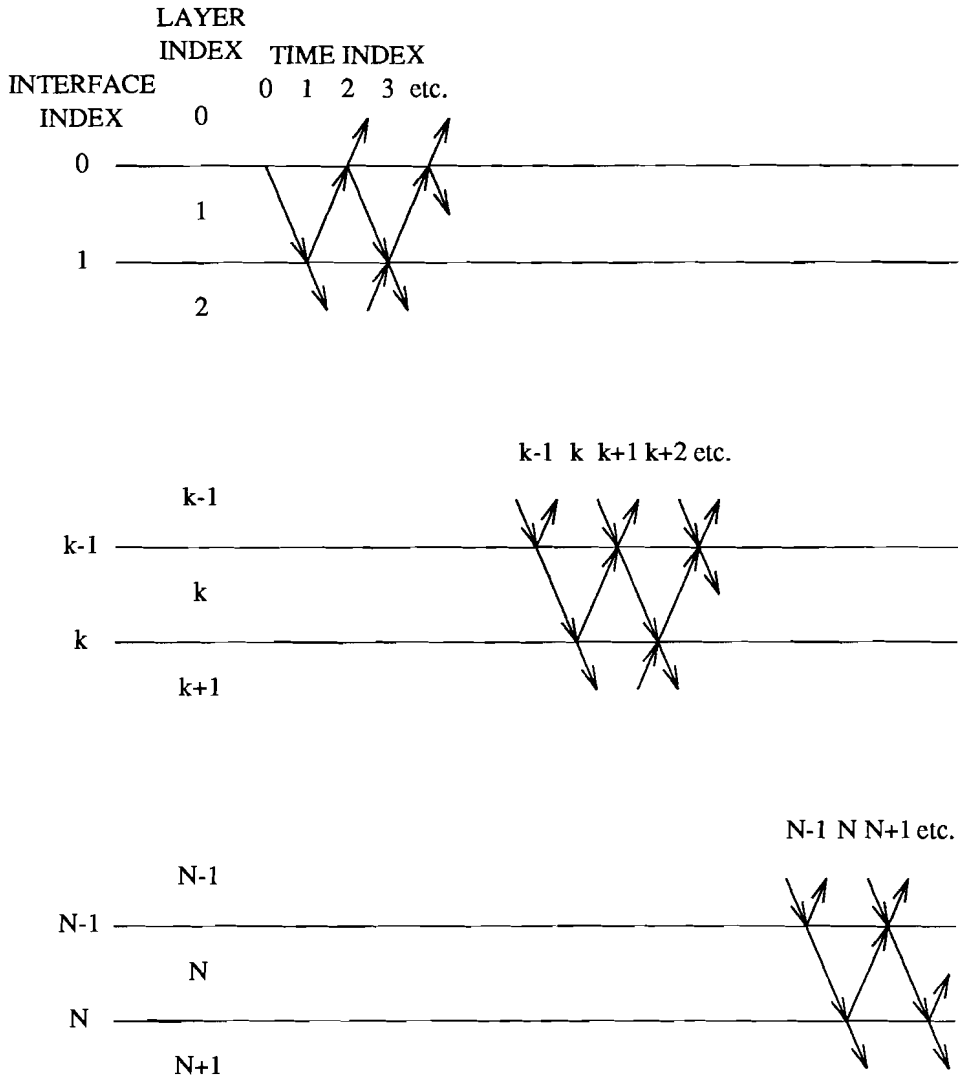

Fig.9: System of indexing for N unit layers between two halfspaces.

Suppose the incident wave is $d_{1,0}$, a downward travelling wave in the top of the first layer upper halfspace which departs from interface 0 at time 0. At time 1 this would have propagated to become $d_{1,1}$ which, upon encountering interface 1, would be partially reflected to produce $u_{1,1}$ and partially transmitted to produce $d_{2,1}$. The fourth type

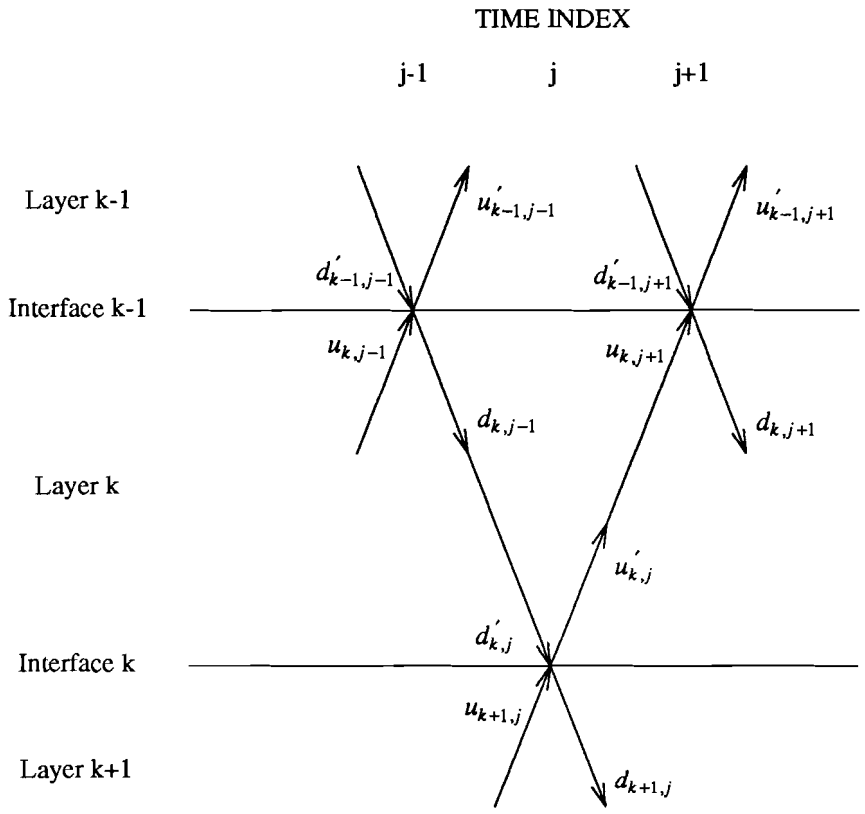

Fig.10: Wave types associated with top and bottom of a layer.

of wave at time 1, $u_{2,1}$, would not exist because no energy would be travelling upward in layer 2 at time 1. By pursuing this argument, it is found, for input $d_{1,0}$, that the waves in layer k are such that

$d_{k,j}$ exists for times $j \geq k-1$ such that $k+j$ is odd,

$d'_{k,j}$ exists for times $j \geq k$ such that $k+j$ is even,

$u_{k,j}$ exists for times $j \geq k+1$ such that $k+j$ is odd,

$u'_{k,j}$ exists for times $j \geq k$ such that $k+j$ is even.

The four wave types therefore may be represented in the z-domain as

$$D_k(z) = \sum_{j=0}^{\infty} d_{k,k+2j-1}\, z^{(k+2j-1)} \quad , \tag{5-1a}$$

$$D_k'(z) = \sum_{j=0}^{\infty} d_{k,k+2j}'\, z^{(k+2j)} \quad , \tag{5-1b}$$

$$U_k(z) = \sum_{j=0}^{\infty} u_{k,k+2j+1}\, z^{(k+2j+1)} \quad , \tag{5-1c}$$

$$U_k'(z) = \sum_{j=0}^{\infty} u_{k,k+2j}'\, z^{(k+2j)} \quad . \tag{5-1d}$$

The pattern of normal propagation within the layered system may be described in terms of these z-transforms.

As shown in fig.10, waves $d_{k,j}'$ and $u_{k+1,j}$ are incident to interface k at time j while $u_{k,j}'$ and $d_{k+1,j}'$ are departing. Thus $u_{k,j}'$ may be considered to consist of the reflected portion of $d_{k,j}'$ and the transmitted portion of $u_{k+1,j}$. Similarly, $d_{k+1,j}$ may be considered to consist of the reflected portion of $u_{k+1,j}$ and the transmitted portion of $d_{k,j}'$. This may be expressed as

$$u_{k,j}' = r_k d_{k,j}' + t_k^* u_{k+1,j} \tag{5-2a}$$

and

$$d_{k+1,j} = r_k^* u_{k+1,j} + t_k d_{k,j}' \tag{5-2b}$$

where r_k and t_k are real numbers, r_k being of unit magnitude or less. They denote the reflection and transmission coefficients, respectively, for propagation from layer k to layer $k+1$. Those in the opposite direction are denoted r_k^* and t_k^*. These expressions may be manipulated into

$$t_k d_{k,j}' = d_{k+1,j} - r_k^* u_{k+1,j} \tag{5-3a}$$

and

$$t_k u_{k,j}' = r_k d_{k+1,j} + (t_k t_k^* - r_k r_k^*)\, u_{k+1,j} \quad . \tag{5-3b}$$

Letting ρ_k and c_k denote the density and speed of compressional wave propagation in the kth layer, respectively, the reflection coefficients are given by the Rayleigh relationship

$$r_k = -r_k^* = \frac{\rho_k c_k - \rho_{k+1} c_{k+1}}{\rho_k c_k + \rho_{k+1} c_{k+1}} \tag{5-4a}$$

and the transmission coefficients are such that

$$t_k = 1 + r_k \quad , \quad t_k^* = 1 - r_k \quad . \tag{5-4b}$$

Combining eq.s(5-2), (5-3) and (5-4) yields

$$t_k d'_{k,j} = d_{k+1,j} + r_k u_{k+1,j} \tag{5-5a}$$

and

$$t_k u'_{k,j} = r_k d_{k+1,j} + u_{k+1,j} \tag{5-5b}$$

or, equivalently,

$$t_k d'_{k,k+2j} = d_{k+1,k+1+2j-1} + r_k u_{k+1,k+1+2j-1} \tag{5-5c}$$

and

$$t_k u'_{k,k+2j} = r_k d_{k+1,k+1+2j-1} + u_{k,k+1+2j-1} \quad . \tag{5-5d}$$

Multiplying by $z^{(k+2j)}$ and summing over $0 \le j \le \infty$ expresses the simultaneous equations (5-5c,d) in terms of the z-transforms (5-1a,b,c,d). They may then be written in the matrix form

$$\begin{bmatrix} U'_k(z) \\ D'_k(z) \end{bmatrix} = \frac{1}{t_k} \begin{bmatrix} 1 & r_k \\ r_k & 1 \end{bmatrix} \begin{bmatrix} U_{k+1}(z) \\ D_{k+1}(z) \end{bmatrix} \tag{5-6}$$

which is the z-domain expression for propagation across interface k.

Since the thickness of each layer is equivalent to one unit of time, propagation through a layer results in a delay of one time unit which is expressed in the z-domain by a multiplicative factor $\{z\}$. When absorption occurs in the layer it produces an attenuation of amplitude and a delay of phase that are frequency dependent and result in a change of wave-form shape. This effect may be modelled mathematically by convolving the wave form with a suitable operator. Following Sherwood and Trorey (1965), a suitable operator for any physically possible absorption law is, first of all, a function of time $a(\tau)$ that is causal, i.e. $a(\tau)=0$ for $\tau<0$, and stable, i.e. $\int_0^\infty a^2(\tau)d\tau < \infty$. The Fourier

transform of such a function exists and can be written in the polar form $|A(\omega)|\, e^{i\alpha(\omega)}$ where ω is frequency in radians per time unit. Its amplitude spectrum $|A(\omega)|$ describes the frequency-dependent attenuation and its phase spectrum $\alpha(\omega)$ describes the frequency-dependent phase delay. Dispersion occurs if $\alpha(\omega)$ is nonlinear. Futterman (1962) shows that this Fourier transform must exhibit the "crossing" symmetry $A(\omega) = \bar{A}(-\omega)$, where the bar indicates complex conjugate, if the principle of superposition of waves is to be valid. Such symmetry exists only if $a(\tau)$ is real valued. Also, if the effect of absorption does not change the polarity of the onset of propagating wave forms, $a(\tau) \geq 0$ for $\tau > 0$. This description includes an absence of absorption as the special case $a(\tau) = \delta(\tau)$ which has value one for $\tau = 0$ and is zero otherwise. Since the Laplace transform of any causal, stable, real nonnegative function has no zeros or poles in the right half of the transform plane, any suitable absorption operator is minimum phase in continuous time and, by definition, has a minimum-phase continuous-time inverse.

The duration of the continuous-time operator is infinite (extending for all positive time) but any digital representation of it is of finite length because its magnitude becomes less than the level of the least significant digital bit after a finite number of samples. Moreover, these representations are not necessarily minimum phase in discrete time. Mitchell and Stokes (1986) give examples of minimum-phase functions of continuous time which become non-minimum-phase discrete functions if sampled within a certain range of sample rates. Each of these examples does have a minimum-phase digital representation that is minimum-phase if sampling is done at a sufficiently high rate, however. Thus sampling rate can be a determining factor in whether or not a discrete absorption operator is minimum phase.

Denoting the absorption operator associated with unit-layer k as $a_k(\tau)$ and the z-transform of its digital representation as $A_k(z)$, the z-transforms of waves with common direction in the top and bottom of layer k are related by

$$U_k(z) = z\, A_k(z)\, U_k'(z) \tag{5-7a}$$

and

$$D_k'(z) = z\, A_k(z)\, D_k(z) \quad . \tag{5-7b}$$

Normal propagation through layer k may therefore be expressed

$$\begin{bmatrix} U_k(z) \\ D_k(z) \end{bmatrix} = \frac{1}{z\, A_k(z)} \begin{bmatrix} z^2 A_k^2(z) & 0 \\ 0 & 1 \end{bmatrix} \begin{bmatrix} U_k'(z) \\ D_k'(z) \end{bmatrix} \tag{5-8}$$

where $A_k(z) = 1$ if there is no absorption.

For an incident wave $d_{1,0}$, the z-transform of the downward travelling waves in the top of layer 1 is

$$D_1(z) = d_{1,0} + \sum_{j=1}^{\infty} d_{1,2j}\, z^{2j} \quad . \tag{5-9}$$

Since the boundary condition at the top of the first layer is $d_{1,2j} = -r_0\, u_{1,2j}$ for all j it may be written

$$D_1(z) = d_{1,0} - r_0 U_1(z) \quad . \tag{5-10}$$

Also, since no upward travelling energy exists in the lower halfspace, the lower boundary condition is

$$U_{N+1}(z) = 0 \quad . \tag{5-11}$$

Letting $\prod$ indicate continued product, equations (5-6) and (5-8) may be combined with conditions (5-10) and (5-11) to produce

$$\begin{bmatrix} U_1(z) \\ d_{1,0} - r_0 U_1(z) \end{bmatrix} = \prod_{k=1}^{N} \frac{1}{t_k z A_k(z)} \begin{bmatrix} z^2 A_k^2(z) & r_k z^2 A_k^2(z) \\ r_k & 1 \end{bmatrix} \begin{bmatrix} 0 \\ D_{N+1}(z) \end{bmatrix} \quad . \tag{5-12}$$

This is a set of simultaneous equations which may be solved for the quantities $\{D_{N+1}(z)/d_{1,0}\}$ and $\{U_1(z)/d_{1,0}\}$. The first of these is the z-transform of the transmissivity sequence in the top of the lower halfspace and the second is that of the reflectivity sequence in the top of the first layer. Each has the form of a quotient of polynomials, i.e.

$$\frac{D_{N+1}(z)}{d_{1,0}} \equiv T_N(z) = \frac{\prod_{k=1}^{N} t_k z A_k(z)}{H_N(z) + r_0 F_N(z)} \tag{5-13}$$

and

$$\frac{U_1(z)}{d_{1,0}} \equiv R_N(z) = \frac{F_N(z)}{H_N(z) + r_0 F_N(z)} \tag{5-14}$$

where $H_N(z)$ and $F_N(z)$ are elements of the continued product matrix

$$\begin{bmatrix} E_N(z) & F_N(z) \\ G_N(z) & H_N(z) \end{bmatrix} = \prod_{k=1}^{N} \begin{bmatrix} z^2 A_k^2(z) & r_k z^2 A_k^2(z) \\ r_k & 1 \end{bmatrix} \tag{5-15}$$

which is sometimes called the propagator matrix of the system. The time sequences corresponding to the solutions are of infinite length except in the trivial case of no layers between the halfspaces. Stability of the solutions requires that the polynomial $\{H_N(z) + r_0 F_N(z)\}$ be the z-transform of a minimum-phase sequence. It should be noted that the polynomial $\{1 + R_N(z)\}$ also corresponds to a minimum-phase sequence (Sherwood and Trorey, 1965). It is the z-transform of the complete synthetic reflection seismogram, direct wave plus primary and multiple reflections, for an impulsive source of plane waves at the surface and a perfectly broad-band surface receiver at zero offset. Expressions for source and receiver at locations other than the surface are obtained by making appropriate modifications to boundary condition (5-10). This involves no essential change in the theory and will not be pursued further here.

It should be noted that the presence of absorption precludes elements of the propagator matrix being written in terms of reverse polynomials as done by Robinson (1967b). Doing so would require that $A_k^{-1}(z) = A_k(z^{-1})$ and thus that $A_k(z)A_k(z^{-1}) = 1$. Since $A_k(z)$ must be real for real z, this could be true only if the absorption operator is all pass (Eisner, 1984) and therefore only if absorption is absent.

The foregoing development is in terms of conceptual "unit layers" whose boundaries are separated by one unit of time. As discussed by Trorey (1962), such a scheme provides the desired result but involves much calculation that is not really necessary because observable effects on seismic pulses are related more to some "average absorption" than to small scale changes. The computation is more efficient if the layer model is arranged into blocks of arbitrary thickness within which the effects of absorption "on average" do not vary. The unit-layer absorption operator $a(\tau)$ then represents the average absorption-per-unit-temporal-thickness of the block and can be called the specific absorption operator of the block. The total absorption operator corresponding to one-way propagation through a block with a temporal thickness of n time units is then equivalent to an n-fold convolution of $a(\tau)$ with itself and the Fourier transform of the total operator is the nth power of the Fourier transform of the specific operator. It is important to realize that the convolution is in continuous time and digitization is done afterwards. The z-transform of a digital representation of the total absorption operator can be denoted $A^{[n]}(z)$ where the square brackets around the exponent are used to make it clear that the indicated convolution occurs in continuous, not discrete, time. The distinction is necessary because, in general, $A^{[n]}(z) = A^n(z)$ only in the ideal limit of infinite digital resolution. The implication is that the block model is valid only if the digital dynamic range is sufficiently large to render this equality approximately true.

There are two types of "constant-absorption" blocks. The simpler type has no internal reflecting interfaces and for that reason is said to be homogeneous. It is represented by an appropriate number of unit layers separated by interfaces with null reflection coefficient. The other type does contain internal reflectors and is represented by an appropriate number of homogeneous blocks with reflecting interfaces between them.

If the system comprises M homogeneous blocks and the temporal thickness of the jth block is n_j time units with specific absorption operator $a_j(\tau)$, the propagator matrix can be written

$$\begin{bmatrix} I_M(z) & J_M(z) \\ K_M(z) & L_M(z) \end{bmatrix} = \prod_{j=1}^{M} \begin{bmatrix} z^{2n_j} A_j^{[2n_j]}(z) & r_j z^{2n_j} A_j^{[2n_j]}(z) \\ r_j & 1 \end{bmatrix} \tag{5-16}$$

where r_j is the reflection coefficient at the bottom of the jth homogeneous block. The transmissivity and reflectivity are then

$$T_M(z) = \frac{z^N \prod_{j=1}^{M} t_j A_j^{[n_j]}(z)}{L_M(z) + r_0 J_M(z)} \quad , \tag{5-17}$$

where $N = \sum_{j=1}^{M} n_j$, and

$$R_M(z) = \frac{J_M(z)}{L_M(z) + r_0 J_M(z)} \quad , \tag{5-18}$$

respectively. These expressions assume that the z-transforms of continuously convolved absorption operators are factorable, i.e. that the total system absorption operator can be represented as a continued product of total block operators. As mentioned previously, the validity of this depends on the digital resolution being sufficiently large.

Chapter 6

Reflectivity Models for Zero-offset Seismograms

The reflectivity of any number of layers of different thicknesses can by expressed by means of eq.s(5-16,18), but most practical situations require a model of only a few layers. Regardless of how many primary reflections may be present on a seismogram, only a few are usually associated with sufficient impedance contrast to generate discernable sequences of reverberations. Only strong reflections are of interest to the modelling procedure and weak ones may be included in otherwise "homogeneous" blocks. For marine seismograms, there is always at least one such block. It is called the water layer but may include the uppermost layer of sea-floor sediment if the water bottom is weakly reflecting. The top of this block, the air/water interface, is an almost perfect reflector and $r_0 = 1$ is a good approximation. The bottom of the block is the first interface reflective enough to generate a discernable sequence of reverberations. Since water does not absorb energy in the seismic range, if the block does not include any absorbent soil it is possible to let $A_1(z) = 1$ and to write

$$R_1(z) = \frac{r_1 z^{2n_1}}{1 + r_1 z^{2n_1}} \tag{6-1}$$

which is the z-transform of the reflectivity of a marine seismogram such as that of fig.1 which exhibits water-layer multiples but no other reverberations. It should be noted that the assumption of no absorption in the water layer is not always valid. A sequence of water-layer multiples that exhibits absorption, apparently due to gas in a thin layer of surficial material on the sea floor being included in the water-layer block, has been found by van der Wey (1989).

Of course, marine seismograms often exhibit a structure more complicated than the reflectivity of a single block. For example, the sea floor can consist of a layer of soft sediment overlying more competent material and the interface thus formed can be sufficiently reflective to generate discernable reverberations between itself and both the top and bottom of the water layer. This requires that the model include a second block

and eq.(5-18) is written

$$R_2(z) = \frac{[r_1 + r_2 z^{2n_2} A_2^{2n_2}(z)]\, z^{2n_1}}{1 + r_1 z^{2n_1} + r_1 r_2 A_2^{2n_2}(z)\, z^{2n_2} + r_2 A_2^{2n_2}(z)\, z^{2(n_1+n_2)}} \quad . \tag{6-2}$$

Such a situation is observed in fig.2 where the second block is bounded above by the water/sediment interface and below by the sediment/bedrock interface. It should be noted in fig.2 that there is more than one layer of sediment but the interfaces between sediments are not sufficiently reflective to generate reverberations. In such a case the second block could be taken to comprise the total thickness of sediment.

The situation is different in portions of fig.3 and fig.4 where an interface between sediments is locally very reflective. The second block of a model for these localities would comprise only the upper sediment layer. A third block could then be included to account for the material between the upper sediment and the bedrock. The z-transform of the reflectivity would then be of the form

$$R_3(z) = \tag{6-3}$$

$$\frac{[r_1 + r_2 z_2^2 + r_3 (z_2 z_3)^2 + r_1 r_2 r_3 z_3^2]\, z^{2n_1}}{1 + r_1 z^{2n_1} + r_2 (z^{n_1} z_2)^2 + r_3 (z^{n_1} z_2 z_3)^2 + r_1 r_2 z_2^2 + r_2 r_3 z_3^2 + r_1 r_3 (z_2 z_3)^2 + {}_1 r_2 r_3 (z^{n_1} z_3)^2}$$

where $z_2 = [z\, A_2(z)]^{n_2}$ and $z_3 = [z\, A_3(z)]^{n_3}$.

Another example requiring a three-block model is shown in fig.6, but the water is so deep that the water-layer multiples fall outside the figure. Similar expressions could be written for four or more blocks, but they rarely would be required in practice.

All the foregoing z-transforms have roots within the unit circle ($2n_1$ of them at $z=0$) and therefore none of them correspond to minimum-phase sequences. These roots can be removed by shifting the origin of time by $2n_1$ units so that the water-bottom reflection occurs at time zero. The single-block model would then have no zeros and therefore be minimum phase after the shift. The other shifted models would have no zeros at the origin, but could still have zeros within the unit circle. For example, the shifted two-block model has one zero which is outside the unit circle only if $r_1 > r_2$. Of course, this need not always be the case and implies that the application of statistical inverse-filtering techniques (that assume minimum phase) to the reflected portions of marine seismograms, cannot be relied upon to suppress reverberations. It will be seen later that it is possible, however, to construct a deterministic filter for suppressing multiples if the required parameters are known or can be estimated by some means such as model fitting.

Chapter 7

Quantitative Determination of Geometric Attenuation

The fact that seismic frequencies are not absorbed in water can be used as the basis of a scheme for estimating the exponent γ in eq.(4-3a), the power law describing the effect of geometric attenuation. Consider the absorption-free single-block model of eq.(6-1). Since the magnitude of the reflection coefficient is less than unity, it can also be written in the power series form

$$R_1(z) = r_1 z^{2n_1} \sum_{j=0}^{\infty} (-r_1 z^{2n_1})^j \quad . \tag{7-1}$$

This corresponds to a temporal sequence consisting of a primary reflection at $2n_1$ time units followed by reverberatory waves at intervals of $2n_1$ time units. Since the waves simply retrace the same ray path, the range of the first reverberatory wave is twice that of the primary wave, that of the second is three times, the third four times, etc. Taking the range of the primary reflection to be the reference range, and assuming it to be in the far field of the source, the geometric attenuation factor is, by eq.(4-3b),

$$g_t = \left[\frac{2n_1 \Delta t}{(j+1)2n_1 \Delta t} \right]^{\gamma} \quad . \tag{7-2}$$

It can be incorporated into the reflectivity by writing eq.(7-1) as

$$R_1(z) = r_1 z^{2n_1} \sum_{j=0}^{\infty} (j+1)^{-\gamma} (-r_1 z^{2n_1})^j \quad . \tag{7-3}$$

Thus the amplitude ratio of two successive wavelets is

$$\frac{\text{amp wavelet } k+1}{\text{amp wavelet } k} = -r_1 \left[\frac{k+1}{k+2} \right]^{\gamma} \tag{7-4}$$

and therefore

$$\log\frac{|\text{amp wavelet } k+1|}{|\text{amp wavelet } k|} = \log|r_1| + \gamma \log\frac{k+1}{k+2} \quad . \tag{7-5}$$

A similar expression can be obtained for the amplitude ratio of two other successive wavelets $(k+n)$, $(k+n+1)$ and it can be subtracted from eq.(7-5) to give

$$\log\frac{|\text{amp wavelet } k+1|}{|\text{amp wavelet } k|} - \log\frac{|\text{amp wavelet } k+n+1|}{|\text{amp wavelet } k+n|} = \gamma\left[\log\frac{k+1}{k+2} - \log\frac{k+n+1}{k+n+2}\right] \tag{7-6}$$

or, equivalently,

$$\gamma = \frac{\log\dfrac{|\text{amp wavelet } k+1|\ |\text{amp wavelet } k+n|}{|\text{amp wavelet } k|\ |\text{amp wavelet } k+n+1|}}{\log\dfrac{(k+1)(k+n+2)}{(k+2)(k+n+1)}} \quad . \tag{7-7a}$$

The simplest application of this relationship involves the amplitudes of the primary sea-floor reflection and its first two multiples. The primary reflection corresponds to $j = 0$ in eq.(7-1) and the multiples to $j = 1$ and $j = 2$. Thus, letting $k = 0$ and $n = 1$ in eq.(7-7a),

$$\gamma = \frac{\log\dfrac{|\text{amp first multiple}|^2}{|\text{amp bottom reflection}|\ |\text{amp second multiple}|}}{\log\dfrac{3}{4}} \quad . \tag{7-7b}$$

This scheme should be implemented only with data recorded over a smooth, flat sea floor so that the estimate is not affected by scattering or focusing of the wave front. Also, the accuracy of the estimate depends on the assumption that there is no absorption present in the water layer. Thus care should be taken that the estimation is done using a sequence of water-layer reverberations that does not exhibit changes in wavelet shape.

Chapter 8

An Example of Estimating Sea-floor Reflection Coefficients

An "approximately zero-offset" reflection profile chosen to illustrate the use of reverberations to estimate reflection coefficients is shown in fig.11. It was recorded in Vancouver Harbour, British Columbia, using a small airgun source and recorded on FM magnetic tape. It exhibits several apparent differences in sea-floor reflectivity. In particular, the presence of a strong sequence of water-layer reverberations indicates that the sea floor is highly reflective within a small locality of the right-hand part of the record. The sea floor seems to be less reflective elsewhere.

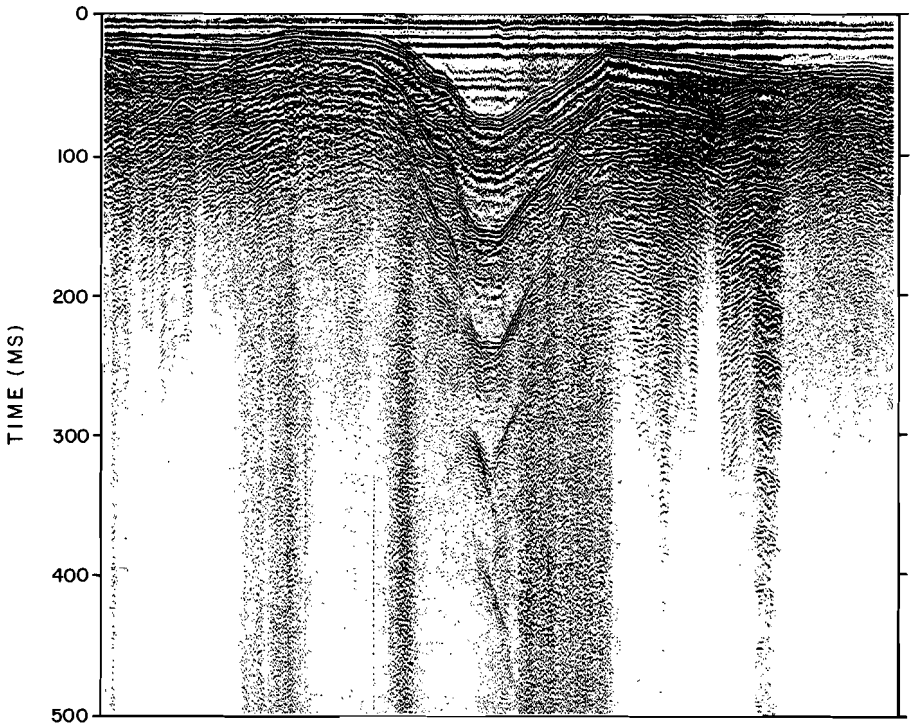

Fig.11: Playback of an FM recording of a seismic profile in Vancouver Harbour.

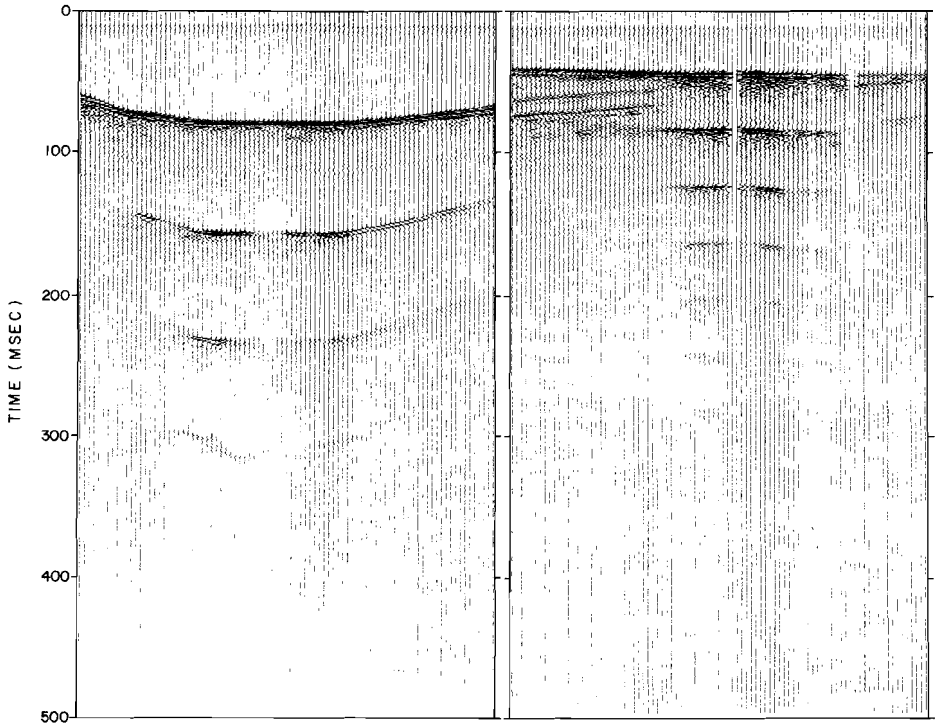

Fig.12: Two groups of traces digitized from fig.11; (a) traces from the sea-floor valley and (b) traces from the area of strong reverberations.

The FM recording was subsequently digitized at an 8 kHz rate and the resulting discrete data have about 10 bits of dynamic range. This does not truly represent the dynamic range of the seismic signal because the strongest wavelets are clipped due to saturation of the magnetic tape. The two groups of digitized traces shown in fig.12 were selected to be analyzed. The group shown in fig.12(a) is taken from the sea-floor valley located near the center of the profile. The group shown in fig.12(b) includes the area of strong reverberations. (Some traces appear to be muted due to erroneous triggering of the digitizer.)

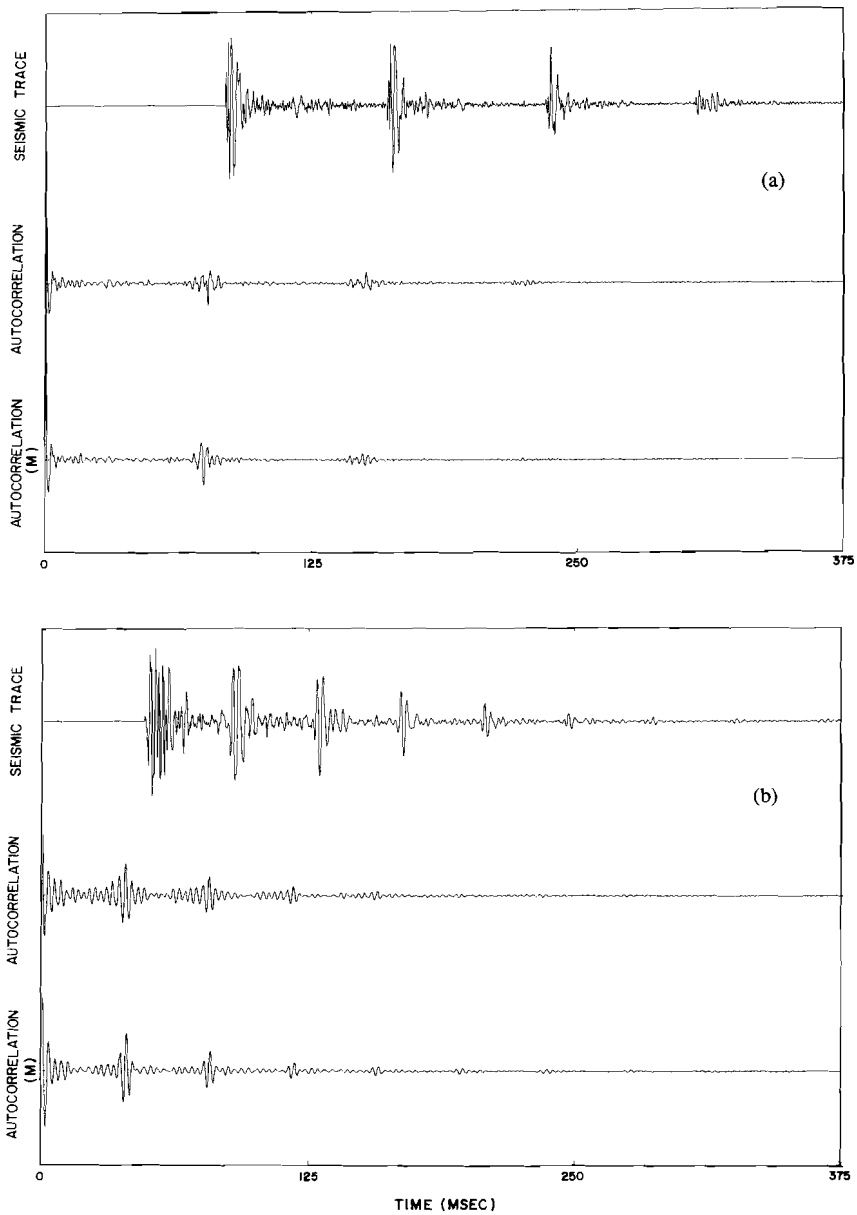

Fig.13: A representative data trace (with direct wave muted) from each group in fig.12 and associated autocorrelations; (a) a trace from the sea-floor valley and (b) a trace from the region of strong reverberations. In each case, the upper autocorrelation is of the data tace as shown and the lower, denoted (M), is of the data trace with the clipped portion muted.

A representative trace from each group of traces in fig.12 is plotted in fig.13; a trace from the sea-floor valley is shown in fig.13(a) and a trace from the region of strong reverberations is shown in fig.13(b). Three plots are associated with each representative trace. In each case, the uppermost plot is the data trace itself with the direct arrival muted. The middle plot is the autocorrelation of the upper plot. The lowermost plot, denoted (M), is the autocorrelation of the upper plot with the clipped portion muted. Amplitude ratios of successive wavelets can be measured from the unclipped portion of the uppermost plot. Wavelet polarity is not clear, however, partly due to the clipping of stronger wavelets. Autocorrelations were calculated in order to improve the observation of relative polarity between successive wavelets. (No geometric corrections were made prior to correlating, therefore only the polarity, not the amplitude, of the correlations is correct.)

The clipping made it impossible to get an estimate of the geometric divergence power law exponent but, since the dominant period of the recorded wavelets is 3 ms (about five metres in water and large compared to the region of turbulent water observed when the airgun was triggered), an assumption of spherical divergence was made. The clipping did not seriously affect the estimation of reflection coefficients because it was possible to compare wavelets of successive higher-order reverberations which were not clipped.

Assuming the geometric attenuation to be due to spherical divergence only, amplitude measurements of successive unclipped multiple wavelets in fig.13(a) indicate a magnitude of about 0.3 for the reflection coefficient of the water bottom in the valley. Similar measurements in fig.13(b) yield a magnitude of 0.6 for the coefficient in the highly reflective locality. The correlation amplitudes in fig.13(a) alternate in polarity while those in fig.13(b) have a common polarity. As can be deduced from the alternating series in eq.(7-1), this implies that the reflection coefficient in the valley is positive while that in the highly reflective area is negative.

It is possible that the amplitudes of the water-layer reverberations in the valley are affected by the curvature of the sea floor. Since the sea floor is concave, the estimate of reflection coefficient might be errorously large due to focusing of the reflected wave front. The correct value then would be somewhat less than +0.3 which, according to measurements reported by Hamilton (1972), is reasonable if the sediment in the valley is mud. Amplitudes in the strong reverberatory sequence would be less affected by focusing because the sea floor is rather flat in the right-hand portion of the profile. The estimated value of -0.6 for the reflection coefficient seems to be anomalous in both magnitude and sign, however. No groundtruth is available for identifying the sea-floor material there, but the fact that it is located near a fabricator of wood products indicates that it may be a mat of decaying wood fibers within which gas is trapped. Such an interpretation is supported by the observation of van der Wey (1989) that the wavelets in this sequence exhibit absorption.

Chapter 9

Estimating the Effect of Absorption in Sea-floor Soils

Absorption changes the shape of propagating wavelets by reducing the amplitude and delaying the phase of higher frequencies relative to the amplitude and phase of lower frequencies. There are two main categories of methods by which to estimate the effect; those implemented in the frequency domain and those implemented in the time domain. Methods in both categories were applied to vertical-reflection marine seismograms by Jannsen et al. (1985) and the results compared. They report that the principal difficulty with frequency domain methods arises from the interference that occurs when more than one wavelet is present in the time gate to be transformed. An illustration of such interference is shown in fig.14. The two wavelets of opposite polarity are present in the time trace of fig.14(a). The dotted curve in fig.14(b) is the Fourier amplitude spectrum of one of them. It is smooth and rather simple in shape. The solid curve superimposed on it is the spectrum of the entire time trace containing both wavelets. It has a complicated shape due to constructive and destructive interference between the spectral components of the two wavelets. Thus it is seen that the presence of the second wavelet causes the true spectrum shape to be almost completely masked. It is this masking that causes spectral methods to fail.

If two seismic wavelets can be isolated in time and their individual spectra determined, their shapes can be compared by dividing one spectrum by the other to obtain their spectral ratio (equivalent to the spectrum of their crosscorrelation). Consider two wavelets $u(t)$ and $v(t)$ and their respective Fourier transforms

$$U(\omega) = Re[U(\omega)] + i\ Im[U(\omega)] = |U(\omega)|e^{i\upsilon(\omega)}$$

and

$$V(\omega) = Re[V(\omega)] + i\ Im[V(\omega)] = |V(\omega)|e^{i\xi(\omega)}$$

where ω is frequency in radians per time unit. If $u(t)$ occurs before $v(t)$ in the same reverberatory sequence so that the onset of $u(t)$ is located at m units of time and that of $v(t)$ is located at $m+n$ units of time, their spectral representations are related by

$$V(\omega) = L\ A^n(\omega)\, e^{in\omega}\, U(\omega) \qquad (9\text{-}1)$$

where L is the amplitude loss due to frequency-independent processes (reflection, transmission and geometric divergence) and $A(\omega)$ is the Fourier transform of the

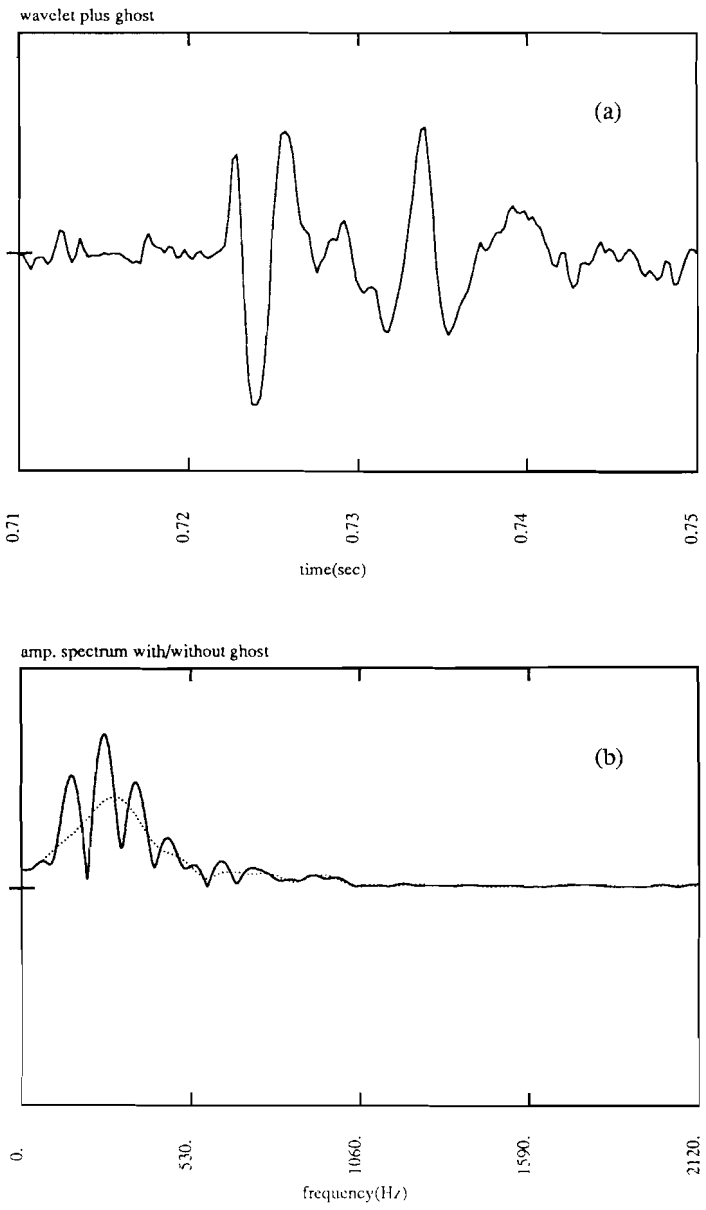

Fig.14: Illustration of the interference that occurs in the frequency domain when more than one wavelet is present in the time domain: (a) two wavelets in the time domain and (b) the Fourier amplitude spectrum of one wavelet alone (dotted curve) and of both wavelets together (solid curve).

specific absorption operator $a(\tau)$ defined in Chapter 5 (τ being "interwavelet time"). For any frequency at which $U(\omega)$ does not vanish this can be rearranged to give

$$A^n(\omega) = |A^n(\omega)|e^{in\alpha(\omega)} = \frac{1}{|L|}\frac{|V(\omega)|}{|U(\omega)|}e^{i[\xi(\omega)-\upsilon(\omega)-n\omega]} \tag{9-2}$$

where $|A^n(\omega)|$ is the amplitude attentuation and $n\,\alpha(\omega)$ is the phase delay between the wavelets. Thus the specific absorption operator $a(\tau)$ has amplitude spectrum

$$|A(\omega)| = \left[\frac{1}{|L|}\frac{|V(\omega)|}{|U(\omega)|}\right]^{\frac{1}{n}} . \tag{9-3}$$

and phase spectrum

$$\alpha(\omega) = \frac{\xi(\omega)-\upsilon(\omega)}{n} - \omega . \tag{9-4a}$$

For purposes of computation it is often convenient to use the trigonometric identities

$\cos(\xi-\upsilon) = \cos\xi\cos\upsilon + \sin\xi\sin\upsilon$ and $\sin(\xi-\upsilon) = \sin\xi\cos\upsilon - \cos\xi\sin\upsilon$

to write the phase spectrum in the form

$$\alpha(\omega) = \frac{1}{n}\tan^{-1}\left[\frac{Im[V(\omega)]\,Re[U(\omega)] - Re[V(\omega)]\,Im[U(\omega)]}{Re[V(\omega)]\,Re[U(\omega)] + Im[V(\omega)]\,Im[U(\omega)]}\right] - \omega . \tag{9-4b}$$

Knowledge of the amplitude and phase spectra then allows the specific absorption operator to be determined by inverse transformation to the time domain.

Letting $K(\omega)$ be the absorption coefficient defined by Futterman (1962), the ratio of amplitude spectra in eq.(9-2) is proportional to an exponential function of frequency such that

$$|A^n(\omega)| = \frac{e^{-n\omega K(\omega)}}{|L|} \tag{9-5}.$$

where c is the average speed of propagation along the ray path between the wavelets. The functional form of $K(\omega)$ has been the subject of much discussion in the literature. Aminzadeh and Mendel (1983) consider it to be either linear or quadratic. They obtain operators for these cases (noncausal operators because phase lag is not taken into account). Many authors, including Trorey (1962) and Hamilton (1972), are of the opinion that a linear absorption coefficient agrees better with experimental evidence than does a quadratic coefficient. Futterman (1962) shows that a causal operator can correspond to a linear absorption coefficient only for frequencies above some arbitrarily low non-zero cutoff frequency. Below the cutoff frequency, the absorption coefficient

must be nonlinear in such a way that arbitrarily low frequencies are unaffected by absorption. The existence of the cutoff has significant consequences in the time domain because it requires the first derivative of the absorption operator to be continuous at its onset time. Such continuity implies that the onset magnitude of a causal operator is arbitrarily small and less than the least significant bit of any digital representation of it. Thus the discrete absorption operator has at least one leading zero due to finite digital resolution. This has the appearance of being a delay of onset time and is indistinguishable from an increase in temporal block thickness. Thus temporal block thickness can be expected to be overestimated in the presence of an "almost linear" absorption coefficient.

Seismic absorption is usually discussed in terms of the quality factor Q. Futterman (1962) shows it to be related to the absorption coefficient K by

$$Q(\omega) = \frac{2\pi}{1 - \exp \frac{-4\pi c\, K(\omega)}{\omega}} \quad . \tag{9-6}$$

Equivalently then,

$$K(\omega) = \frac{-\omega}{4\pi c} \ln \left[1 - \frac{2\pi}{Q(\omega)} \right] \quad . \tag{9-7}$$

Substituting this into eq.(9-5) and taking the logarithm,

$$\ln |A^n(\omega)| = \frac{n\,\omega}{4\pi} \ln \left[1 - \frac{2\pi}{Q(\omega)} \right] - \ln |L| \quad . \tag{9-8}$$

This is a linear function of ω if Q is constant. Since it can be linear only above the cutoff frequency, Q is said to be "nearly constant". Below the cutoff, Q becomes unboundedly large at very low frequencies so that the effect of absorption vanishes. The slope of the linear portion is

$$S = \frac{n}{4\pi} \ln \left[1 - \frac{2\pi}{Q} \right] \tag{9-9}$$

and therefore

$$Q = \frac{2\pi}{1 - \exp \frac{4\pi S}{n}} \quad . \tag{9-10}$$

In this way the value of a "nearly constant" Q can be determined from the slope of the logarithm of the ratio of the amplitude spectra of two wavelets in the same reverberatory sequence.

Jannsen et al.(1985) conclude that, if the data are noisy, or if individual wavelets cannot be isolated, the most consistent estimates of absorption are obtained by modelling in the time domain. This may be done using eq.s(5-16,18) if a functional form is assumed for the absorption operator. If an assumption of "nearly constant" Q is made, the method of Carpenter (1966) can be used to obtain a causal absorption operator. The procedure is to first calculate a "similarity function" for a specified low cutoff frequency and then to scale it according to parameters Q, the absorption "quality factor" of the material, and T, the time of propagation in the absorbing material for the lowest (unabsorbed) frequencies. As an example, he gives a numerical listing for the "similarity function" corresponding to a cutoff frequency of .01 Q/T cycles per time unit. The similarity function is plotted in fig.15 as a dimensionless curve the area beneath which is unity. The operator appropriate to a specified combination of Q and T is obtained by multiplying the vertical axis by Q/T and the horizontal by T/Q. The area spanned remains unity and the result is the amplitude of the desired operator as a function of time from its onset, i.e. "interwavelet" time.

By way of illustration, four time-domain models have been computed using the three-block system of eq.(6-3). The four models are similar in that they have the same reflection coefficients and no absorption in the first and third blocks. The values of the reflection coefficients are reasonable for "water over clay over sand over sandstone bedrock". The second block exhibits absorption in three of the models, its effect being calculated by Carpenter's method assuming "nearly constant" values of Q. System parameters are:

$$r_0 = 1.0$$

$$r_1 = 0.2\,,\quad n_1 = 500\,,\quad A_1^{[1000]}(z) = 1.0$$

$$r_2 = 0.2\,,\quad n_2 = 45\,,\quad A_2^{[90]}(z) = C_Q^{[90]}(z)$$

$$r_3 = 0.6\,,\quad n_3 = 175\,,\quad A_3^{[350]}(z) = 1.0 \qquad .$$

where $C_Q^{[90]}(z)$ is the z-transform of Carpenter's operator for the reflected path in the second (clay) block. Calculations were done for four different values of Q in block 2; $Q \rightarrow \infty$ (no absorption) , Q=500 , Q=100 and Q=20 . The corresponding four discrete total absorption operators for the layer are shown in fig.16. The operator for the absorption-free case is specified to be a unit impulse at time zero. The other three are obtained from Carpenter's method by scaling the curve of fig.15 according to $T = 90$ for each value of Q.

It can be seen that the three operators obtained by Carpenter's method have leading elements zero. As discussed previously, this is due to causality and the digital resolution being finite. In continuous time, as Q increases without limit Carpenter's operator retains its areal span of unity by approaching an impulse of infinite amplitude at time zero. That is not the case in discrete time, however, because the first derivative of the absorption operator is continuous at its onset. In discrete time, the first element is always zero and, as Q becomes large, the operator approaches an impulse located at the time of the second element. The amplitude of the impulse is such that unit area is preserved, i.e. if the digitization interval is the unit of time then the amplitude of the

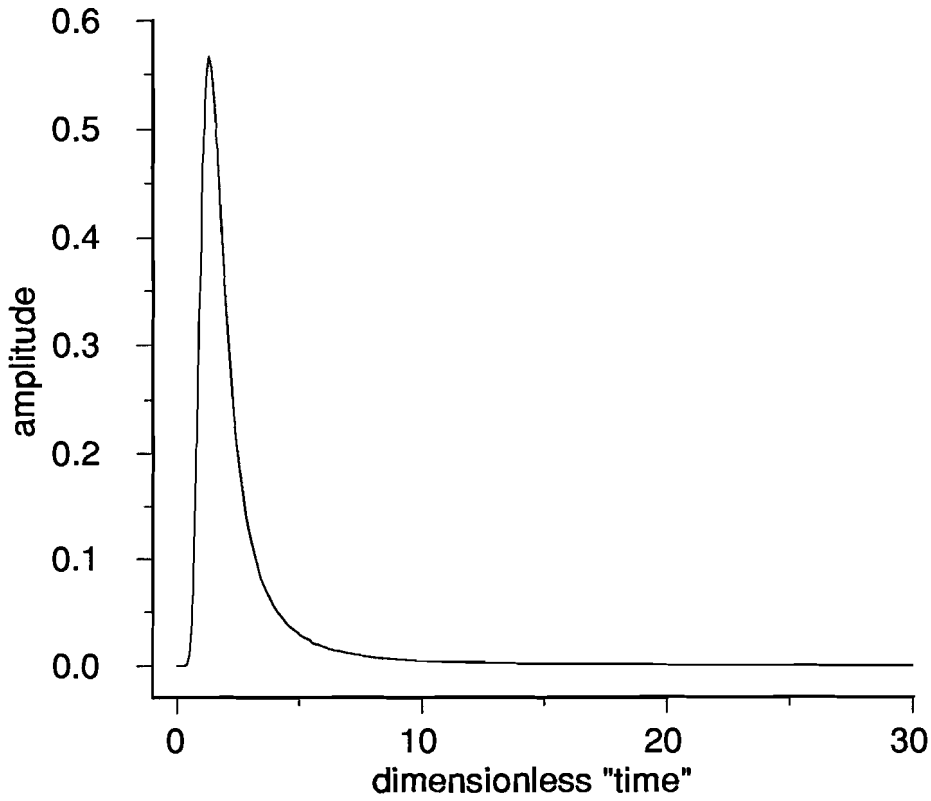

Fig.15: Carpenter's curve for determining absorption operators with a low-frequency cutoff of .01 Q/T .

impulse is one. At the other extreme, as Q becomes small, the onset of the operator can be quite gradual in continuous time and the number of leading zeros in its digital representation is determined by the digital resolution. Thus the discrete operator always has at least one leading zero which results in a timing error of at least one digitization interval. This effect is clearly observed in fig.16 where the digital resolution is such that there is one leading zero for Q=500 and Q=100 and three for Q=20 .

Nondivergent (plane-wave) reflectivity sequences calculated according to eq.(5-18) and incorporating the absorption operators of fig.16 are shown in fig.17. The calculations were done using a program of Veldhuizen (1989). The resulting sequences constitute models for the geometrically corrected "whitened" seismograms of eq.(4-9). The thickness of the second block is in error by amounts corresponding to the number of leading zeros in the absorption operators. The sequences shown in fig.18 are similar to those of fig.17 but include the spherical divergence factor of eq.(4-3c) with the reference range being the range of the water-bottom reflection. If convolved with a far-field source wavelet, the sequences of fig.18 model the noise-free term on the right-hand side of eq.(4-7b).

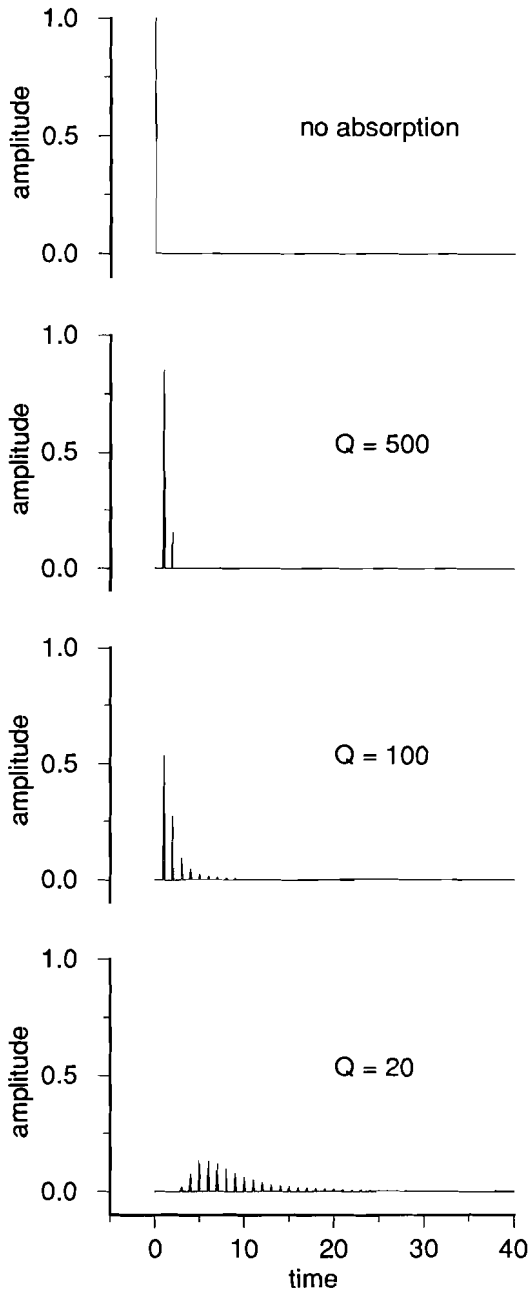

Fig.16: Discrete total absorption operators for the illustrative models.

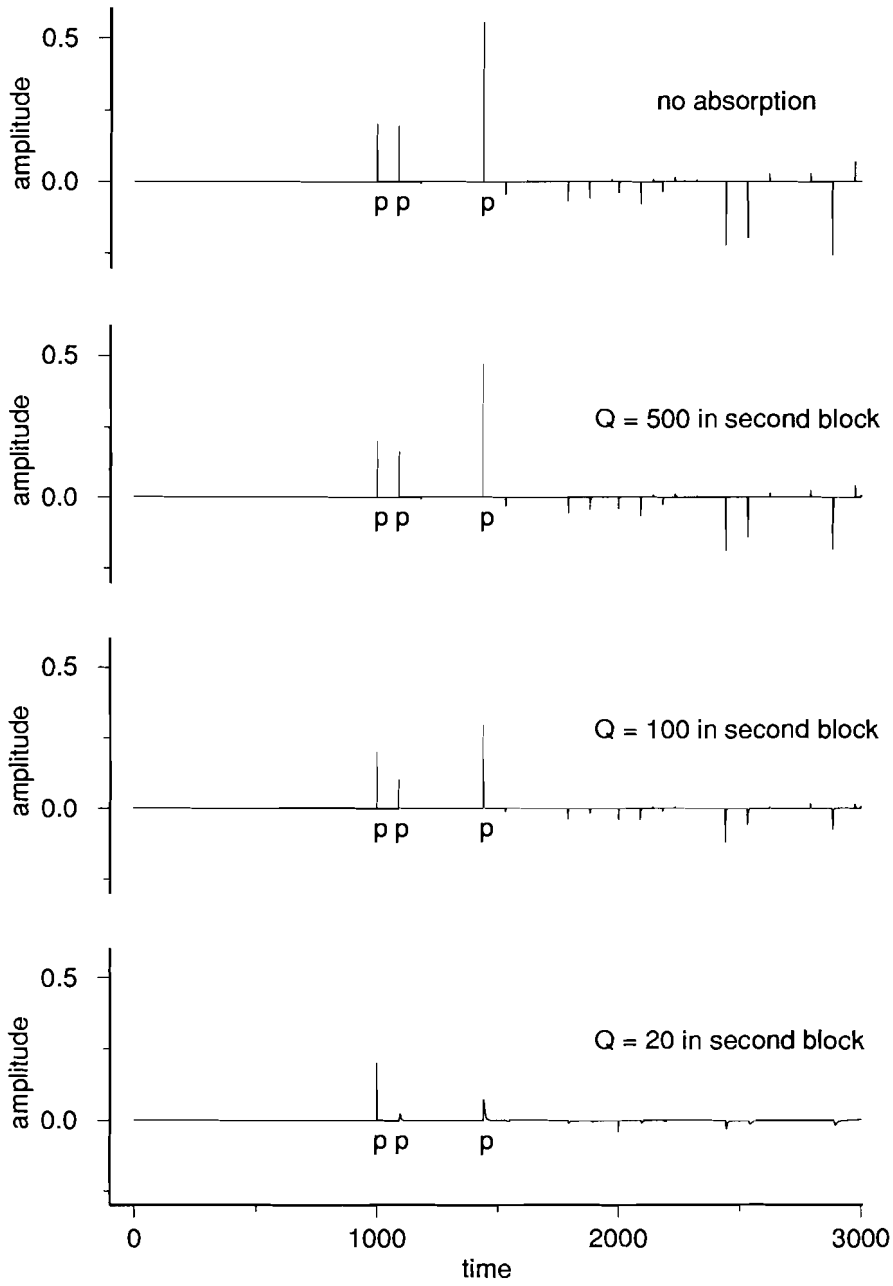

Fig.17: Non-divergent (plane-wave) reflectivity sequences for the illustrative models. (p indicates primary events, all other events are multiples)

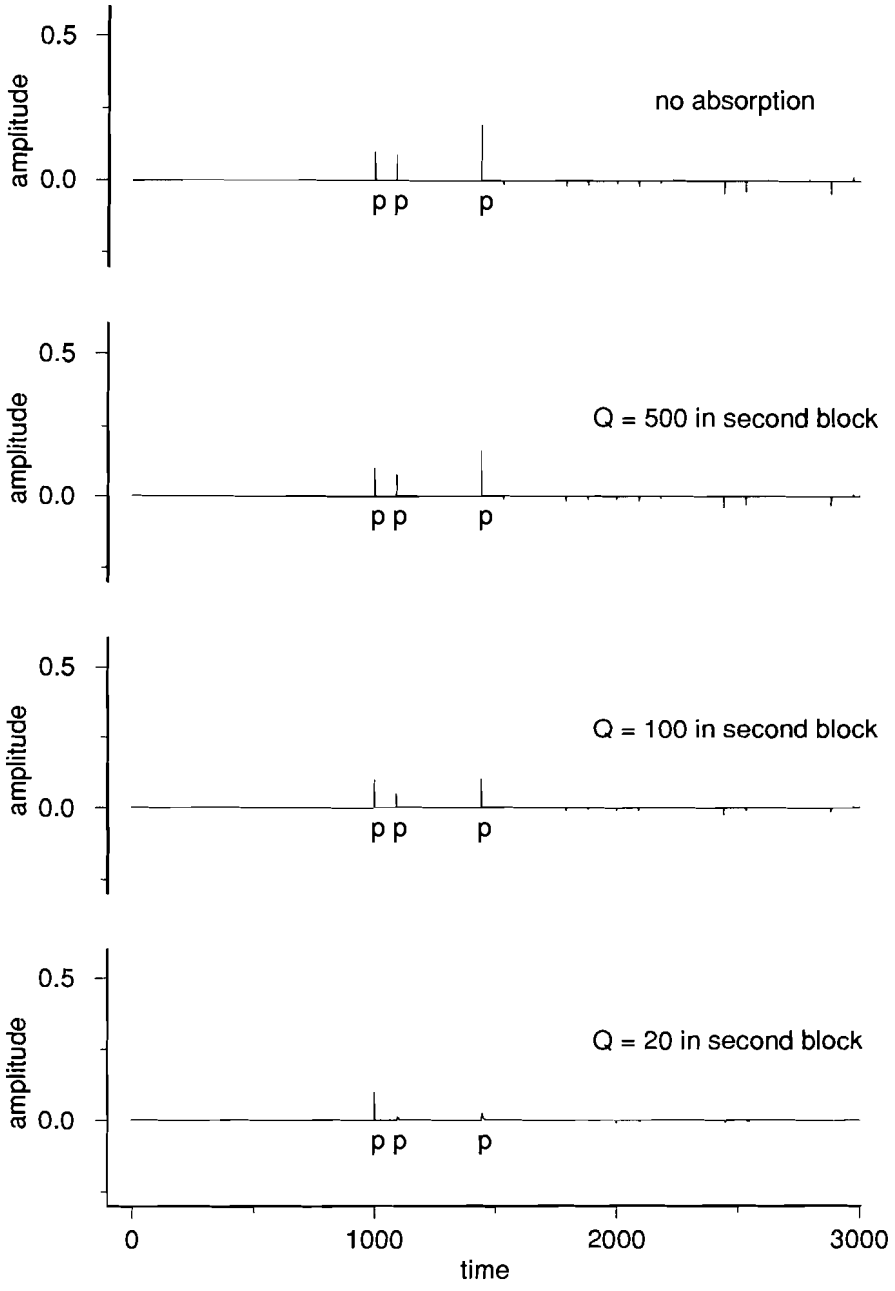

Fig.18: Spherically-divergent reflectivity sequences for the illustrative models. (p indicates primary events, all other events are multiples)

Chapter 10

The Dereverberation Filter

The minimum-phase finite time sequence corresponding to the polynomial $\{L_M(z) + r_0 J_M(z)\}$ in eq.s(5-17,18) is called the dereverberation filter of the system. The name is derived from the fact that, if it is convolved with either the reflectivity or the transmissivity, the result is a finite sequence that is free of reverberations. The temporal structure of the dereverberation filter may be elucidated by writing out eq.(5-16) for simple systems. The z-transform of the filter for a single block is

$$1 + r_0 r_1 z^{2n_1} A_1^{[2n_1]}(z) \quad . \tag{10-1}$$

In the absence of absorption this corresponds to a sequence of $(2n_1 + 1)$ elements; the first element being of unit amplitude, the last being of amplitude $r_0 r_1$ and the others being of amplitude zero. If absorption is present, the last element is convolved with the total absorption operator of the block and the number of elements in the sequence is increased by one less than the number of samples in the digital representation of the total absorption operator. The z-transform of the filter for two homogeneous blocks is

$$1 + r_0 r_1 z^{2n_1} A_1^{[2n_1]}(z) + r_1 r_2 z^{2n_2} A_2^{[2n_2]}(z) + r_0 r_2 z^{2(n_1+n_2)} A_1^{[2n_1]}(z)\, A_2^{[2n_2]}(z) \,. \tag{10-2}$$

In the absence of absorption this corresponds to a sequence of $(2n_1 + 2n_2 + 1)$ elements, four of which are nonzero. In the presence of absorption, this number is increased by two less than the sum of the number of samples representing the total absorption operator of the first block plus the number of samples representing the convolution of the total absorption operators of both blocks.

The number of elements in the dereverberation filter increases rapidly with the number of blocks. The dereverberation filter for a system of M homogeneous blocks comprises a sequence of 2^M nonzero elements in the absence of absorption and appropriately more in its presence. Continuing to write out z-transforms for successive values of M and doing some straightforward algebra, it is found that, if the digital resolution is high enough, the general case can be written in the factored form

$$L_M(z) + r_0 J_M(z) = \prod_{j=1}^{M} [1 + r_j z^{2n_j} A_j^{[2n_j]}(z)\, B_{j-1}(z)] \tag{10-3}$$

where

$$B_0(z) = r_0$$

and

$$B_j(z) = \frac{r_j + z^{2n_j} A_j^{[2n_j]}(z)\, B_{j-1}(z)}{1 + r_j z^{2n_j} A_j^{[2n_j]}(z)\, B_{j-1}(z)} \qquad \text{for } 1 \le j \le M \ . \tag{10-4}$$

This nonlinear relationship provides a recursive link between the factors of eq.(10-3). The factor corresponding to $j=1$ is a polynomial and therefore has a finite number of zeros but no poles. The factors corresponding to $j>1$ are rational functions (quotients of polynomials) that have a finite number of both zeros and poles. (This prevents their corresponding sequences being used in practice as filters to "strip" reverberatory sequences from the reflectivity one layer at a time.) It is interesting to note how the dereverberation filter can be stable in the presence of the poles of the rational functions. The zeros of the factor for any particular j are located at

$$1 + r_j z^{2n_j} A_j^{[2n_j]}(z)\, B_{j-1}(z)] = 0$$

and, by recursive relation (10-4), its poles are located at

$$1 + r_{j-1} z^{2n_{j-1}} A_{j-1}^{[2n_{j-1}]}(z)\, B_{j-2}(z)] = 0 \ .$$

But this set of poles is identical to the set of zeros of the factor for $j-1$. Thus, when the factors are multiplied, the zeros of one cancel the poles of the next. The result is that the z-transform of the dereverberation filter for any number of blocks has a finite number of zeros and no poles. None of the zeros are located within the unit circle and the filter is minimum phase.

If the values of system parameters are known, or can be estimated, the dereverberation filter of the system simply can be written out. For example, as indicated by eq.(6-3), the z-transforms of the dereverberation filters for the three-block illustrative models of Chapter 9 are of the form

$$1 + .04\, z^{90} C_Q^{[90]}(z) + .12\, z^{350} + .12\, z^{440} C_Q^{[90]}(z)$$

$$+ .2\, z^{1000} + .2\, z^{1090} C_Q^{[90]}(z) + .024\, z^{1350} + .6\, z^{1440} C_Q^{[90]}(z) \ .$$

The time sequences shown in fig.19 correspond to this polynomial for each of the four "nearly constant"values of Q in the second block.

It is instructive to examine the structure of the dereverberation filter in the Fourier domain. Writing eq.(10-4) on the unit circle $z = e^{i\omega t}$ and expressing complex quantities in polar form, it is found that the amplitude and phase spectra of the sequence

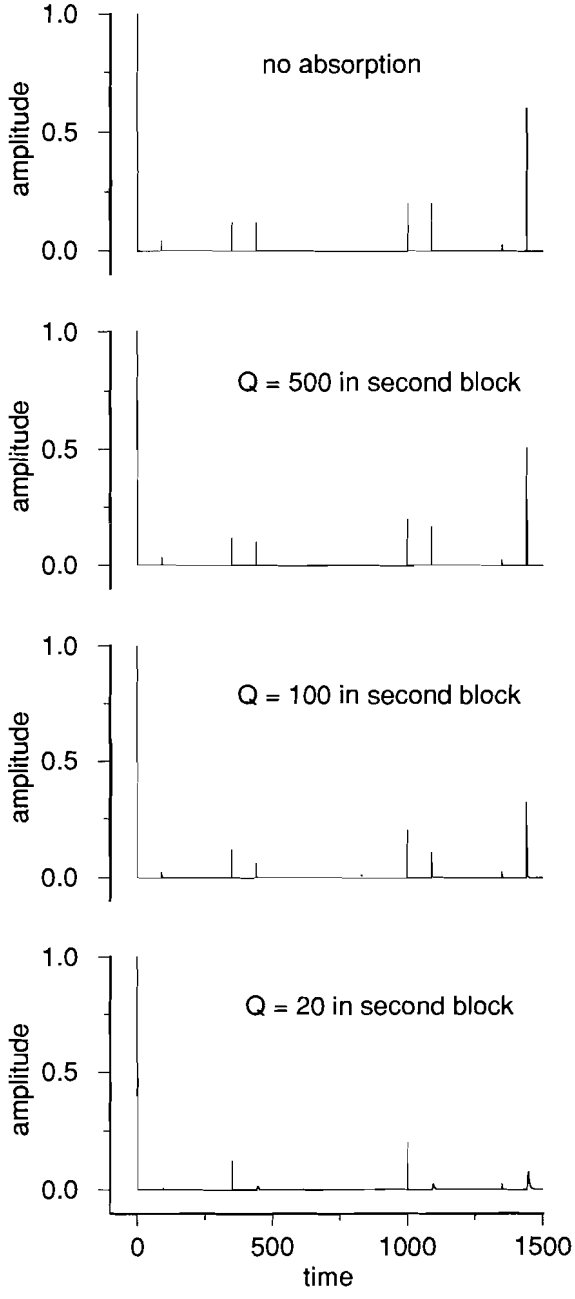

Fig.19: Dereverberation filters corresponding to the illustrative models.

corresponding to $B_j(z)$ are

$$|B_j(\omega)| = \left[\frac{r_j^2 + |P_j(\omega)|^2 + 2r_j|P_j(\omega)|\cos\phi_j(\omega)}{1 + r_j^2|P_j(\omega)|^2 + 2r_j|P_j(\omega)|\cos\phi_j(\omega)}\right]^{1/2} \tag{10-5}$$

and

$$\beta_j(\omega) = \tan^{-1}\left\{\frac{(1-r_j^2)|P_j(\omega)|\sin\phi_j(\omega)}{r_j(1+|P_j(\omega)|^2) + (1+r_j^2)|P_j(\omega)|\cos\phi_j(\omega)}\right\}, \tag{10-6}$$

respectively, where

$$|P_j(\omega)| = |A_j^{[2n_j]}(\omega)|\,|B_{j-1}(\omega)|$$

and

$$\phi_j(\omega) = 2n_j\omega + 2n_j\alpha_j(\omega) + \beta_{j-1}(\omega) \quad .$$

Thus the amplitude spectrum of the dereverberation filter for a system of M homogeneous blocks can be written

$$\prod_{j=1}^{M}\left[1 + r_j^2|P_j(\omega)|^2 + 2r_j|P_j(\omega)|\cos\phi_j(\omega)\right]^{1/2} \tag{10-7}$$

and its phase spectrum is

$$\sum_{j=1}^{M}\tan^{-1}\left\{\frac{r_j|P_j(\omega)|\sin\phi_j(\omega)}{1 + r_j|P_j(\omega)|\cos\phi_j(\omega)}\right\} \quad . \tag{10-8}$$

By eq.(10-7), the amplitude spectrum of the dereverberation filter is zero at frequencies such that

$$\cos\phi_j(\omega) = \frac{-(1 + r_j^2|P_j(\omega)|^2)}{2r_j|P_j(\omega)|}$$

which, for real frequencies, can be satisfied only if

$$r_j|P_j(\omega)| = \pm 1 \quad .$$

Since $-1 \le B_0 = r_0 \le 1$ and $|A_j^{[2n_j]}(\omega)| \le 1$, the process of induction can be applied to eq.(10-4) to show that

$$| B_j(\omega) | \le 1 \qquad \text{for all values of } j \ . \tag{10-9}$$

The equality applies only if $|r_0|=1$ and there is no absorption. In that case $|P_j(\omega)|=1$ and the sequence corresponding to $B_j(z)$ is an all-pass filter with phase spectrum

$$\beta_j(\omega) = \tan^{-1}\left\{\frac{(1-r_j^2)\sin[2n_j\omega + \beta_{j-1}(\omega)]}{2r_j + (1+r_j^2)\cos[2n_j\omega + \beta_{j-1}(\omega)]}\right\} \tag{10-10}$$

where $\beta_0(\omega) = 0$ because B_0 is real. Taking these conditions together, it is seen that there are zeros in the amplitude spectrum of the dereverberation filter only if there is no absorption and there are two interfaces such that $|r_0|=|r_M|=1$. In that case the system is a perfectly elastic wave trap bounded by interface 0 and interface M and its characteristic frequencies are

$$2n_j\omega + \beta_j(\omega) = (2k+1)\pi \qquad \text{if } r_M = +1$$

or

$$2n_j\omega + \beta_j(\omega) = 2k\pi \qquad \text{if } r_M = -1$$

where k is an integer, $j \le M$ and $\beta_j(\omega)$ is given by eq.(10-10).

Chapter 11

The "Dereverberated" Reflectivity

If the dereverberation filter is convolved with the reflectivity sequence of eq.(5-18), the result is a time sequence with z-transform

$$[L_M(z) + r_0 J_M(z)]\, R_M(z) = J_M(z) \quad . \tag{11-1}$$

The structure of the corresponding sequence is not immediately apparent, but it can be elucidated by writing out eq.(5-16) for a few values of M, i.e.

$$J_1(z) = r_1 z^{2n_1} A_1^{[2n_1]}(z)$$

$$J_2(z) = J_1(z) + r_2 z^{2(n_1+n_2)} A_1^{[2n_1]}(z) A_2^{[2n_2]}(z)$$

$$J_3(z) = J_2(z) + r_3 z^{2(n_1+n_2+n_3)} A_1^{[2n_1]}(z) A_2^{[2n_2]}(z) A_3^{[2n_3]}(z)$$
$$+ r_1 r_2 r_3 z^{2(n_1+n_3)} A_1^{[2n_1]}(z) A_3^{[2n_3]}(z)$$

etc.

If the process is continued it is found that, in the absence of absorption, the dereverberated reflectivity is a sequence of impulses located at the arrival times of primary reflections from the bottoms of the homogeneous blocks (with amplitudes equal to the reflection coefficients at those interfaces) plus, for three or more blocks, other impulses that are not associated with reflections in the usual sense. Rather, these other impulses are associated with normal modes, or resonances, of the system that cannot be described in terms of ray paths. Considering the impulses associated with primary reflections to be first-order events in that their amplitudes are determined by a single reflection coefficient, the others can be considered to be higher-order events because their amplitudes are determined by products of more than one reflection coefficient.

If the z-transform of the sequence of primary events associated with M homogeneous blocks is denoted $P_M(z)$ and that of the sequence of higher-order events denoted $O_M(z)$, the dereverberated reflectivity can be written in the general form

$$J_M(z) = P_M(z) + O_M(z) \quad . \tag{11-2}$$

The z-transform of the primary sequence can be expressed

$$P_M(z) = \sum_{j=1}^{M} r_j z^{2N_j} \prod_{k=1}^{j} A_k^{[2n_k]}(z) \tag{11-3}$$

where $N_j = \sum_{k=1}^{j} n_j$.

No simple closed-form expression has been found for the z-transform of the sequence of higher-order events, but it is such that

$$\begin{aligned}
O_1(z) &= 0 \\
O_2(z) &= O_1(z) \\
O_3(z) &= O_2(z) + r_1 r_2 r_3 [q_1 q_3] \\
O_4(z) &= O_3(z) + r_1 r_3 r_4 [q_1 q_4] + r_2 r_3 r_4 [q_1 q_2 q_4] + r_1 r_2 r_4 [q_1 q_3 q_4] \\
O_5(z) &= O_4(z) + r_1 r_4 r_5 [q_1 q_5] + r_2 r_4 r_5 [q_1 q_2 q_5] + r_1 r_4 r_5 [q_1 q_4 q_5] \\
&\quad + r_3 r_4 r_5 [q_1 q_2 q_3 q_5] + r_2 r_3 r_5 [q_1 q_2 q_4 q_5] + r_1 r_2 r_5 [q_1 q_3 q_4 q_5] \\
&\quad + r_1 r_2 r_3 r_4 r_5 [q_1 q_3 q_5] \\
O_6(z) &= O_5(z) + \text{additional higher–order terms associated with } M=6 \\
&\text{etc.}
\end{aligned} \tag{11-4}$$

where the square brackets indicate convolution in continuous time and q_j denotes the polynomial $\{ z^{2n_j} A_j^{[2n_j]}(z) \}$. It may be noticed that the higher-order events are associated with multiples of odd numbers of reflection coefficients in all possible combinations.

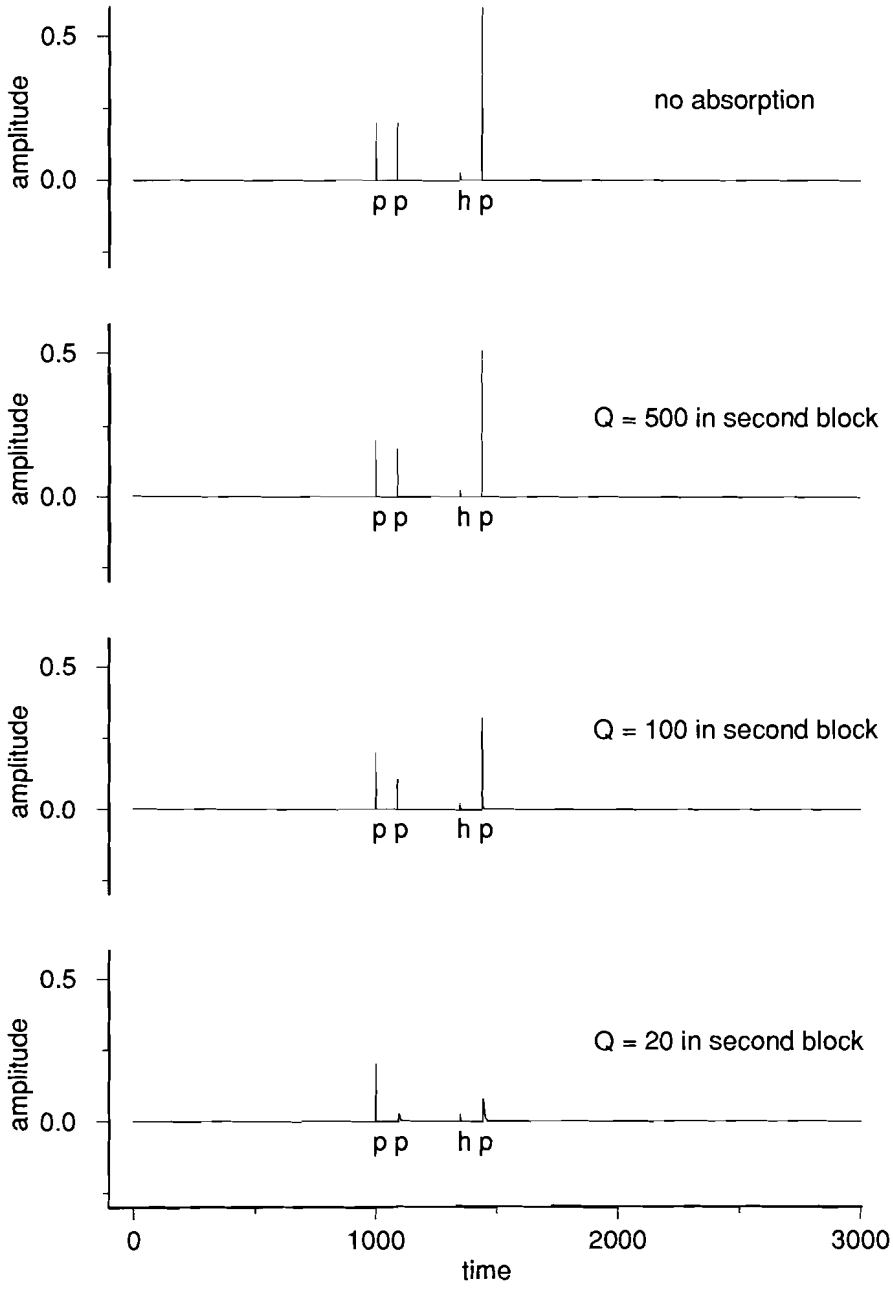

Fig.20: Deverberated non-divergent reflectivity sequences for the illustrative models. (p indicates a primary event, h indicates a higher-order event)

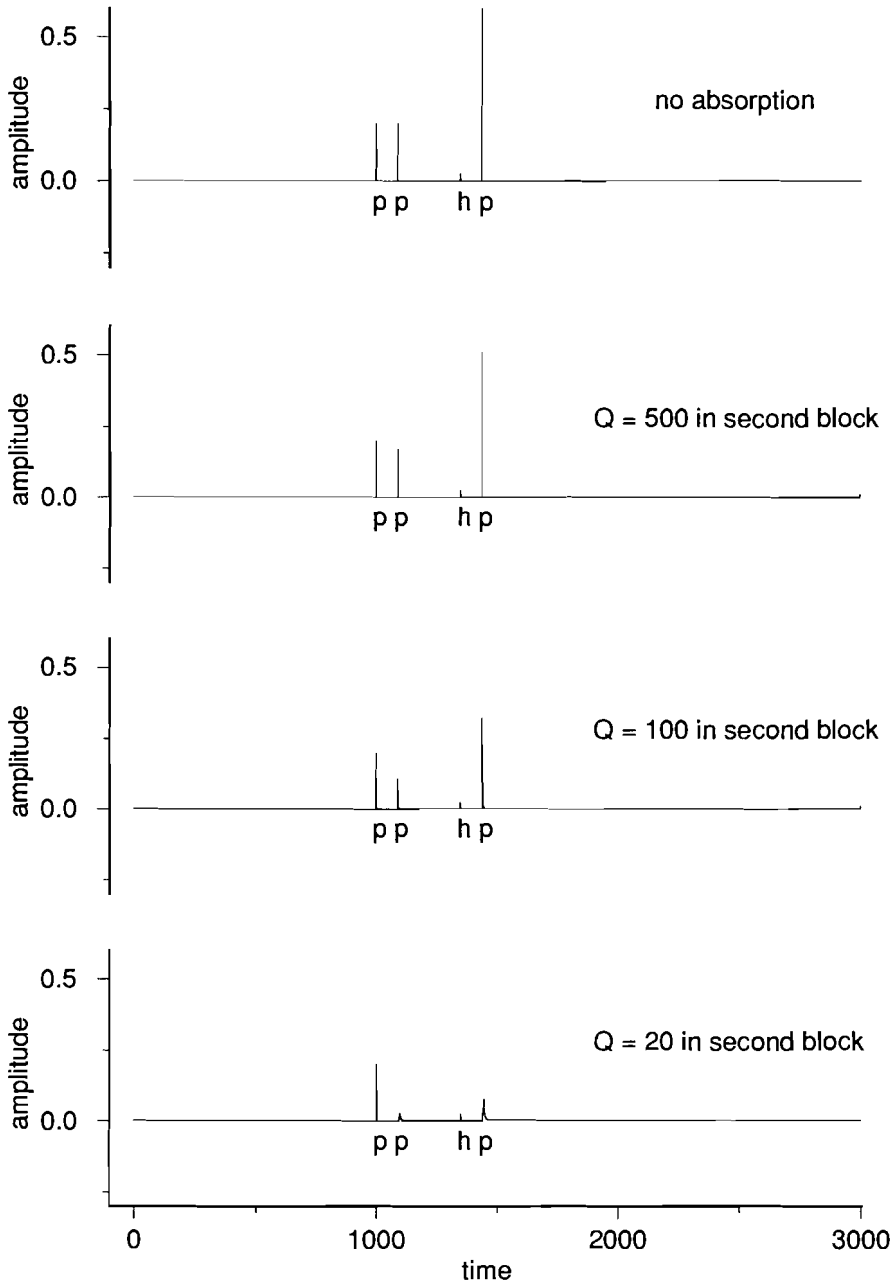

Fig.21: Convolution of dereverberation filters with divergent reflectivity sequences after the application of spherical divergence corrections. Note that there is no obvious distortion in comparison with fig.20. (p indicates a primary event, h indicates a higher-order event)

If the higher-order events could be assumed to be of negligible amplitude, the dereverberated reflectivity could be considered to comprise only primary events. This is, of course, exactly true for systems of one or two homogeneous blocks and would probably be a close approximation for most absorption-free systems of three blocks. If only the second block of a three-block system was absorbing, however, the second and third primaries would be attenuated while the higher-order event was not. This could result in the amplitude of the higher-order event being greater than that of a primary event. (An example of this is seen in fig.20 for Q=20.) Such an assumption could also be invalid for absorption-free systems of four or more blocks, an example being when $r_2 < r_1 r_3 r_4$ in $O_4(z)$ above. Thus it is not possible to simply disregard the higher-order events but, since their locations and amplitudes are known, their presence in the dereverberated reflectivity sequence should cause no difficulty.

The results of convolving the dereverberation filters of fig.19 with the appropriate plane-wave reflectivity sequences of fig.17 are shown in fig.20. Each dereverberated sequence comprises three primary events and one higher-order event. The primary events are located at their correct times for all values of Q, the action of the filter having compensated for the leading zeros in the absorption operators. In the case of no absorption, the primary amplitudes are equivalent to the corresponding reflection coefficients. In the presence of absorption, these amplitudes are reduced. It can be seen that the higher-order event is not affected by absorption and therefore cannot correspond to a wave that propagates through the second block. Its amplitude is not negligible and, for Q=20 , is greater than that of the second primary event. It is possible that the amplitude of the higher-order event could serve as a constraint on estimating the amount of primary amplitude reduction due to absorption.

As a means of checking the distortion caused by applying geometrical corrections in the presence of absorption, the sequences of fig.18 were corrected for spherical divergence and then convolved with the dereverberation filters of fig.19. The results are shown in fig.21. If distortion occurred, it is not obvious in these examples.

Chapter 12

Conclusions

Sequences of multiple reflections other than those confined to the water layer have been observed on single-channel marine seismic profiles. They are commonly observed in industrial waterways where their low rate of decay indicates anomalously high reflection coefficients. They have also been found in apparently natural sea-floor situations of soft soil overlying more competent material where their decay rate is consistent with moderate reflection coefficients. Although such sequences are usually considered to be a form of noise, they can be a source of useful information. Indeed, they may be the only source of information for mechanically sensitive soils such as those which might fail under earthquake loading or of which undisturbed samples cannot be recovered. In areas of industrial outfalls, they provide a means of monitoring, and perhaps even identifying, accumulations of certain effluents.

Both the observation and the analysis of multiple sequences are facilitated if certain conditions are satisfied during data acquisition. The water surface should be calm and both the source and the hydrophone array should be deployed at a very shallow depth. The dimensions of source and receiving array should be small enough that the water bottom is located in the Fraunhofer far field of both. The duration of the source pulse should be as short as possible and always less than the water-bottom reflection time. The offset distance between the source and hydrophones should be less than one-fifth the water depth. The data should be acquired digitally with as large a dynamic range, band width and signal-to-noise ratio as possible. Ideally, the only frequency filter used would be a low-cut filter on the hydrophone output to prevent the preamplifier from being saturated by high-amplitude low frequencies when the array is very close to the source. The digitizing rate should be so high that several samples occur on the steepest part of the pulse. The record length should be long enough that all observable multiples are recorded.

Under these conditions, the reflected portion of field data may be modelled in terms of a far-field source wavelet, a function describing the effect of geometric attenuation, a plane-wave reflectivity sequence and a noise sequence. In the absence of geometric attenuation and absorption, a model of only one dimension (record time) is sufficient to model sea-floor soils that are relatively flat lying. The inclusion of geometric attenuation requires a second temporal dimension, "interwavelet time", that measures the duration of a wavelet relative to its onset. The two dimensions are independent if there is no absorption (or dispersion). There are two methods of accounting for geometric attenuation; one applying a "correction" to the data and the other including the effect in the model. The choice of which to use is mainly dictated by the signal-to-noise ratio. If field data are sufficiently free of noise they can be

spectrally "whitened" to reduce wavelet duration. This is done by inverse filtering if the source wavelet is known or by predictive deconvolution if it is not known but can be assumed to be minimum phase. The "whitened" data can then be corrected for geometric attenuation and the result modelled as if it were simply a reflectivity sequence. If there is too much noise for spectral "whitening" to be feasible and wavelets are of significant duration, the effect of geometric attenuation must be included in the model by applying it to the plane-wave reflectivity sequence. The result is then convolved with the far-field source wavelet in order to obtain the model.

The effect of geometric attenuation is often expressed as a power law. The exponent of the power law depends on the shape of the wave front, being unity for spherical waves and zero for plane waves. If the shape of the wave front is not known, the value of the exponent must be determined empirically. A scheme has been described by which an empirical estimate of the power law exponent can be obtained from the water-layer multiple sequence. It exploits the fact that water is absorption-free in the range of seismic frequencies.

An expression has been derived which gives the plane-wave reflectivity sequence in terms of the temporal thickness of layers, the reflection coefficients at interfaces and the absorption characteristics within layers. The reflectivity sequence contains all possible multiple sequences. Each sequence consists of impulses located at a time interval equal to the total temporal thickness of the layers giving rise to the sequence. In the absence of absorption the impulses have no duration, i.e. they are "spikes", and their amplitudes decay at a rate governed by the reflection coefficients involved. The effects of absorption are to increase the decay rate and to progressively broaden the impulses as high frequencies are preferentially attenuated. A reflectivity sequence may be calculated for any number of layers, but sequences corresponding to more than a few layers are rarely required. Reflectivity sequences are never minimum phase unless shifted in time so that their first nonzero element (corresponding to the reflection from the sea floor) is located at time zero. If so shifted, the reflectivity of a single layer is always minimum phase. This is not necessarily true for systems of more than one layer. In particular, the shifted reflectivity of a two-layer non-absorbing system comprising water and soil over bedrock is minimum phase only if the magnitude of the reflection coefficient between water and soil is larger than that between soil and bedrock. If the coefficient between soil and bedrock is larger, as it appears to be on some profiles presented in Chapter 2 (i.e. fig.2 and, possibly, fig.6), the reflectivity sequence is not minimum phase. In such a case, statistical techniques of multiple suppression that assume minimum phase (such as predictive deconvolution with a long operator) would fail.

A scheme has been described by which the effect of absorption can be determined from the spectra of individual wavelets within a reverberatory sequence. It assumes that above some arbitrarily low cutoff frequency the power loss per seismic cycle is independent of frequency. In that case the seismic quality factor Q is said to be "nearly constant". Such an effect can be modelled using the causal operator of Carpenter (1966). Examples of operators for various values of Q illustrate how this is done. The discrete representations of these operators have at least one leading zero. These leading zeros are equivalent to timing errors and can be reduced only by increasing the digitization rate and digital resolution.

Plane-wave reflectivity sequences associated with realistic three-layer models and incorporating "nearly constant Q" absorption have been computed for various values of Q. The presence of the leading zeros in the absorption operators are seen to be indistinguishable from changes in layer thickness and therefore can be considered to be a source of error when estimating model parameters. The effect of spherical geometric attenuation has been applied to these sequences to simulate divergent reflectivity sequences.

If the temporal thickness of layers, reflection coefficients and absorption characteristics are determined (or estimated) in some manner, it is possible to describe a finite-length sequence that attenuates multiple events when convolved with zero-offset data that have been corrected for geometric attenuation. It is called the dereverberation filter and is a minimum-phase sequence whose z-transform can be written as the continued product of as many factors as there are layers. Each factor therefore corresponds to a minimum-phase sequence. One factor is a polynomial but the others are rational functions that have a number of poles. This prevents their use as individual filters to "strip" reverberatory sequences for the seismogram one layer at a time. The factors are related in a recursive way that succinctly (and deterministically) describes the structure of the dereverberation filter. The recursive relationship is nonlinear regardless of whether or not absorption is present. Filters obtained by means of it are more generally applicable than are filters obtained by linear inversion which requires that the primary events be uncorrelated. Dereverberation filters for the illustrative three-layer models have been presented.

The result of convolving a dereverberation filter with its corresponding reflectivity sequence has been examined in detail. The deverberated reflectivity sequence comprises a number of events; a primary event located at the travel time of the reflection from the bottom of each layer plus, for systems of three or more layers, higher-order events that are not associated with ray paths. The amplitudes of the primary events are equal to the reflection coefficients at the interfaces. The amplitudes of higher-order events are equal to the product of an odd number (three or more) of reflection coefficients. They are therefore generally of small magnitude, but they can be significant in certain situations. One such situation has been illustrated. Dereverberated reflectivity sequences are never minimum phase because they have at least one leading zero. For a one-layer system, the sequence produced by shifting the time origin to the location of the reflection from the bottom of the layer is minimum phase if the total absorption operator for the layer is minimum phase in discrete time (which depends on the digitization rate). Time-shifted dereverberated reflectivities of systems of more than one layer can be minimum phase or not, depending on the relative magnitudes of reflection coefficients as well as the properties of absorption operators in discrete time. The effect of dereverberation has been illustrated by convolving the filters obtained previously with the reflectivity sequences of the various models. Results for one model illustrate the fact that a higher-order event can be of greater magnitude than a primary event after dereverberation. The dereverberation filter of each model has been convolved with both the plane-wave reflectivity sequence and the simulated divergent reflectivity after correction for spherical geometric attenuation. Even though the filter is strictly correct only for the plane-wave sequence, no obvious distortion results from its application to the corrected divergent sequence. Although no general conclusion can be drawn from this particular result, it indicates that, at least in

some cases, real data that has been corrected for geometric attenuation might be successfully dereverberated by means of the deterministic filter.

Many of the procedures described herein postulate digitization rates that are higher than usual. Extremely high digitization rates make it expensive both in time and in money to simply store raw data in memory for later processing. It would be better to do at least some of the processing in near-to-real time. If wavelets are separable, the processing required is basically simple; adequate geometric corrections being the most severe problem. It could be done very efficiently by using digital hydrophone arrays and hardware dedicated to specific algorithms. Then only the preprocessing output and relevant parameters would need to be stored. If wavelets are not separable, previously determined, or average, parameters could be tried. If the results are not satisfactory for any reason, parameters could be changed and the data reacquired immediately. This would amount to a "cut-and-try" field philosophy but in many instances would be preferable to extensive post-survey processing, especially when profiling results are required without delay, as is often the case when sampling or dredging and in other engineering situations.

Appendix A

The Control of Noise During Single-channel Seismic Profiling

Introduction

The intention here is to discuss types of noise commonly encountered during high-resolution marine seismic profiling and to describe procedures that have been found to be effective for reducing their effects. Many users of single-channel marine seismic profiling obtain data of drastically reduced quality due to the presence of noise. Unnecessarily noisy situations are tolerated because either the user does not recognize it or is not familiar with appropriate remedies. An inability to observe subbottom reflections, particularly in saturated unconsolidated soils, is often due to a noise level that precludes recognition of the seismic signals. When results are not satisfactory, the first suspicion should be that noise is responsible, not that there is a lack of penetration or that there are no reflectors to observe. If noise is low, recording gain can be increased to permit observation of extremely weak reflections.

Since no realizable data acquisition system can be entirely noise free, the total elimination of noise is not a practical objective. Rather, the objective should be to reduce system noise to whatever level is required in order to achieve the desired resolution. This usually entails minimizing noise within a desired frequency band and spacial configuration. The noise level outside the signal's band width can be reduced by the system's band-pass filters. Noise propagating outside the signal's spacial configuration can be attenuated by system geometry. Insofar as noise is coincident with signal, however, it must be reduced at its source.

Any loss of resolution is considered to be the result of noise in the system. The sources of resolution loss can be categorized as electrical, operational or geometrical. Useful techniques for minimizing the effects of many such sources have been developed during research and practice. Successful utilization of these techniques does require some planning, effort and sensitivity to the problem, however. The most effective method of reducing total system noise is to approach it in a logical manner, category by category. This is not as difficult a procedure as might be supposed, but it must be followed rigorously. No identifiable noise source should be neglected because it does not seem to be a major source. Success in reducing total system noise is usually the result of many small improvements.

The Resolution of Seismic Signals and the Definition of Noise

Signals produced by seismic sources are characterized according to frequency content, pulse length and consistency of pulse shape. The capability of a seismic signal to resolve smaller detail improves as its power spectrum becomes broader and smoother, as its pulse length becomes shorter and as its pulse shape becomes more repeatable from shot to shot. The specification of a desired resolution serves to identify which combinations of these characteristics are acceptable. Noise is defined to be any effect that degrades resolution. The level of noise in a given situation is quantified relative to the level of the signal. The relative quantity is called the signal-to-noise ratio. Theoretically, it can be "improved" by either increasing the signal or decreasing the noise.

Although the various types of seismic sources are often referred to as if each type inherently provides a certain resolution, achievable resolution largely depends on the power level of operation. For example, although boomer sources are usually considered to be capable of higher resolution than airgun sources, a small-capacity airgun can sometimes resolve smaller detail than can a high-energy boomer. In fact, the operating level of most conventional sources is usually more critical to resolution than is the type of source because, with increasing power level, the tendency is toward a preferential enhancement of lower frequencies and a longer, more erratic pulse. This has been quantified as the Rayleigh-Willis relation (Kramer, Peterson and Walter, 1968). The implication is that, if resolution is to be maintained, there is little freedom to improve the signal-to-noise ratio by increasing the signal strength. The only alternative is to decrease the noise level at its source.

The Reduction of Electrical Noise

The control of electrical noise requires that all electronic equipment be of good quality and be mutually compatible. It should be well maintained and thoroughly bench checked before being installed on board ship. The installation should be closely supervised by a competent technician. Since most electrical noise encountered on a ship is associated with grounding, the supervising technician should take care that a good grounding procedure is followed consistently during installation. Ground "loops" should be avoided. Since ship's ground often fluctuates when shipboard equipment such as pumps, refrigerators, radios, radars, etc. switch on and off, the seismic receiving equipment (hydrophone array, amplifier, recorder, oscilloscope, etc.) should be powered by an isolated supply and grounded separately. When profiling on salt water the receiving system should be grounded directly to the sea. The sea ground should be heavily weighted so that it tows more than a metre below the surface to avoid patches of fresh water that can occur. Surficial fresh water often accumulates near shore after an extended period of calm weather and A.C. noise increases when the receiver ground is towed into it. When profiling on fresh water, it may be necessary to use a "floating" ground on the receiving system. A major source of electrical noise that is often overlooked is the key pulse line by which the receiving system triggers the source. The electrical connection it forms should be eliminated by triggering through an optical

isolator. This is especially important when using high-voltage sources such as boomers or sparkers.

Electrical noise can also be caused by induction. Power cords and signal cords should be well separated, an easily remembered rule being "Power lines on port side, signal lines on starboard side". All electrical lines should be as short as possible and any excess length should be looped in figure-8 patterns rather than being coiled. Radars, radios and other high-voltage ship's equipment should not be operated during data acquisition. It is often necessary to operate a microwave positioning system and special care should be taken that it and all cables related to it are well removed from signal lines and the recording equipment.

These precautions will not necessarily eliminate all electrical noise, but they will simplify the task of locating remaining sources. All sources of electrical noise should be identified and their effects minimized while the ship is still at dock side. A few hours spent here will be rewarded amply at sea.

The Reduction of Operational Noise

The most common sources of operational noise are the survey vessel, other activities in the survey area, towing procedure and sea state. The easiest way to diagnose which sources are contributing to a particular noise problem is to listen to a speaker tapped into the hydrophone signal line. This allows the recognition power of the ear to be used for identifying sounds that would not be obvious on a visual presentation. For example, the ear immediately distinguishes between the clanking of machinery and the gurgling of water, but the two have a very similar appearance on a record. Mechanical sounds indicate that either the survey vessel or nearby machinery is the source. When the sound of water is heard, either the towing of equipment or wave action is creating noise. When the operational noise is low, the speaker is quiet except for the sound of the seismic source quickly followed by a decreasing train of reverberations and echoes. If the source is a low-power boomer, the sound is reminiscent of the sonar in old submarine movies. If the source is a large airgun, a roar is heard.

The best way to minimize the noise of the survey vessel is to choose a quiet ship. Older wooden work boats with slow turning engines and dry exhaust are usually very quiet if the shaft, propeller and rudder mounts are in reasonably good condition. Vessels with steel hulls and powerful, hard-mounted engines tend to be noisy, especially at higher engine speeds. Underwater exhaust is noisy on any vessel, particularly in combination with an outboard drive. Variable pitch propellers and bow thrusters also tend to be very noisy.

If a quiet ship is not available, the next best solution is to tow the hydrophones at some distance. This is not always the simple solution it seems to be, especially in shallow water. Depending on the type of sea floor, the required tow distance may be found to be rather great because the ship's noise, being reflected from the sea floor and trapped in the water layer, strikes the hydrophones broadside and decreases slowly with distance. If a large hydrophone tow distance is used, the source must also be towed to avoid destroying the source-receiver geometry that is so important in shallow-water

work. If the source is towed, it is usually necessary to attach floatation to its heavy power cable. Further complications arise because long tow distances hamper manoeuverability and become more than a nuisance when profiles must be run near to shore.

Noise due to other activities in the work area may be associated with the survey work or may be totally unrelated. That associated with the work is easiest to control. A common source is a support vessel approaching or accompanying the survey vessel. Support vessels should stand by at a large distance during data acquisition. Other sources, such as dredges, may have periodic interruptions for maintenance or location change. An attempt should be made to schedule work in the immediate vicinity during such interruptions. If the source is traffic in a shipping lane, work must be done as the opportunity arises. This problem can be quite severe. For example, the noise from a labouring steel-hulled tug has been observed to obliterate seismic data at a distance of several kilometres. Profiling was interrupted for more than two hours while it passed through the survey area.

Tow noise is decreased by fairing all towed equipment and cables so that the "strumming" caused by vortex shedding is eliminated. The hydrophones should be extremely fair and not oscillate under tow. If eel-type hydrophone arrays are used, they should not be coiled tightly for storage or shipment. If they cannot be kept straight, they should be loosely looped in a figure eight pattern and then laid straight in a warm place for as long as possible before use.

Sea-state noise is best avoided by attempting to schedule work during periods of good weather. If work must be done in a choppy sea, its noise may be reduced by deploying the hydrophones in the lee of the survey vessel or, if they must be astern, by increasing their tow depth. Any increase of tow depth should be kept minimal, however, in order to limit the loss of resolution caused by the surface (ghost) reflections.

The Improvement of Resolution by System Geometry

Certain geometrical aspects of source and receiver deployment are important for the attainment of high resolution because they affect the length and shape of the signal pulse. Included among these are the distance between source and hydrophone array, the physical dimensions of source and/or hydrophone arrays and the depth below the water surface that the array is deployed. A poor choice of any of these can degrade resolution and therefore each constitutes a potential source of noise.

The distance by which the source is offset from the hydrophones is important because it influences the seismic power that is transmitted through the sea floor and thus made available for providing subbottom information. As offset distance increases, the angle of incidence between the seismic wave front and the water bottom varies from 0^o (normal incidence) to 90^o (grazing incidence). Normal incidence occurs when the offset distance is zero. If the speed of propagation in the water is constant, grazing incidence occurs at infinite offset. If the speed of propagation increases with depth, grazing incidence occurs at a finite offset distance. Seismic power in the water exists as compressional waves (p-waves) because water has no rigidity. If the subbottom material exhibits rigidity, power transmitted through the sea floor can exist as both

Type of Sediment	Measured		Calculated values of b		
	a	d	k=0.9	k=1.0	k=1.1
light clay	0.97	1.3	.437	.359	.276
silt	1.00	1.7	.594	.556	.514
dense clay	1.00	2.2	.666	.640	.612
sand	1.15	2.0	.809	.785	.761

Table A-1: Typical Parameter Ratios Across Water/Sediment Interfaces

compressional and shear waves (s-waves). In general, a p-wave incident to the sea floor is partitioned into a reflected p-wave, a transmitted p-wave and a transmitted s-wave. By conservation of energy, the total power reflected and transmitted is equal to the incident power. Expressions for ratios of reflected and transmitted energy (or power) to incident energy (or power) at a liquid/solid interface are given by Ergin (1952). Each ratio is a function of angle of incidence as well as contrasts in density and speed of propagation between the liquid and the solid. A well-known result of elastic wave theory is that the speed of propagation of p-waves, c , and that of s-waves, s , are related to the elastic parameters incompressibility, κ , rigidity, μ , and density, ρ , by

$$c^2 = \frac{1}{\rho}\left[\kappa + \frac{4}{3}\mu\right] \qquad \text{and} \qquad s^2 = \frac{\mu}{\rho} \ .$$

In terms of contrasts across a liquid/solid interface, since a liquid exhibits no rigidity, it is possible to combine these and write

$$b^2 = \frac{3}{4}\left[a^2 - \frac{k}{d}\right] \qquad \text{(A-1)}$$

where a is the ratio of the p-wave speed in the solid to that in the liquid,
b is the ratio of the s-wave speed in the solid to the p-wave speed in the liquid,
k is the ratio of the incompressibility of the solid to that of the liquid and
d is the ratio of the density of the solid to that of the liquid.

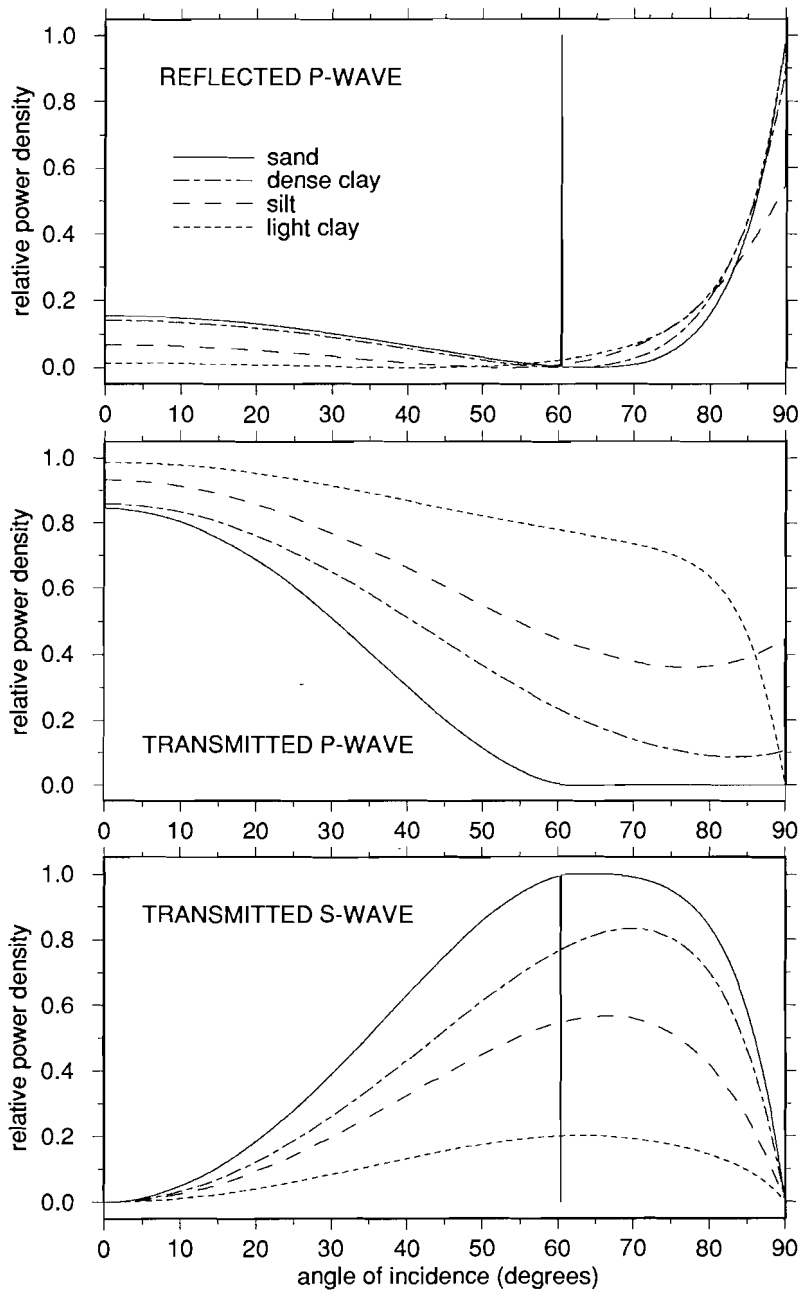

Fig.A-1: Ratios of the power of reflected and transmitted waves to the power of a p-wave in water incident to typical marine sediments assuming that the ratio of the incompressibility of the sediment to that of water is equal to 0.9 .

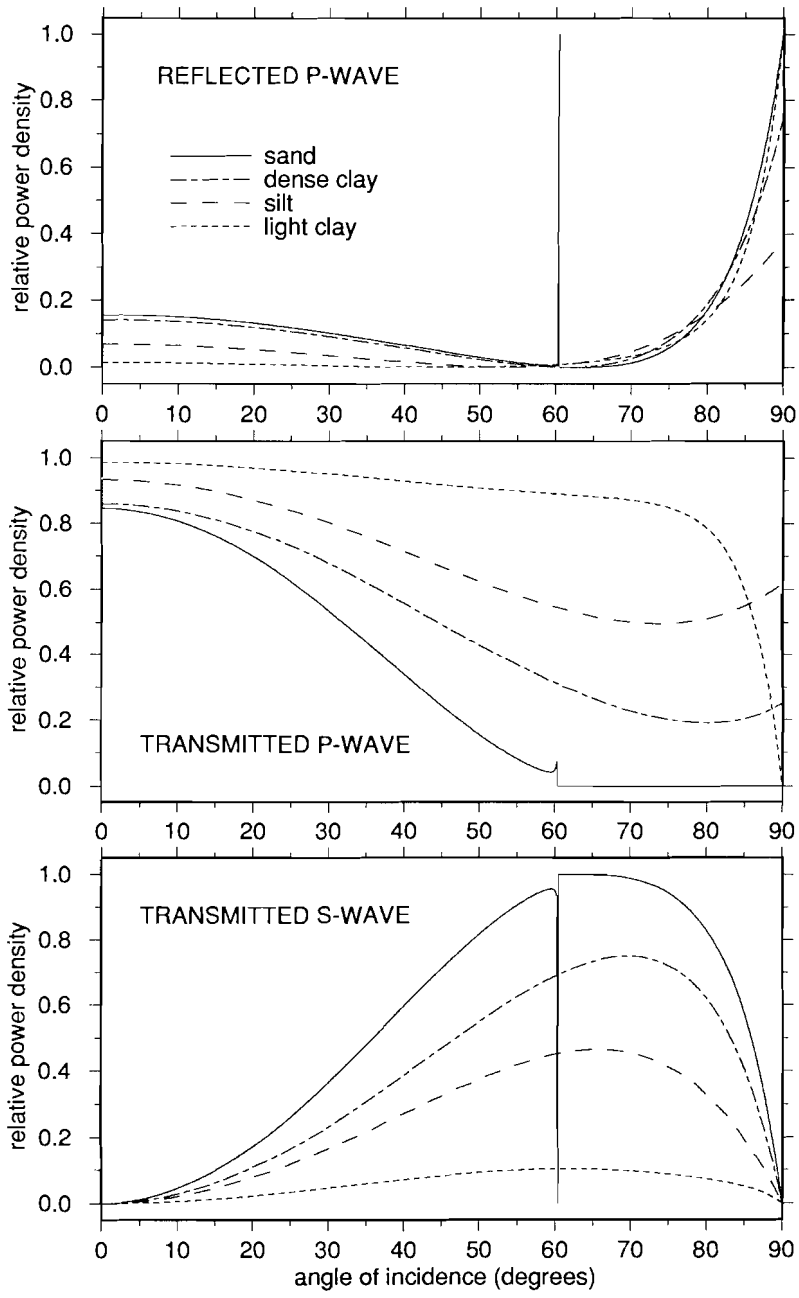

Fig.A-2: Ratios of the power of reflected and transmitted waves to the power of a p-wave in water incident to typical marine sediments assuming that the ratio of the incompressibility of the sediment to that of water is equal to 1.0 .

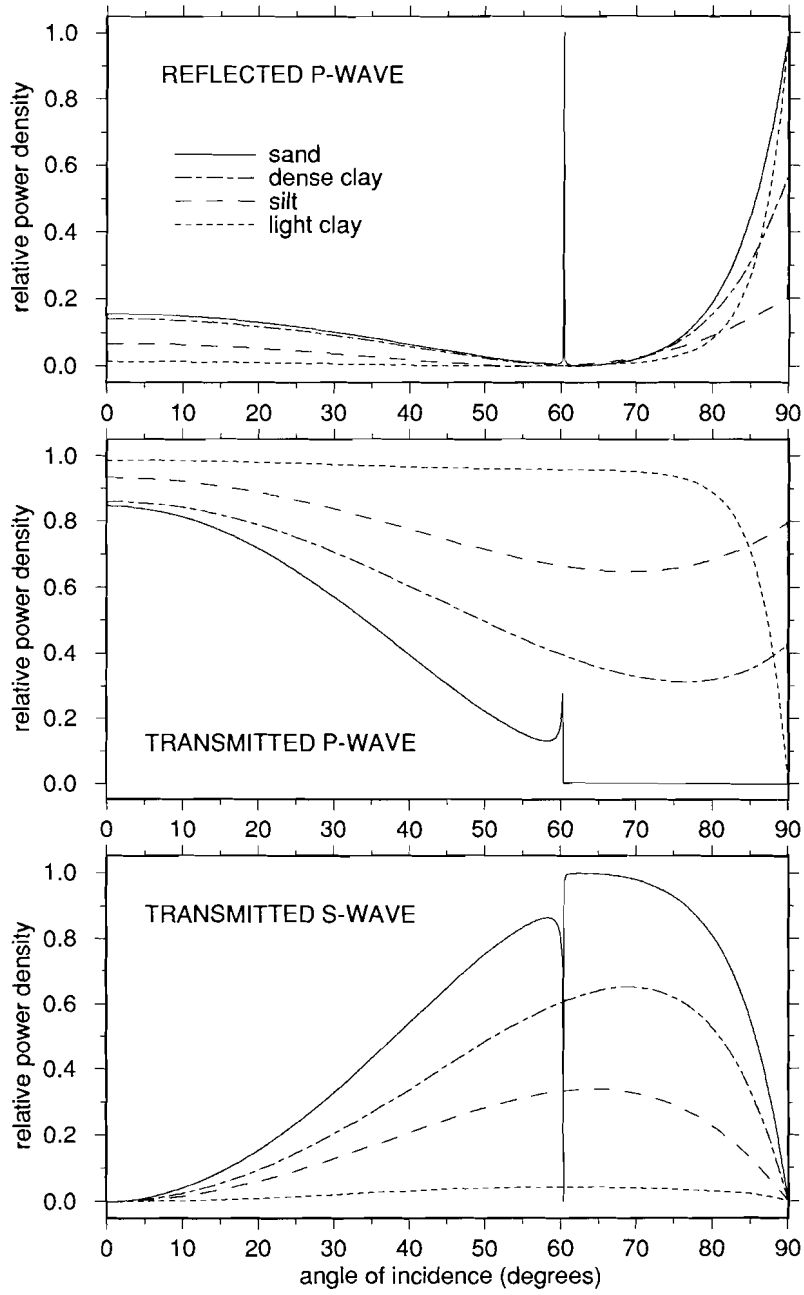

Fig.A-3: Ratios of the power of reflected and transmitted waves to the power of a p-wave in water incident to typical marine sediments assuming that the ratio of the incompressibility of the sediment to that of water is equal to 1.1 .

Measurements of density and p-wave speed in marine sediments have been published by Hamilton (1972). Since $\rho \simeq 1$ and $c \simeq 1500$ metres per second in water, it is possible to use those measurements to determine typical values of ratios a and b for various types of sea-floor material. A set of such values is given in the "measured" columns of Table A-1. Except for special cases in which gas is present, one expects sea-floor sediments to be fully saturated with water and their incompressibility to be similar to that of water. Thus it is reasonable to assume a value of k near unity and use eq.(A-1) to calculate typical values of b.

Reflected and transmitted power-density ratios calculated per Ergin (1952) for the tabulated values are plotted versus angle of incidence in Fig.A-1 for k=0.9, in Fig.A-2 for k=1.0 and in Fig.A-3 for k=1.1. It can be seen that, regardless of the value of k, the maximum density of transmitted compressional power occurs at normal incidence. The curves are rather flat up to almost ten degrees, however, so there is not much loss of transmitted power if the offset distance is slightly different from zero. That is fortunate because there is, of course, a practical limit to how small the offset can be. Obviously, the hydrophones should not be so close to the source that they sustain damage. They can, however, be quite close if the hydrophone signal passes through a low-cut filter prior to amplification to prevent saturation of the preamplifier by high-amplitude low frequencies. The minimum feasible offset usually depends on the level of noise associated with the towing of the source. When the hydrophones are positioned near the source they pick up the sound of turbulent water which is broad band and cannot be filtered out. As they are moved closer noise level becomes unacceptable and thus establishes the minimum distance that can be used.

The principal concern in regard to array dimensions is to avoid configurations that produce interference patterns detrimental to resolution. When an array of hydrophones and/or sources is used, both the spacing of array elements and the total size of the array are significant quantities. Element spacing is often equidistant, but that is not necessary. The distance between array elements should be short compared to the wavelengths of interest in order to reduce the height of side lobes in the spacial response of the array. If the output of the array is a sum of the outputs of individual elements, possibly incorporating linear time shifts (but not nonlinear time shifts), the total size of the array should be such that the ray paths to and from the shallowest reflector of interest can be considered to be parallel. In single-channel work the shallowest reflector of interest is usually the sea floor. Parallel ray paths are described by Fraunhofer diffraction (Born and Wolf, 1959). Thus the dimensions of source and/or receiver arrays should be small enough that the sea floor is in their Fraunhofer far field. They should not be smaller than necessary, however, in order to retain as much as possible the advantages of their use (directivity, noise rejection, etc). Therefore there is good reason to determine the array size that is suitable to any particular situation. The way of doing this can be illustrated by an example. The geometry of a common field situation, a point source and linear hydrophone array deployed on the water surface, is shown in Fig.A-4. The length of the array is L and the source is offset in line with it by a distance X. The depth of the water is D. The shortest and longest reflection distances

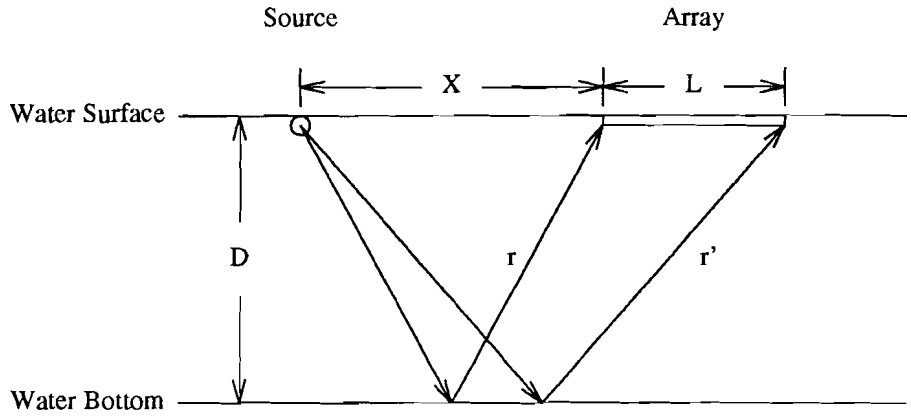

Fig.A-4: Reflection geometry of source offset in line from linear hydrophone array.

from source to receiver, r and r', respectively, are such that

$$r^2 = X^2 + 4D^2 \qquad \text{and} \qquad r'^2 = (X+L)^2 + 4D^2 \ .$$

Subtracting the first from the second,

$$r'^2 - r^2 = (r'+r)(r'-r) = L\,(2X+L) \ .$$

Letting $(r'-r) = \Delta r$,

$$\Delta r = \frac{L\,(2X+L)}{2r+\Delta r} = \frac{L\,(2X+L)}{2r}\,\frac{1}{1+\dfrac{\Delta r}{2r}} \ .$$

Since $r > \Delta r$,

$$\Delta r = \frac{L\,(2X+L)}{2r}\sum_{n=0}^{\infty}\left[\frac{-\Delta r}{2r}\right]^n = L\,(2X+L)\left[\frac{1}{2r} - \frac{\Delta r}{4r^2} + \frac{\Delta r^2}{8r^3} - \frac{\Delta r^3}{16r^4} + \cdots\right]$$

and there is some term in the series beyond which higher-order terms may be neglected. The Fraunhofer approximation retains only the first term. (Retaining the first two terms

is called the Fresnel approximation.) The Fraunhofer assumption is that $\Delta r / r^2$ is a negligibly small quantity and therefore that

$$\Delta r \approx \frac{L\,(2X + L)}{2r}$$

which may be solved for

$$L \approx \sqrt{X^2 + 2r\Delta r} - X \quad .$$

If a signal of wavelength λ is in phase at all elements of the array, the distances propagated to the elements cannot vary by more than a small portion of λ. This requires that $\Delta r \ll \lambda$. The length of the array must therefore be such that

$$L \ll \sqrt{X^2 + 2r\lambda} - X \tag{A-2}$$

which, at zero offset, reduces to

$$L \ll 2\sqrt{\lambda D} \quad . \tag{A-3}$$

If the signal is a seismic wavelet, λ is its dominant wavelength. Considering the wavelet to be comprised of a continuous distribution of frequencies, its dominant wavelength is the speed of propagation divided by a dominant component of its power spectrum. Frequencies higher than that will correspond to shorter wavelengths and, in practical situations, there will be a highest frequency of interest that corresponds to some λ_{min}, the shortest wavelength of interest. If the band width of the wavelet is sufficiently broad, $\lambda_{min} \ll \lambda$ and the maximum array length appropriate to the situation can be estimated to be

$$L_{max} \quad \text{on the order of} \quad \sqrt{\lambda_{min} D} \quad \text{if} \quad \lambda_{min} \ll D \quad . \tag{A-4}$$

This is a useful rule-of-thumb for designing eel-type hydrophone arrays to receive seismic pulses of short duration such as those produced by "boomer"-type sources.

The depth below the water surface at which the source and hydrophones are deployed is an important geometrical parameter because the effective signal pulse consists of a primary pulse followed by its reflection from the surface. As the depth below the water surface increases, the surface reflection lags further behind the primary pulse, thereby increasing the total length of the effective signal pulse and adversely affecting resolution. Of course, the source and hydrophones must be located some distance below the surface in order to function properly, but resolution is improved by that distance being minimal. It should also be as constant as possible because if the depth of tow varies, perhaps due to sea state or tow instability, the surface reflection time will vary from shot to shot and the effective signal pulse will be inconsistent from trace to trace and result in a loss of resolution.

Conclusions

The resolution available on marine seismic profiles is closely related to the signal-to-noise ratio. Since resolution tends to decrease as source power increases, the most effective way of increasing the signal-to-noise ratio is to reduce noise at its source. Significant improvements usually can be obtained by considering potential noise sources in a systematic fashion. An outline of principal concerns which always should be addressed has been given here. Efforts made to satisfy these concerns usually will improve results and sometimes can make the difference between sufficient resolution and no data at all.

Appendix B

The Theoretical Structure of Power Spectra

The structure of stochastic power may be further investigated by appealing to certain results of probability theory. That theory describes statistical properties of a stochastic process in terms of its *probability distribution function*. A probability distribution function is a monotone nondecreasing function defined over the range of the stochastic parameter. Its value varies from zero at the lower end of the range to unity at the upper end. If the autocovariance function of a weakly stationary process is normalized by the dispersion of the process, it may be described in terms of the probability distribution function $P(\omega)$ by the Riemann-Stieltjes integral

$$\frac{\phi(\tau)}{\phi(0)} = \int_{\Omega} e^{i\tau\omega}\, dP(\omega) \tag{B-1}$$

where Ω is the range $(-\pi/\Delta\tau < \omega \leq \pi/\Delta\tau)$ and the stochastic parameter τ is discretely spaced at interval $\Delta\tau$ such that $\tau=n\Delta\tau$, n being an integer. If τ is measured in τ-units, ω is measured in radians per τ-unit.

A theorem by Lebesque states that $P(\omega)$ may be uniquely decomposed into three "elemental" distribution functions, i.e.

$$P(\omega) = P_a(\omega) + P_b(\omega) + P_c(\omega) \tag{B-2}$$

where $P_a(\omega)$ is a set of step functions that are, at most, countably infinite in number,
$P_b(\omega)$ is a continuous function with derivative zero almost everywhere,
$P_c(\omega)$ is absolutely continuous, i.e. continuous with bounded variation.

Each component function would be a probability distribution function if it were normalized to its value at $\omega=\pi/\Delta\tau$. The phrase "almost everywhere" is intended to mean "at all points of the interval of definition except at a set of isolated points which may be, at most, denumerably infinite in number."

The first component may be written as a sum of Heaviside step functions of varying amplitude. Since the Heaviside function is not defined at the point of the step, mathematical completeness requires the existence of the second component to define it there. If the value of each Heaviside function were defined at the step, as could be done, for example, by requiring continuity-on-the-right, $P_b(\omega)$ could be included in

$P_a(\omega)$ and $P(\omega)$ would be decomposed into only two distribution functions, the first being

$$P_a(\omega) = \sum_k p_k \, h(\omega-\omega_k) \quad , \tag{B-3}$$

where $h(\omega)$ is the continuous-on-the-right unit step function. The coefficients p_k are positive and equal to the magnitudes of the steps. Summation is over the set of points that are the locations of the steps. Since the third component is absolutely continuous, it may be described by

$$P_c(\omega) = \int_{-\pi/\Delta\tau}^{\omega} p(\lambda)\, d\lambda \quad , \tag{B-4}$$

where $p(\omega)$ is the derivative of $P_c(\omega)$. It is called the *density function* of the process and, by definition, is nonnegative, bounded and approaches zero as $|\omega| \rightarrow \pi/\Delta\tau$. Combining eq.s (B-1) thru (B-4) it is possible to write

$$\phi(\tau) = \sigma(\tau) + \psi(\tau) \tag{B-5}$$

where

$$\sigma(\tau) = \phi(0) \sum_k p_k \, e^{i\tau\omega_k} \tag{B-6}$$

and

$$\psi(\tau) = \phi(0) \int_{\Omega} p(\omega)\, e^{i\tau\omega}\, d\omega \quad . \tag{B-7}$$

This shows that, in the general case, the autocovariance function of a weakly stationary process can be separated into two parts, both of which are scaled by the dispersion of the process.

The first part, $\sigma(\tau)$, is proportional to the discrete Fourier transform of the distribution of step functions and is periodic because the series is a linear combination of periodic functions. Since the number of step functions is countable, it is possible to define an interval, $\Delta\omega$, sufficiently small that the locations of the steps may be written $\omega_k = k\,\Delta\omega$ where k is an integer. In terms of this interval, the period of $\sigma(\tau)$ is $2\pi/\Delta\omega$, i.e. $\sigma(\tau) = \sigma(\tau \pm 2\pi k/\Delta\omega)$ for all τ and k. If $\sigma(\tau)$ is considered to be an autocovariance function, there is a stochastic process $Y(t)$ that corresponds to it. It can be proved that, if $\sigma(\tau)$ is periodic, any particular value $Y(t=a)$ can be predicted with zero mean-square-error by a linear combination of values $Y(t<a)$. For this reason, $\sigma(\tau)$ is said to correspond to a *purely deterministic* process. The power spectrum of a purely deterministic process consists of a set of discrete spectral lines located at frequencies ω_k with amplitudes p_k.

The second part, $\psi(\tau)$, is proportional to the continuous Fourier transform of the density function $p(\omega)$. Considered to be an autocovariance function, $\psi(\omega)$ corresponds to a stochastic process that may or may not be purely deterministic, depending on the nature of $p(\omega)$. A weakly stationary stochastic process is defined to be *purely nondeterministic* if, and only if, its distribution function is absolutely continuous, i.e. $R(\omega) \equiv R_c(\omega)$, and its density function is such that

$$\left| \int_{\Omega} \log p(\omega)\, d\omega \right| < \infty \quad . \tag{B-8}$$

This condition is satisfied only if the zeros of $p(\omega)$ comprise a set of points that contributes nothing to the integral, i.e. a set of isolated points that are, at most, countably infinite in number. This is equivalent to the probability being zero that the corresponding process is totally devoid of any particular spectral component. Inequality (B-8) is known as the Paley-Wiener criterion (Paley and Wiener, 1934). If it is satisfied, the normalized autocovariance function is the Fourier transform of the density function, i.e. eq.(B-7) forms a Fourier pair with

$$\phi(0)p(\omega) = \frac{1}{2\pi} \sum_{\tau=-\infty}^{\infty} e^{-i\tau\omega} \psi(\tau) \quad . \tag{B-9}$$

The continuous function $\phi(0)p(\omega)$ is called the *spectral density* and is the power spectrum of a purely nondeterministic process. The spectral density is real valued, nonnegative and passes through the origin, i.e. $p(0) = 0$. If the stochastic process is real, the spectral density is symmetrical about $\omega = 0$.

It should be noted that convergence of the infinite series in eq.(B-9) requires that $\psi(\tau)$ vanish as τ increases. This implies that a purely nondeterministic process is uncorrelated for large lag values. The amplitude of its autocovariance function tends to decrease with increasing lag value, except for local maxima, and approaches zero as its limiting value. This is in contrast to the autocovariance function of a purely deterministic process which has correlation maxima periodically as the lag values become unbounded. Therefore, a lack of correlation at large lag values is a characteristic useful for identifying purely nondeterministic processes.

A complete discussion of deterministic and nondeterministic processes is presented in Grenander and Rosenblatt (1957). In general, a weakly stationary stochastic process can be partly deterministic and partly nondeterministic. Its power spectrum is then the sum of a line spectrum and a continuous spectrum. The line spectrum, given by eq.(B-6), is the Fourier series of a periodic process and the continuous spectrum, given by eq.(B-7), is the Fourier transform of an aperiodic process. The periodic process is said to be purely deterministic and its spectrum comprises amplitude values at discrete frequencies that are separated by ranges of frequencies throughout which amplitudes are identically zero. The aperiodic process is said to be purely nondeterministic and its spectrum has nonzero amplitudes everywhere except at a discrete set of frequencies that are, at most, countably infinite in number.

For physical processes that oscillate about a null point, such as seismic waves, one such discrete zero amplitude is located at zero frequency. This is intuitively plausible since, for such processes, a nonzero amplitude at zero frequency represents a D.C. component. A D.C. component is periodic since $\sigma(\tau) = \sigma(\tau \pm 2\pi k/\Delta\omega)$ for every nonzero choice of $\Delta\omega$. If it is not removed prior to spectral transformation it will cause low-frequency distortion.

Finally, by the Paley-Wiener criterion, if the spectrum of a process is zero over any continuous range of frequencies it is entirely periodic. All band-limited processes are therefore periodic.

References

Aminzadeh, F. and Mendel, J. 1983. Normal incidence layered system state-space models which include absorption effects. Geophysics **24**, 259-271.

Born, M. and Wolf, E. 1959. Principles of optics. Pergamon Press.

Carpenter, E.W. 1966. Absorption of elastic waves - an operator for a constant Q mechanism. United Kingdom Atomic Energy AWRE Report, reprinted in Seismic Wave Attenuation, Geophysics Reprint Series No.2, pp.418-430. Society of Exploration Geophysicists.

Eisner, E. 1984. Minimum phase for continuous time and discrete time functions. Geophysical Prospecting **32**, 533-541.

Ergin, K. 1952. Energy ratio of the seismic waves reflected and refracted at a rock-water boundary. Bul.Seism.Soc.Am. **42**, 349-372.

Futterman, W. I. 1962. Dispersive body waves. Journal of Geophysical Research **67**(13), 5279-5291.

Goupillaud, P. L. 1961. An approach to inverse filtering of near-surface layer effects from seismic records. Geophysics **26**, 754-760.

Grenander, U. and Rosenblatt, M. 1957. Statistical analysis of stationary time series. Wiley and Sons, New York.

Hamilton, E. L. 1972. Compressional-wave attenuation in marine sediments. Geophysics **37**, 620-646.

Haskell, N.A. 1953. The dispersion of surface waves on multilayered media. Bulletin of the Seismological Society of America **43**(1), 17-34.

Jannsen, D., Voss, J. and Theilen, F. 1985. Comparison of methods to determine Q in shallow marine sediments from vertical reflection seismograms. Geophysical Prospecting **33**, 479-497.

Meissner, R. and Theilen, F. 1986. Experimental Studies of the Absorption of Seismic Waves. Final Report for the Federal Ministery of Research and Technology, DGMK Project 254 "Absorption of Seismic Waves (ASW).

Mitchell, A. R., and Stokes, W. D. 1986. Sampling and minimum phase from both a continuous and discrete point of view. Geophysical Prospecting **34**, 807-821.

Nyquist, H. 1928. Certain topics in telegraph transmission theory. A.I.E.E. Transactions, April, 617-644.

Paley, R.E.A.C. and Wiener, N. 1934. Fourier transforms in the complex domain. American Mathematical Society Colloquium Publication No. 19.

Port Huron Daily Times. 1890. Special August edition on completion of the railway tunnel.

Kramer, Peterson and Walter. 1968. Seismic Energy Sources 1968 Handbook, Bendix United Geophysical Corporation, Pasadena, California.

Robinson, E. A. 1967a. Statistical communicatioon and detection. Hafner, New York.

Robinson, E. A. 1967b. Multichannel time series and analysis with digital computer programs. Holden-Day, San Francisco.

Shannon, C. E. 1949. Communication in the presence of noise. Proceedings of the I.R.E. **37**, 10-21.

Sherwood, J. W. C., and Trorey, A. W. 1965. Minimum-phase and related properties of the response of a horizontally stratified absorptive earth to plane acoustic waves. Geophysics **30**, 191-197.

Thompson, W.T. 1950. Transmission of elastic waves through a stratified solid medium. Journal of Applied Physics **21**, 89-93.

Trorey, A. W. 1962. Theoretical seismograms with frequency and depth dependent absorption. Geophysics **27**, 766-785.

van der Wey, A. 1989. Comparison of deconvolution methods for high- resolution zero-offset marine seismic data. M.Sc. thesis for the Department of Exploration Geophysics, State University of Utrecht, The Netherlands.

Veldhuizen, H. 1989. Seismic absorption: shipboard modelling with a P.C. M.Sc. thesis for the Department of Exploration Geophysics, State University of Utrecht, The Netherlands.

Wiener, N. 1958. Nonlinear problems in random theory. The M.I.T. Press.

Ziolkowski, A. 1984. Deconvolution. D. Reidel Publishing Company, Dordrecht, Holland.

Acknowledgments

The work discussed herein has been in progress for a number of years. It seems appropriate to trace its development and make acknowledgements in chronological order.

The possibility of exploiting the information content of multiple sequences was suggested to me more than twenty-five years ago by Rudy Prince, then of Geophysical Services Incorporated. At about the same time discussions with Bill Shell, also of G.S.I., raised questions concerning the logic that justified the use of long predictive deconvolution filters to attenuate marine multiples. A continuing interest in the subject was initiated. A brief conversation with John Berg of Texas Instruments convinced me that a more complete education would be required to pursue it. It was obtained in graduate school at St. Louis University with the help of William Stauder S.J. and an NDEA Title IV fellowship. A two-year series of courses given by N. J. Vlaar, then visiting the geophysics department in St. Louis, deserves special acknowledgment. It provided not only a strong foundation in theoretical seismology but also an introduction to measure theory. Another year spent in the company of Prof. Vlaar at the Vening Meinesz Laboratorium in Utrecht permitted further delving into measure theory, probability theory in particular, until some small spark of understanding finally began to glimmer.

The opportunity to enter a branch of seismology that was developing rapidly at the time, high-resolution single-channel marine reflection profiling, was provided by the marine geology group of Prof. J. W. Murray at the University of British Columbia. The broad-band character of this type of data presents serious obstacles to realistic mathematical description and working with R. D. Macdonald and J. J. Kennedy of that group produced field methods that resulted in data that could be modelled adequately. The interest of project engineers in the British Columbia Hydro and Power Authority and in H. A. Simons (International) Ltd. provided many opportunities to perfect those methods. The acquisition of data in the St. Clair River was conceived and organized by Paul Brander. The opportunity to use that work as the basis for a dissertation was provided by Prof. Klaus Helbig. His patience and the digital capabilities of his department were of much practical assistance throughout. Finally, my wife Liliana provided tremendous personal support as well as a tireless proofreading service.

Curriculum Vitae

3-11-39: Born in Moberly, Missouri, U.S.A.

1957-61: Undergraduate student, Department of Geophysics, Saint Louis University.
Research entitled "The Source Mechanism of Some Aleutian Earthquakes from S-Wave Data" supervised by Prof. William Stauder, S.J.
Received Bachelor of Science degree in Geophysical Engineering.
Successfully wrote examinations for Missouri State Board for Architects and Professional Engineers

1961-62: Geophysical engineer, Chevron Oil Company, Houston and Calgary
Responsible for reduction of field data on seismic exploration crews.

1962-66: Exploration Party Chief, Geophysical Service Incorporated, New Orleans
Responsible for operation of a marine seismic exploration crew in the Gulf of Mexico and supervision of a research group applying digital processing techniques to marine seismic data.

1966-68: Graduate student, Department of Geophysics, Saint Louis University.
Wrote computer program for prediction of earth tides, researched a procedure for determination of earth's crustal structure by comparison of P and pP earthquake phases and completed requirements (except dissertation) for doctoral degree in geophysics.

1967-68: Special Consultant, Sinclair Oil Company, Tulsa.
Studied shallow-water reverberations in the Gulf of Alaska and calibrated three-component borehole seismometers for Vibroseis test site.

1968-69: NATO visiting scientist, Vening Meinesz Laboratory, Utrecht.
Wrote the course text and lectured on the application of communications theory to geophysical problems and prepared a manuscript on the maximum entropy criterion in spectral analysis.

1969-70: Chief programmer for analysis and research, Atlantic-Richfield Oil Company, Plano.
Responsible for development of computer programs to process seismic exploration data.

1971-74: Geophysicist to the marine geology group, Department of Geological Sciences, University of British Columbia, Vancouver.
Responsible for development of improved seismic amplifiers, hydrophone arrays, procedures and computer programs for high-resolution seismic profiling.
Senior scientist during several cruises of the research vessel CFAV "Endeavour" acquiring and interpreting single-channel seismic profiles along the coast of British Columbia.
Prepared maps and manuscripts concerning the submarine geology of the Strait of Juan de Fuca, the continental shelf of Vancouver Island and adjacent basins of the northeast Pacific Ocean, the Explorer oceanic plate, Dixon Entrance and the Queen Charlotte Islands, various fjords and lakes in British Columbia.

1972-present: President of Thalassic Data Limited, Vancouver.
A corporation founded by members of the University of British Columbia marine geology group for the purpose making results of research available to industry.
Responsible for geophysical aspects of work undertaken by the company, organization and supervision of field crews and interpretative personnel, sea-floor mapping and report writing.
Completed commercial contracts include an electric transmission cable across the Straits of Georgia and effluent outfalls at various municipalities, pulp mills and mines along the west coast of Canada.
Research funded by the company included a sea-floor penetrometer and vibrocorer, a PC-based digital seismic acquisition system, seismic sources, hydrophone arrays and optimal field procedures.
Research funded by clients included estimation of sea-floor properties from amplitude vs. offset measurements.
Contributor to "Civil Engineering in the Oceans IV", San Francisco, 1979.

1979-present: Geophysical consultant to engineering management, West Vancouver.
Services include planning and implementation of marine geotechnical studies, writing of terms of reference and technical specifications, reviewal of bid documents and client representation during data acquisition and interpretation.
Project involvement includes a gas pipeline across the Straits of Georgia, an electric transmission cable across Sunda Strait, port facilities on both coasts of Canada and being an expert witness to the British Columbia Utilities Commission.

1987-present: Research associate for marine geophysics, Institute of Earth Sciences, State University of Utrecht
Responsible for promoting an in-house expertise concerning the recording, processing and interpretation of high-resolution marine seismic profiles, the development of a multichannel digital system for recording and shipboard processing of marine seismic data, supervising student research and teaching a course in signal processing.